TRANSPORTATION RESEARCH RECORD 1071

Rail Track and Structures

TRB
TRANSPORTATION RESEARCH BOARD
NATIONAL RESEARCH COUNCIL
WASHINGTON, D.C. 1986

Transportation Research Record 1071
Price $11.20
Editor: Julia Withers
Compositor: Lucinda Reeder
Layout: Marion L. Ross

modes
2 public transit
3 rail transportation

subject areas
21 facilities design
25 structures design and performance
40 maintenance
62 soil foundations
63 soil and rock mechanics

Transportation Research Board publications are available by ordering directly from TRB. They may also be obtained on a regular basis through organizational or individual affiliation with TRB; affiliates or library subscribers are eligible for substantial discounts. For further information, write to the Transportation Research Board, National Research Council, 2101 Constitution Avenue, N.W., Washington, D.C. 20418.

Printed in the United States of America

Library of Congress Cataloging-in-Publication Data
National Research Council. Transportation Research Board.

Rail track and structures.

(Transportation research record, ISSN 0361-1981 ; 1071
1. Railroads–Track–Congresses. I. National Research Council (U.S.). Transportation Research Board. II. Series.
TE7.H5 no. 1071 380.5 s 86-23464
[TF240] [625.1'4]
ISBN 0-309-04065-5

Sponsorship of Transportation Research Record 1071

GROUP 2–DESIGN AND CONSTRUCTION OF TRANSPORTATION FACILITIES
David S. Gedney, Harland Bartholomew & Associates, chairman

Soil Mechanics Section
Raymond A. Forsyth, California Department of Transportation, chairman

Committee on Engineering Fabrics
Verne C. McGuffey, New York State Department of Transportation, chairman
J. R. Bell, Robert G. Carroll, Jr., Steven M. Chrismer, Jerome A. Dimaggio, Graham Rudy Ford, S. S. Dave Guram, Curtis J. Hayes, Gary L. Hoffman, Robert D. Holtz, Thomas P. Hoover, Donald J. Janssen, James H. Keil, Thomas C. Kinney, Robert M. Koerner, Jim McKean, Gregory N. Richardson, Harry H. Ulery, Jr., Dennis B. Wedding, David C. Wyant

Railway Systems Section
Robert E. Kleist, Association of American Railroads, chairman

Committee on Railroad Track Structure System Design
Robert E. Kleist, Association of American Railroads, chairman
Ben J. Johnson, Railroad/Transit Consultant, secretary
Louis T. Cerny, William R. Hamilton, John B. Heagler, Jr., Thomas B. Hutcheson, Arnold D. Kerr, Mohammad S. Longi, W. Scott Lovelace, Philip J. McQueen, Howard G. Moody, Myles E. Paisley, Gerald P. Raymond, J. Frank Scott, Alfred E. Shaw, Jr., Charles L. Stanford, W. S. Stokely, Daniel H. Stone, Marshall R. Thompson, Erland A. Tillman, George H. Way, Jr., John G. White, J. W. Winger

Task Force on Rail Transit System Design
Erland A. Tillman, Daniel, Mann, Johnson, and Mendenhall, chairman
Donald A. Shoff, secretary
Anthony T. Bruno, Robert E. Clemons, James F. Delaney, Ronald H. Dunn, William R. Hamilton, Robert D. Hampton, Amir N. Hanna, Ben J. Johnson, William D. Kiley, Mohammad S. Longi, Vincent P. Mahon, Robert J. Murray, Thomas J. O'Donnell, Roy T. Smith, Charles L. Stanford

Maintenance Section

Committee on Railway Maintenance
Albert J. Reinschmidt, Association of American Railroads, chairman
William B. O'Sullivan, Federal Railroad Administration, secretary
Richard F. Beck, James R. Blacklock, H. D. Campbell, David M. Coleman, C. L. Coy, Ronald H. Dunn, Alfred E. Fazio, Amir N. Hanna, Thomas B. Hutcheson, Robert A. Kendall, Richard G. McGinnis, Willis H. Melgren, Guenther W. Oberlechner, Ernest T. Selig, William J. Semioli, Walter W. Simpson, Harry E. Stewart, Vincent R. Terrill

Elaine King and Neil F. Hawks, Transportation Research Board staff

Sponsorship is indicated by a footnote at the end of each paper. The organizational units, officers, and members are as of December 31, 1985.

NOTICE: The Transportation Research Board does not endorse products or manufacturers. Trade and manufacturers' names appear in this Record because they are considered essential to its object.

1074

Contents

Procurement and Selection of Direct-Fixation Fasteners for Transit Projects

AMIR N. HANNA

ABSTRACT

Direct-fixation fasteners are used by U.S. and Canadian transit properties to secure rails to concrete in tunnels and on elevated structures. These fasteners utilize elastomeric pads, steel plates, insulating components, and anchoring devices. Bonded and unbonded type fasteners have been used. Direct-fixation fasteners provide five primary functions. They maintain gage and alignment, control longitudinal rail movements, provide resilience, and assure electrical insulation. In addition, they help attenuate noise and vibrations. Generally, procurement specifications set forth minimum performance requirements as a guide for the design and manufacture of direct-fixation fasteners. Compliance with these specifications is evaluated by laboratory tests. Several applications of direct-fixation fasteners have shown problems ranging from failure of fastener components to electrical leakage. In this paper, the practices used by transit properties for the procurement of direct-fixation fasteners are reviewed, the requirements for direct-fixation fasteners are outlined, and the methods employed for evaluating fastener designs are presented. Also, recommendations for improving fastener performance are presented.

Direct-fixation fasteners are used by U.S. and Canadian transit properties to secure rails to concrete in tunnels and on elevated structures. These fasteners utilize elastomeric pads, steel plates, insulating components, and anchoring devices. Direct-fixation fasteners are unbonded or bonded. An unbonded fastener utilizes a steel plate resting on an elastomeric pad. A bonded fastener utilizes one or two steel plates bonded to an elastomeric pad.

Unbonded fasteners that utilize separate plates and pads have been used on transit projects in Miami (Florida) and Philadelphia (Pennsylvania) as well as in Calgary and Edmonton (Alberta, Canada), and Toronto (Ontario, Canada). Figure 1 shows this type of fastener as used on the Metropolitan Dade County (MDC) transit system in Miami. Bonded fasteners with a single steel plate bonded to the top of an elastomeric pad have been used on transit projects in Atlanta (Georgia) and Baltimore (Maryland). Bonded fasteners with two steel plates and an elastomeric pad bonded between them have been used on transit projects in Buffalo (New York), Chicago (Illinois), Detroit (Michigan), Pittsburgh (Pennsylvania), San Francisco (California), Vancouver (British Columbia, Canada), and Washington, D.C. Figure 2 shows this type of fastener as being used in the Advanced Light Rapid Transit (ALRT) system in Vancouver. To permit accurate gaging of track during construction and regaging to compensate for rail wear, most direct-fixation fasteners have provisions for lateral adjustment.

Direct-fixation fasteners provide similar functions to those provided by cross-tie fasteners. They maintain gage and alignment, restrain longitudinal rail movements, provide resilience, and assure electrical insulation (1). However, because of the elimination of ballast, direct-fixation fasteners exhibit considerably lower spring-rate values to help improve ride quality and attenuate noise and vibrations. Generally, procurement specifications set forth minimum performance requirements as a guide for the design and manufacture of fasteners. Compliance with these specifications is evaluated by laboratory tests (2,pp.29-39). Also, procurements have stipulated compliance with qualification requirements as a requisite for acceptance of a fastener design.

Construction Technology Laboratories, 5420 Old Orchard Road, Skokie, Ill. 60077.

PROCUREMENT PRACTICES

Procurement documents do not ordinarily include detailed fastener designs. They consist of a series of laboratory performance tests with acceptance criteria and a minimum of dimensional constraints to ensure interchangeability, economy, and ease of maintenance. Also, procurement documents stipulate sampling and limited quality control tests. This approach gives

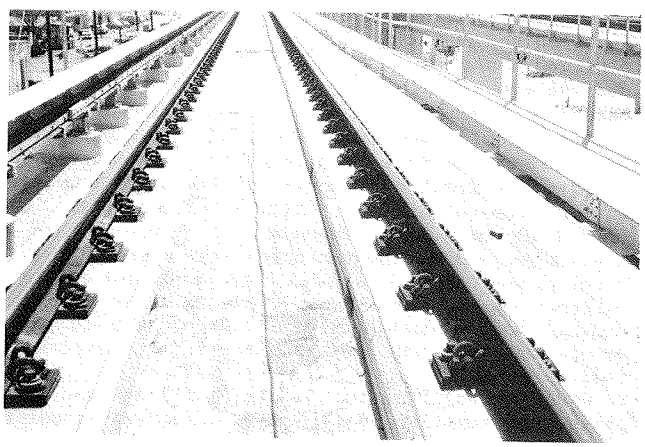

FIGURE 1 Direct-fixation track on MDC in Miami.

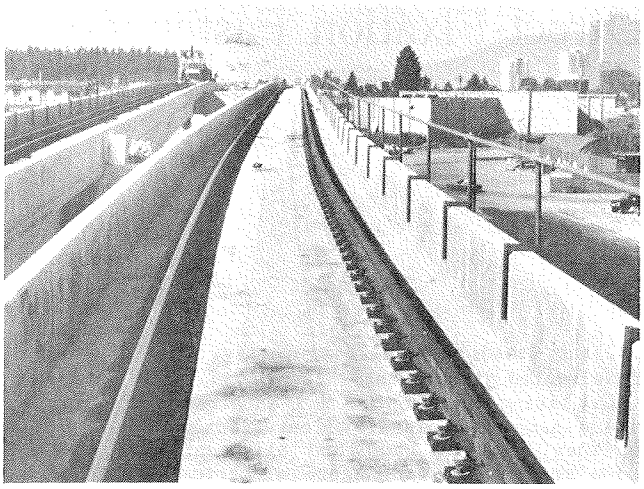

FIGURE 2 Direct-fixation track on ALRT in Vancouver.

the suppliers the freedom to develop solutions within the specified parameters and thus enables procurement from multiple competitive sources. However, other procurement methods have been employed by transit properties. These methods include (a) 1-phase procurement, (b) 2-phase procurement, and (c) sole-source procurement.

In a 1-phase procurement, the bidder is expected to furnish, after contract award, a product meeting the requirements stipulated in the procurement specifications. Availability of an acceptable design before a contract award is not required. However, compliance with qualification test requirements is generally required before acceptance of the proposed design. Also, compliance with production test requirements is generally required before acceptance of the manufactured product. This practice has been used in the procurement of fasteners for several transit projects including those in Atlanta, Baltimore, Miami, and Washington, D.C. This procurement practice could result in extensive delays if the initially proposed fastener design does not meet the specified requirements and subsequent design modifications and reevaluations are required. In several procurements, exceptions and deviations from specifications were permitted by the transit properties because of time restraints.

In a 2-phase procurement, prequalification of fastener design is a requisite for consideration. This prequalification is performed by the supplier or by the transit property as the first phase of procurement. When prequalification is performed by the transit property, potential fastener designs are selected and subjected to a prequalification testing program. Based on test results, the most promising designs are identified and considered in the second phase of procurement. The selected design may be subjected to additional qualification and production tests to ensure that properties of the manufactured product are similar to those of the fasteners used in the prequalification tests. This practice has been used for the procurement of fasteners for a transit project in the Vancouver ALRT system. In this case, prequalification tests were performed on three fastener types, two of which were selected and considered for procurement. The fastener design ultimately selected was then subjected to a series of qualification tests.

When prequalification is performed by the supplier, the supplier is expected to furnish--together with the bid documents--adequate test data to indicate the likelihood of compliance of the proposed design with the stipulated requirements. Generally, the selected design will be subjected to a full qualification testing program before acceptance by the transit property. This practice has been employed for the procurement of fasteners for a transit project for the Southeastern Pennsylvania Transportation Authority (SEPTA) in Philadelphia. The 2-phase procurement has the advantage of identifying the most promising designs before the contract award and thus avoiding possible delays for design modification and reevaluation. Also, this practice permits procurement from multiple competitive sources.

In a sole-source procurement, the transit property selects, based on previous performance, available test data, or other considerations, one or more fastener designs for procurement. However, the supplier is generally required to perform additional testing to verify compliance of design with specification requirements. This practice has been employed for procurement of fasteners for a transit project in the Massachusetts Bay Transportation Authority (MBTA) in Boston. An advantage of this practice is shortening procurement time. However, it has the potential of reducing competition unless several designs are selected for consideration.

QUALIFICATION TESTING REQUIREMENTS

Direct-fixation fastener evaluations include static, dynamic, and repeated-load tests, electrical tests, and corrosion tests. Static tests evaluate fastener response to statically applied loads. Dynamic tests evaluate fastener response to dynamically applied or short-term cyclic loads. Repeated-load tests evaluate the serviceability of fastener components. Electrical tests evaluate the electrical insulation properties of the fastening assembly. Corrosion tests evaluate the effect of severe environmental conditions on the corrosion resistance of fastener components.

Examples of the static tests include the following:

1. A vertical load test to evaluate the effect of vertical loads on rail vertical deflection;
2. A lateral load test to evaluate the effect of lateral load on rail head lateral deflection when a vertical load is applied;
3. A lateral restraint test to evaluate the effect of lateral shear applied to the rail base on rail lateral displacement; and
4. A longitudinal restraint test to evaluate the effect of longitudinal forces on rail longitudinal movement.

Some examples of dynamic tests include (a) a vertical uplift test to evaluate the effect of alternating downward-upward vertical loads on rail vertical deflection, and (b) a dynamic-to-static stiffness ratio test to evaluate the effect of statically and dynamically applied vertical loads on rail vertical deflection, thus comparing the fastener's dynamic and static stiffness values.

Some examples of repeated-load tests include (a) a vertical and lateral repeated-load test to evaluate the effect of the repeated loads on the serviceability of fastener components, (b) an uplift repeated-load test to evaluate the effect of repeated uplift forces on the serviceability of fastener components, and (c) a push-pull test to evaluate the effect of cyclic push-pull loads or displacements on the serviceability of fastener components.

Some examples of electrical tests include (a) a voltage withstand test to evaluate the effect of high-voltage direct current on fastener components,

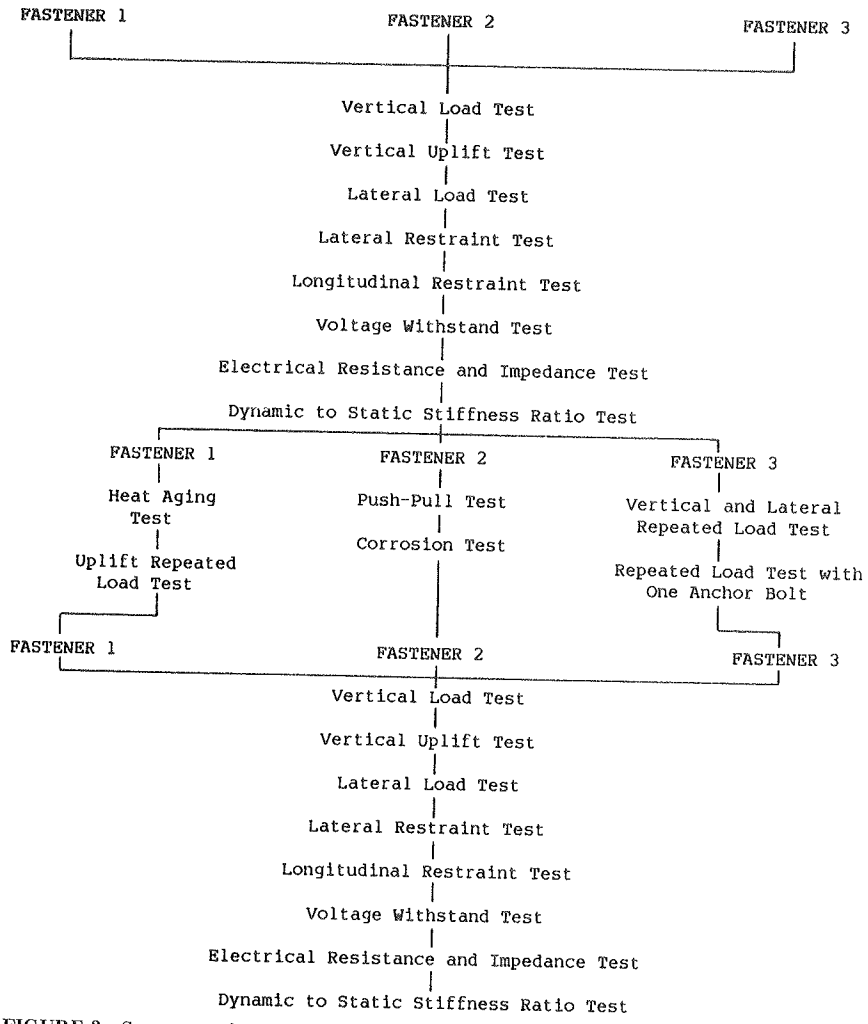

FIGURE 3 Sequence of qualification tests.

(b) a resistance test to evaluate the electrical resistance of wet and dry fasteners, and (c) an impedance test to evaluate the electrical impedance of wet fasteners.

The salt spray test is an example of a test generally specified to evaluate fastener resistance to corrosion.

Qualification and prequalification tests are generally performed on a number of fasteners. Figure 3 shows the test sequence employed for the prequalification testing of direct-fixation fasteners for a transit project in SEPTA in Philadelphia (3). Slightly different testing programs have been specified for the procurement of fasteners for other transit projects.

Recent specifications for direct-fixation fasteners have stipulated test conditions for the laboratory evaluation of fasteners. Test loads and environment are based on expected vehicle weight and dynamic effects and track and vehicle conditions. For test conditions, fasteners are expected to meet the following requirements (3-12):

1. A spring rate between 80,000 and 300,000 lb/in.;
2. A maximum rail head lateral deflection of 0.3 in.;
3. A longitudinal restraint of not less than 2,000 lb for subway fasteners and not more than 1,000 lb for aerial fasteners;
4. A dynamic-to-static stiffness ratio of not more than 1.5;
5. A ratio of upward-to-downward deflection of not more than 2.05;
6. No failure during 3 million cycles of simultaneously applied vertical and lateral repeated loads;
7. No failure during 1.5 million cycles of upward and downward vertical loads;
8. No failure during 25,000 cycles of longitudinal push-pull-type load or displacement;
9. A resistance to 15 kV of direct current;
10. A minimum resistance of 10.0 and 1.0 megohms for dry and wet fasteners, respectively;
11. A minimum impedance of 10,000 ohms for wet fastener components; and
12. A resistance to corrosion and salt spray.

Recent investigations have shown that the use of fasteners with low spring-rate values has a favorable effect on noise and vibration levels. Fasteners with spring rates as low as 50,000 lb/in. have been used in test installations to evaluate their effect on noise vibration levels. Figure 4 shows a test installation at the Washington Metropolitan Area Transit Authority (WMATA) in Washington, D.C., that uses fasteners of this type.

Also, procurement specifications have included qualification testing programs for the evaluation of fastener anchor inserts. These tests are generally

FIGURE 4 Low spring-rate, direct-fixation track on WMATA in Washington, D.C.

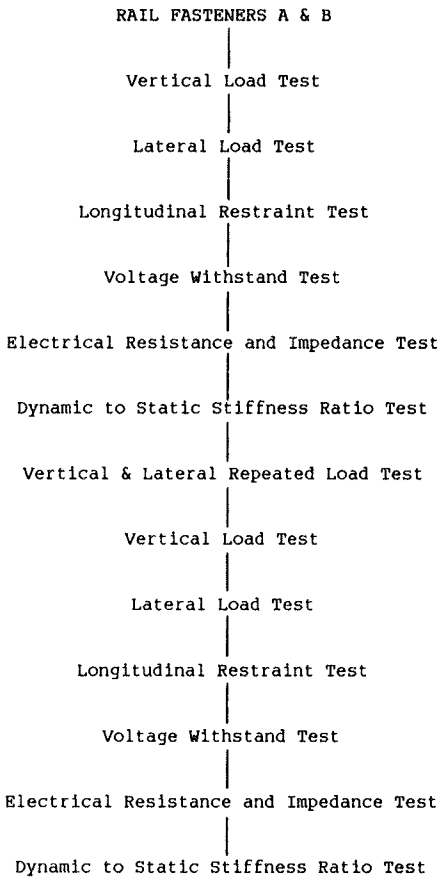

FIGURE 5 Sequence of production tests.

performed on a number of anchor inserts embedded in a concrete test block. These tests evaluate the effect of torsion and uplift forces on the bond between the insert and concrete. Examples of anchor insert tests include torsion and restrained and unrestrained pull-out tests. Recent procurement specifications have stipulated that the anchor inserts must have a resistance to (a) a 400-ft-lb torque, (b) a 20,000-lb uplift force in a restrained pull-out test, and (c) a 12,000-lb uplift force in an unrestrained pull-out test (3).

PRODUCTION TESTING REQUIREMENTS

In addition to the qualification testing program required for the evaluation of fastener designs, procurement documents have generally specified production testing programs for the evaluation of the manufactured product (3-11). This testing program is intended to monitor fastener quality during production and assure its similarity to the design fasteners used in the qualification testing program. Sampling frequency and the extent of testing is specified in the procurement document. Production tests include selected static, dynamic, and repeated-load tests, and electrical tests. Figure 5 shows the test sequence intended for the production testing of direct-fixation fasteners for a transit project on SEPTA in Philadelphia (3).

FASTENER PROBLEMS AND POTENTIAL SOLUTIONS

Experience to date has shown acceptable performance of direct-fixation fasteners on several transit systems. However, some applications of direct-fixation fasteners have shown problems ranging from failure of fastener components to electrical leakage (13, pp.3-28).

Two problems have occurred on some transit properties. These are (a) the failure of the anchorage system and (b) the rapid corrosion of fastener components. Failures of anchoring devices are generally attributed to inherent design deficiencies of the anchoring system, poor construction practices, or lack of adequate quality control during the installation of anchor bolts or inserts. Rapid corrosion of fastener components is caused by inadequate drainage and the resulting wet condition of the fasteners or lack of corrosion protection. Another serious fastener problem is damage of the serrations used in some fastener designs for adjusting track gage. Loss of the serrations makes it practically impossible to ensure proper track gage.

To help reduce track problems and to assure passenger comfort and safety, the following measures should be adopted by the transit industry:

1. Stringent qualification testing programs should be performed before acceptance of design to assure good performance in track. The testing program should be stringent enough to meet service needs, but not so stringent as to require over-designed systems with unneeded and costly characteristics.
2. Adequate quality control programs should be implemented during production to assure that production units are of equal or better quality than those used in design qualification testing.
3. Suitable construction and installation procedures should be followed to eliminate damage to track components during construction.
4. Adequate maintenance programs should be im-

plemented to slow track deterioration, increase service life, and assure safety.

Recent experience with direct-fixation fasteners at the Washington Metropolitan Area Transit Authority has led to a research program to develop better understanding of fastener loading environment and to improve procurement specifications (14,pp.185-212). The program was conducted by the Transportation Systems Center of UMTA. The objective of the program was, in part, to obtain realistic estimates of fastener service loads. This was accomplished by specially designed load cells installed between the direct-fixation fastener and the concrete insert. Once installed and calibrated, vertical, lateral, and torsional forces exerted on the fastener could be measured in track under service conditions. Test data have indicated that fasteners are subjected to vertical loads significantly lower than those specified in qualification testing programs. Measured lateral loads, however, generally exceeded those used in laboratory fastener tests. Therefore, the fasteners are subjected to loading conditions that produce a higher lateral-to-vertical load ratio than specified for qualification testing programs. Also, test data have indicated, as expected, that the distribution of vertical and lateral wheel loads is influenced by the vertical and lateral stiffness of the fastener, respectively.

Based on results of the field measurements, new specifications have been developed for the procurement of direct-fixation fasteners for future WMATA projects (15). The significant deviations in these specifications from those commonly used by other transit systems include the following:

1. The fastener should exhibit a lower vertical spring-rate value, about 70,000 lb/in., to allow for a better distribution of vertical wheel loads to adjacent fasteners and to provide greater attenuation of vibrations.
2. The fastener should be significantly softer laterally to permit better distribution of lateral wheel loads to adjacent fasteners.
3. The pattern and magnitude of vertical and lateral load used for fastener qualification tests are modified to simulate data obtained from field measurements. Also, the number of load applications required for the evaluation of fastener serviceability has been increased from 3 million to 9 million to represent a reasonable service duration.

It should be recognized that data generated from this research program were obtained for specific track designs, operating conditions, and rolling stock characteristics. Data obtained may not be valid for other conditions. Consequently, a great deal of research and development is still needed to properly identify track loading environment and to improve specifications. With suitable information on loading environment, however, optimum and economical track designs can be developed for other specific locations.

CONCLUDING REMARKS

Direct-fixation fasteners are used by U.S. and Canadian transit properties to secure rails to concrete in tunnels and on elevated structures. These fasteners provide five primary functions. They maintain gage and alignment, control longitudinal rail movements, provide resilience, assure electrical insulation, and help attenuate noise and vibrations.

To assure the ability of direct-fixation rail fasteners to provide their intended functions, specifications give minimum performance requirements. These requirements are utilized as a guide for the design and manufacture of rail fasteners. Compliance with these specifications is evaluated by laboratory tests. In these tests, fastener performance is evaluated under specific loads or in a specified environment. This is accomplished by comparing fastener response to acceptance criteria set forth in specifications.

No nationally acceptable standard or recommended practice has yet been developed for fastener evaluation. Therefore, specifications have been developed for individual projects in the United States and Canada. Although test procedures and acceptance criteria vary, specifications generally include tests on complete fastening assemblies to evaluate the fastener's ability to perform the following functions:

1. Provide adequate resilience,
2. Resist uplift forces without damage to fastening components,
3. Control longitudinal rail movements,
4. Restrain lateral rail movement and hold proper gage,
5. Resist repeated vertical and lateral loads without damage to fastening components,
6. Provide adequate electrical insulation, and
7. Exhibit adequate corrosion resistance.

To help develop a nationally acceptable practice for fastener evaluation, it is recommended that a major research and development effort be undertaken to identify the effects of fastener properties, rolling stock characteristics, track configuration, operating conditions, and environment on fastener loads. With these results, an accurate evaluation of fastener designs can be obtained expeditiously to select optimum and economical track designs for each specific application.

Because of time constraints, transit properties have frequently tolerated many exceptions and deviations from specification requirements. Therefore, to help enforce specifications, it is recommended that technical prebid or prequalification submissions be required to eliminate faulty and nonconforming designs from consideration. As an alternative, adequate time should be allowed during the procurement process to enable the transit property to reject nonqualifying designs and seek alternatives.

Finally, it should be recognized that tolerances in material properties, component dimensions, or manufacturing processes could significantly influence fastener characteristics and performance. Therefore, adequate qualification and production test programs should be enforced to ensure compliance of the manufactured fasteners with the intended requirements.

REFERENCES

1. A.N. Hanna. That "Other" Type of Track. Railway Track and Structures, Vol. 81, May 1985, pp. 43-47.
2. A.N. Hanna. Evaluation of Direct Fixation Fasteners by Laboratory Tests. Proc., Direct Fixation Fastener Workshop. Report UMTA-MA-06-0153-85-3. U.S. Department of Transportation, June 1985.
3. Contract Documents and Specifications for Procurement of Direct Fixation Rail Fasteners. Contract CTP1. Southeastern Pennsylvania Transportation Authority, Philadelphia, Oct. 1984.
4. Contract Specifications--Trackwork 8--Direct Fixation Fastener Procurement. Contract 2Z4408U. Washington Metropolitan Area Transit Authority, Washington, D.C., Nov. 1979.

5. Contract Specifications Book--Track Fastening Procurement. Contract X0-04-8. Mass Transit Administration, Baltimore, Md., Nov. 16, 1978.
6. Contract Specifications for Direct Fixation Fastener Procurement. Contract Y541--Stage I Rapid Transit System. Metropolitan Dade County Transportation Improvement Program, Miami, Fla., Jan. 1981.
7. O'Hare Extension Trackwork--Detail Specifications. Contract OE-21. Chicago Transit Authority, Chicago, Ill., March 1980.
8. Direct Fixation Fasteners Project Manual. Contract 2Z0085. Niagara Frontier Transportation Authority, Buffalo, N.Y., 1981.
9. Advanced Light Rapid Transit System. Metro Canada Limited, Vancouver, British Columbia, 1982.
10. Direct Fixation Rail Fasteners Procurement. Contract CQ833. Port Authority of Allegheny County, Pittsburgh, Pa., Aug. 1982.
11. Detroit Central Automated Transit System. Contract 3Z0663. Urban Transportation Development Corporation, Inc., Detroit, Mich., 1984.
12. Specifications for MBTA Contract No. 097-403 Systemwide Trackwork--Southwest Corridor Project. Massachusetts Bay Transportation Authority, Boston, 1983.
13. P. Witkiewicz. A Survey of Direct Fixation Fasteners Systems in North America--Existing Types and Associated Problems. Proc., Direct Fixation Fastener Workshop. Report UMTA-MA-06-0153-83-3. U.S. Department of Transportation, June 1985.
14. A. Sluz. Measurement of Direct Fixation Fastener Load Environment on the Washington Metropolitan Area Transit Authority Metrorail System. Proc., Direct Fixation Fastener Workshop. Report UMTA-MA-06-0153-83-3. U.S. Department of Transportation, June 1985.
15. Trackwork 10--Direct Fixation Fastener Procurement. Washington Metropolitan Area Transit Authority, Washington, D.C., July 1984.

Publication of this paper sponsored by Task Force on Rail Transit System Design.

The Reduction of Wheel/Rail Curving Forces on U.S. Transit Properties

CHARLES O. PHILLIPS and HERBERT WEINSTOCK

ABSTRACT

Summarized in this paper are recent government-sponsored studies to determine the effectiveness of various methods for reducing wheel/rail curving forces and resulting wear and component failure on U.S. transit properties. It describes the factors affecting the trade-off between curving performance and truck stability as it affects ride quality and the potential for derailment. A simplified description of truck-curving mechanics is presented, outlining three sources of lateral wheel/rail forces and three key methods for reducing those forces. References to more detailed papers and reports are included. Finally, the results of wheel/rail force measurements made for various truck and track configurations are presented and compared with theory. It is concluded that reductions in curving forces of up to 75 percent can be obtained by using tapered wheels and softening the longitudinal primary suspension or incorporating steerable trucks, or both.

Wheel/rail wear and related component failures have plagued transit systems since their inception at the turn of the century. In recent years, however, reports of such problems have occurred with increasing frequency. The Transportation Systems Center (TSC) sponsored by UMTA, U.S. Department of Transportation, has conducted studies and experiments to determine the causes and methods of reducing the incidence of high wear and component failure rates. Measuring wheel/rail wear and determining the factors that cause it are difficult and time-consuming. An interim step is to measure the wheel/rail forces that are a significant cause of the wear. Methods of reducing these forces can more rapidly be determined. Subsequently, the actual reduction in wear and component failures resulting from selected force reduction methods can be established over a longer period of

Transportation Systems Center, U.S. Department of Transportation, Cambridge, Mass. 02142.

time. Summarized in this paper is the result of the TSC's studies and experiments related to reducing wheel/rail forces. The paper (a) describes the stability versus curving performance of existing transit trucks; (b) provides an outline of curving mechanics; and (c) estimates the reduction in curving forces achieved by the use of tapered wheels, softening the longitudinal primary suspension, and incorporating steerable trucks.

BACKGROUND

New transit trucks introduced in the 1960s and 1970s to attract ridership with smooth, high-speed, comfortable performance proved to have high wheel/rail wear rates. Initially, transit engineers suspected high yaw resistance between truck and car body as a cause of wear because the new trucks supported the vehicle body through side bearers rather than through the center pins of the older design. Truck designers hastened to show that these forces were not high enough to account for the increase in wear. Through studies reported here, the main cause was determined to be the stiff elastomeric primary suspension elements incorporated to replace steel-spring, pedestal-type suspensions of the older designs. The use of elastomers enabled the longitudinal stiffness to exceed what was needed for dynamic stability at transit speed maximums of 60-70 mph. By softening the longitudinal suspension, curving forces could be reduced without reducing the stability to the point that it would affect ride quality or the potential for derailment. These theories have been subsequently verified by measurements and the revenue use of softened suspensions for periods exceeding 2 years at both the Port Authority Transit Corporation (PATCO) and the Washington Metropolitan Area Transportation Authority (WMATA).

Two other controversies existed. The first concerned cylindrical versus tapered wheels. Although railroads used only 1:20 tapered wheels, several transit systems had, in the past, resorted to cylindrical transit wheels. Work reported here shows that tapered wheels and, in particular, a worn Heumann tapered-wheel profile cause lower level wheel/rail forces and provide adequate stability for present truck designs.

The second controversy concerned the importance of providing sufficient superelevation in curves to allow balance speed for normal operations. Work reported here shows superelevation to be reasonably insensitive toward reducing curving forces and wear in the face of high frictional forces. Furthermore, it was pointed out that high superelevations at low speeds as encountered in reversing loops could cause derailment in the presence of minor track misalignment.

Finally, the Budd Company/H. List steerable truck designs, which were developed in part with UMTA program funding and which are presently in revenue service on the Philadelphia PATCO system, are compared under the same conditions and instrumentation with a conventional and softened suspension Budd Pioneer 3 truck.

TRUCK STABILITY VERSUS CURVING PERFORMANCE

The factors affecting the trade-off between truck stability and curving performance are the interaxle shear stiffness and the interaxle bending stiffness. The shear stiffness, as shown in Figure 1, is related to the resistance to lateral displacement between the two axles and is primarily affected by the primary suspension lateral stiffness. The bending

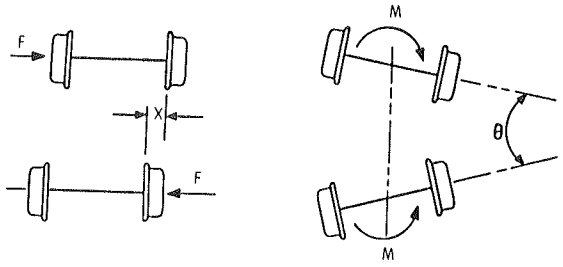

FIGURE 1 Schematic representation of generalized stiffness coefficients.

stiffness is related to the resistance to angular displacement between the two axles and is primarily affected by the primary suspension longitudinal stiffness.

Table 1 gives the stiffness of various transit trucks in current use on U.S. transit properties. Data on vertical stiffness affecting ground and truck vibration are included but not discussed here. Figure 2 shows some of these stiffnesses and relates them

TABLE 1 Transit Truck Suspension Stiffness Characteristics

Property	Manufacturer Truck	Vertical Stiffness (lb/in.)	Bending Stiffness (in./lb)	Shear Stiffness (lb/in.)
CTA	Wegmann	14,560	1.3×10^7	6.3×10^3
MARTA	Rockwell	150,000	1.2×10^8	2.6×10^4
MBTA-Blue	GSI	6,500	6.1×10^7	9×10^3
MBTA-Orange	GSI	7,500	7.3×10^7	10.7×10^3
PATCO	Budd	160,000	2.3×10^8	5.9×10^4
PATH	GSI	32,000	2.4×10^8	4.3×10^4
WMATA	Rockwell	90,000	1.3×10^8	1.8×10^4
WMATA	Breda	10,500	1.1×10^8	1.5×10^4

Note: CTA = Chicago Transit Authrotiy, MARTA = Metropolitan Atlanta Rapid Transit Authority, MBTA = Massachusetts Bay Transit Authority, PATCO = Port Authority Transit Corporation, PATH = Port Authority Trans-Hudson, and WMATA = Washington Metropolitan Area Transportation Authority,

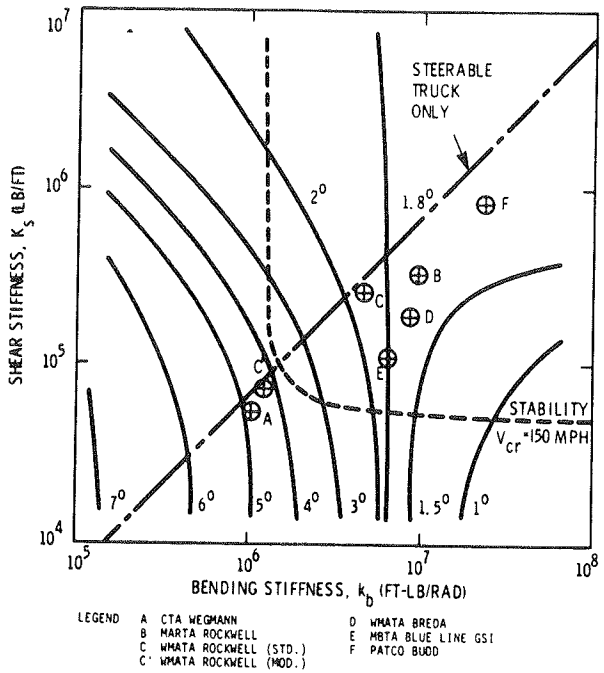

FIGURE 2 Truck curving and stability versus bending and shear stiffness (preliminary).

to truck curving performance and stability. Curving performance is indicated by the angular curvature in degrees that the truck can negotiate without hard flanging, which produces high wheel/rail wear. Stability is indicated by a single critical speed of 150 mph above which hunting and instability occur. As a comparison, the Chicago Transit Authority (CTA) Wegmann truck with a relatively soft suspension can negotiate a 5-degree curve without hard flanging and remain stable at speeds of less than 150 mph, but well above the CTA operating speed of 55 mph. The PATCO Budd truck with a stiffer suspension can negotiate a curve of only less than 1.8 degree without hard flanging and has a critical speed well above 150 mph, as compared with a maximum operating speed at PATCO of 75 mph.

This information is intended to be qualitative to allow comparison and to determine trade-off potential. It does not include the effects of varying the wheel profile, the wheel/rail adhesion coefficients, and the hard flanging. A more practical wear index based on the work performed is described later. Conventional trucks discussed fall below the diagonal line. Steerable trucks with interaxle connecting linkages allow greater freedom for performance trade-offs and can occur above as well as below the line.

Curving performance versus stability is discussed in greater depth in the literature (1).

TRUCK CURVING MECHANICS

Wheel-flange wear and rail gage-face wear result the lateral wheel/rail forces produced as a truck negotiates a curve. The causes of these forces have been imperfectly understood, resulting in a continuing controversy over the methods to reduce them. The following discussion is an attempt to outline in simple terms the present understanding of this phenomenon. It is broken down into seven conditions as follows:

- Condition A: Centrifugal Force
- Condition B. Pivot Force
- Condition C: Wheel/Rail Friction Force
- Condition D: Combined Forces
- Condition E: Tapered Wheels
- Condition F: Soft Suspension and Tapered Wheels
- Condition G: Steerable Truck

Three sources of lateral wheel/rail forces are described in Conditions A, B, and C. Condition D combines them for comparison and to represent the actual forces encountered during curving. Conditions E, F, and G describe three methods for reducing these forces.

Condition A: Centrifugal Force

Figure 3 shows the most easily understood component of curving (or centrifugal) force. To isolate this condition, the wheel/rail friction coefficient and the truck/carbody pivot torque are assumed to be zero. Under these conditions, the centrifugal force F_c acting outward on the car body is reacted by the lateral wheel/rail force F_l, acting inward on the four high-rail wheel flanges. The formula for F_c is presented as a function of the velocity v and the track superelevation E.

Figure 4 shows the wheel/rail force F_l acting on one truck at balance speed, where it is defined to be zero, and for an unbalance of 3 in., where it is calculated to be approximately 1,000 lb for an 80,000-lb car. For conditions where the friction coefficient is not assumed to be zero, the low-rail wheels as well as the high-rail wheels will take up the reactive force. It is assumed that the force would be divided equally among the eight wheels of the two trucks and that the resulting wheel/rail force, F_l, would then be reduced to 500 lb.

Condition B: Pivot Force

Figure 5 shows the second component of curving force, the truck/car body frictional pivot force. As a truck enters a curve and is forced to pivot in relation to the car body, the resulting resistance to turning is

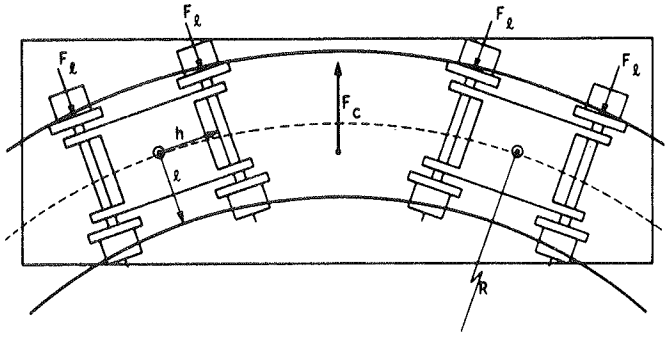

CENTRIFUGAL FORCE ON CAR

$Fc = W[\ v^2/gR - E/2\ell]$

LATERAL WHEEL/RAIL FORCE

$F\ell = Fc/4$

FRICTION COEFFICIENT $\mu = 0$ CONICITY $\alpha = 0$
TRUCK PIVOT TORQUE $T = 0$ SUSPENSION STIFF

W = CAR WEIGHT
V = VELOCITY
g = ACCELERATION OF GRAVITY
R = CURVE RADIUS
E = SUPER ELEVATION
ℓ = 1/2 TRACK GAGE
h = 1/2 TRUCK WHEEL BASE

FIGURE 3 Condition A: centrifugal force.

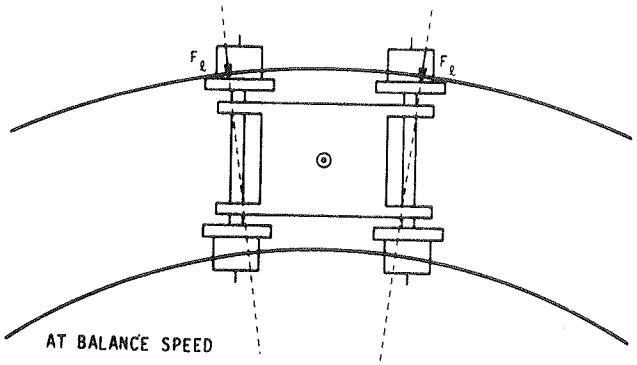

AT BALANCE SPEED

$F\ell = 0$

WITH AN UNBALANCE OF 3" FOR $\mu = 0$

$F\ell = 0.05\ W/4 = 0.05 \times 80{,}000$ LBS./4 = **1,000 LBS.**

FOR $\mu = \mu^*$

$F\ell = 0.05\ W/8 = 0.05 \times 80{,}000$ LBS./8 = **500 LBS.**

FRICTION COEFFICIENT $\mu = 0$ CONICITY $\alpha = 0$
TRUCK PIVOT TORQUE $T = 0$ SUSPENSION STIFF

FIGURE 4 Condition A: centrifugal force (wheel/rail force F_1 acting on one truck at balance speed).

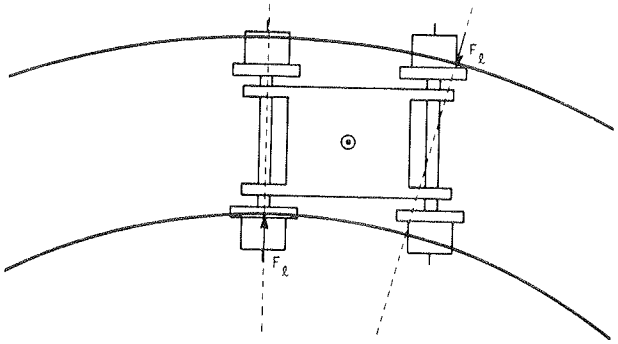

LATERAL WHEEL FORCE AT BALANCE SPEED

$F\ell = T/2h$

$F\ell$ = 80,000 INCH-LBS./2 x 43 INCHES = **1,000 LBS.**

TRUCK PIVOT TORQUE $T = T^*$ CONICITY $\alpha = 0$
FRICTION COEFFICIENT $\mu = 0$ SUSPENSION STIFF

FIGURE 5 Condition B: pivot force.

reacted by the lead-axle, high-rail wheel and the trailing-axle, low-rail wheel for the lead truck and by the opposite wheels for the trailing truck. To isolate and simplify this phenomenon, the friction coefficient is assumed to be zero. The truck pivot torque is assumed to be 80,000 in.-lb, and the half-gage width is assumed to be 43 in., based on measured data for the WMATA sidebearing Rockwell truck (2). Under these conditions, the lead truck high-rail lateral wheel force is calculated to be approximately 1,000 lb. In the constant radius portion of the curve, this force would be zero, except for fluctuations attributed to track geometry and wear irregularities. As the truck leaves the curve, the forces are reversed.

Condition C: Wheel/Rail Friction Force

Figure 6 presents the most important and most poorly understood component of curving force, the wheel/rail friction force. To isolate this condition, the truck is assumed to be operating at balance speed and the truck pivot torque is assumed to be zero. The friction coefficient is assumed to be 0.5. Under wet or lubricated conditions, the friction coefficient is lower. As a result of the wheel/rail friction force,

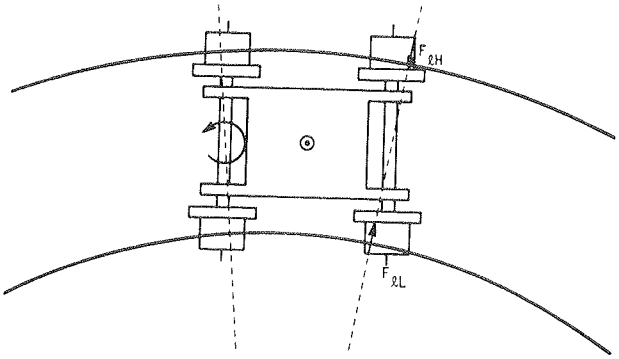

LATERAL WHEEL FORCE AT BALANCE SPEED

HIGH RAIL	LOW RAIL
$F\ell = 1.2\ \mu W/8$	$F\ell = \mu\ W/8$
$F\ell = 1.2 \times 0.5 \times 80{,}000$ LBS./8 =	$F\ell = 0.5 \times 80{,}000$ LBS./8 =
6,000 LBS.	**5,000 LBS.**

FRICTION COEFFICIENT $\mu = \mu^*$ CONICITY $\alpha = 0$
TRUCK PIVOT TORQUE $T = 0$ SUSPENSION STIFF

FIGURE 6 Condition C: wheel/rail friction force.

t.. d-axle, high-rail wheel experiences an inward force of approximately 6,000 lb and the low-rail wheel an outward force of 5,000 lb, as calculated for an 80,000-lb transit car with a friction coefficient of 0.5. These forces decrease with increasing radius but are reasonably independent of speed. They can be accounted for as follows.

The trailing axle assumes an almost radially aligned position, but in the absence of wheel taper, a moment is created because of the greater distance to be traveled by the outside high-rail wheel versus the inside low-rail wheel. This moment is transmitted by the truck frame to the lead axle, which causes the high-rail wheel to flange against the high rail and create a high angle of attack for both the high- and low-rail wheels. This angle of attack causes lateral forces to be created, acting outward on the treads of the low- and high-rail wheels as the wheels tend to go straight rather than curve. These combined forces are reacted by the inward flange force on the high-rail wheels as they contact the gage side of the high rail. The result of the outward tread force and the more-than-twice-as-great inward flange force is an inward high-rail wheel force as previously defined. These forces pushing inward on the wheels of the leading axle are reacted by spreading forces outward on the rails. This complex wheel/rail interaction is described in much greater detail in the literature (3).

Condition D: Combined Forces

Figure 7 shows the combination of the lateral wheel forces as previously described. Although in actual-

LATERAL WHEEL FORCES FOR A 3-INCH UNBALANCE FOR μ = 0.5

CONDITION	Fℓ HIGH RAIL	%	Fℓ LOW RAIL
A	500	7	-500
B	1,000	13	0
C	6,000	80	5,000
D	7,500 LBS.	100	4,500 LBS.

LATERAL WHEEL FORCES AT BALANCE FOR μ = 0.5

CONDITION	Fℓ HIGH RAIL	%	Fℓ LOW RAIL
A	0		0
B	1,000	14	0
C	6,000	86	5,000
D	7,000 LBS.	100	5,000 LBS.

FRICTION COEFFICIENT $\mu = \mu^*$ CONICITY α = 0
TRUCK PIVOT TORQUE T = T* SUSPENSION STIFF

FIGURE 7 Condition D: combined forces.

ity these forces are interactive and not directly additive, they are simply added here for comparative purposes.

The total lateral wheel rail force on the lead axle of the lead truck for a 3-in. unbalance is 7,500 lb for the high rail and 4,500 lb for the low rail. For balance conditions with centrifugal forces reduced to zero, the forces are 7,000 lb and 5,000 lb, respectively. The pivot force is assumed to be positive as it increases the flange force on the high-rail wheel and to not affect the nonflanging low-rail wheel.

As can readily be seen, the wheel/rail friction force of Condition C predominates. For small radius curves and high coefficient of friction, it can be 80-90 percent of the total force, with the result that lateral wheel/rail force during curving are insensitive to speed and not significantly affected by superelevation. This contradicts a theory accepted by a least some people and properties in the industry but is verified by the studies and experiments reported here. [For further discussion, see report by Grief and Weinstock (3).]

Condition E: Tapered Wheels

As shown in Figure 8, introducing tapered wheels reduces the lateral wheel/rail friction force on the high-rail wheel as much as 30 percent, as measured at the WMATA system in Washington, D.C. (6,7). The condition presented here assumes balance speed for a zero centrifugal force, as described in Condition D.

This force reduction is caused by the reduction in the moment on the trailing axle because the tapered wheel allows the high-rail wheel to travel further with less slippage than does the cylindrical wheel. A similar moment on the leading axle is also reduced, further reducing the high-rail, lead-axle lateral force.

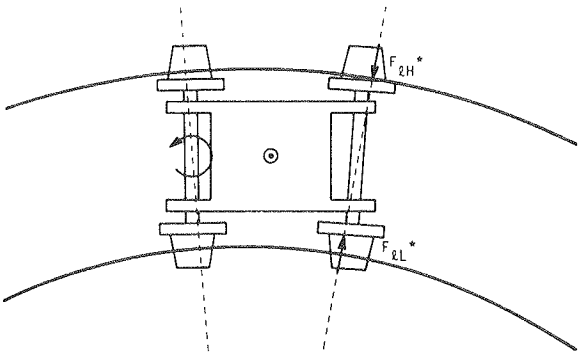

LATERAL WHEEL FORCE AT BALANCE

Fℓ = 0.30 x 6,000 LBS. + 1,000 LBS. = 2,800 LBS.

SUSPENSION SOFT FRICTION COEFFICIENT $\mu = \mu^*$
CONICITY $\alpha = \alpha^*$ TRUCK PIVOT TORQUE T = T*

FIGURE 9 Condition F: soft suspension and tapered wheels.

Condition F: Soft Suspension and Tapered Wheels

As shown in Figure 9, a softened longitudinal primary suspension in addition to tapered wheels reduces the lateral wheel/rail friction force on the high rail as much as 70 percent, as measured at the WMATA system in Washington, D.C. (6). The same assumptions of balance and pivot force are made as in Condition E.

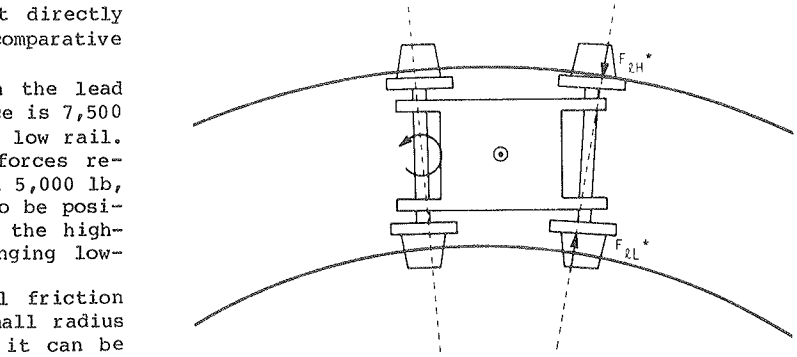

LATERAL WHEEL FORCE AT BALANCE

Fℓ = 0.70 x 6,000 LBS. + 1,000 LBS. = 5,200 LBS.

CONICITY $\alpha = \alpha^*$ FRICTION COEFFICIENT $\mu = \mu^*$
SUSPENSION STIFF TRUCK PIVOT TORQUE T = T*

FIGURE 8 Condition E: tapered wheels.

This significant reduction is caused by the tendency toward radial alignment of both the leading and trailing axles that is allowed by the reduction in longitudinal or bending stiffness, as previously described. On the trailing axle, this change in alignment occurs naturally because of the moment between the axle and the frame of the truck. The radial alignment of the lead axle is less obvious and is caused by (a) the combination of a couple between the lead and trailing axle and (b) the flange contact of the high-rail wheel beneath the running surface of the track, creating a forward force on the axle at the high-rail wheel.

Condition G: Steerable Truck

Figure 10 shows the steerable truck condition created by further softening of the longitudinal suspension and interconnecting the axles with steering arms or linkages to allow complete radial alignment of the axles. Under ideal conditions with sufficient taper and large radius curves, the wheel/rail friction forces can be reduced to practically zero. Allowance is still made here for the pivot force needed to align the axles while entering or leaving the curve. For small radius curves, the self-steering truck shown here is unable to generate sufficient force to align the axles. By interconnecting the linkages with the car body, a forced steering configuration

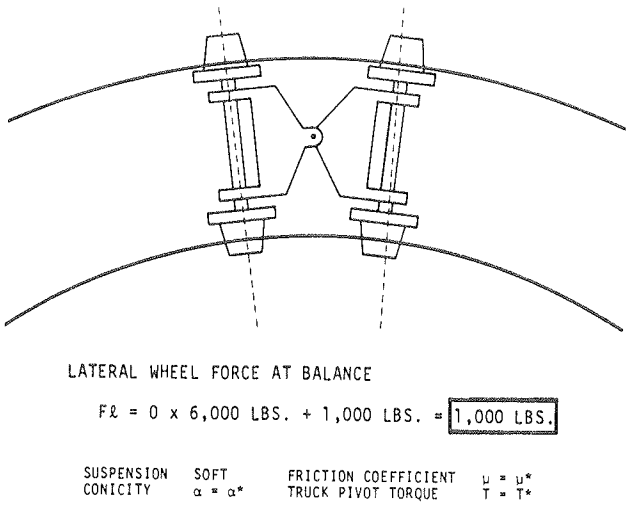

FIGURE 10 Condition G: steerable truck.

is created that provides additional force for radial alignment. Because practical tapers cannot allow for the negotiation of small-to-medium curves without wheel slippage, wheel/rail friction forces are still significant, even with forced steering.

MEASUREMENT AND MODELING RESULTS

Figure 11 shows lateral wheel/rail force as a function of speed as measured on the tight turn loop, a 150-ft radius test curve at the Transportation Test Center in Pueblo, Colorado. It demonstrates the insensitivity to speed predicted by the wheel/rail friction-force component described under Condition C. Forces of 9,000 lb on the high-rail wheel and 6,000 lb on the low-rail wheel are in reasonable agreement with the general condition described under Condition D. The computer predictions presented here are described in greater detail in the literature (7).

Figures 12 and 13 show lateral wheel/rail force as a function of track curvature in degrees as measured by WMATA. They demonstrate the significant reduction in forces accomplished by changing from a cylindrical-wheel, stiff primary-suspension truck configuration to a tapered-wheel, soft primary-suspension truck. The computer predictions are described in greater detail in the literature (8).

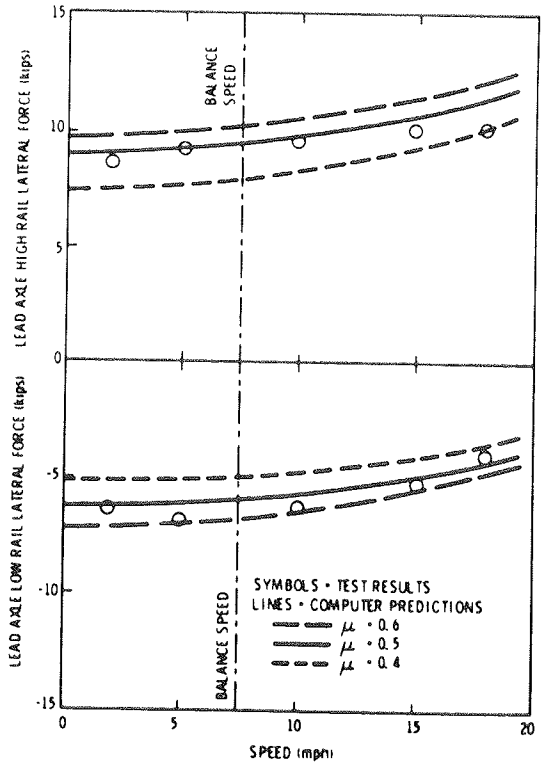

FIGURE 11 Lead axle, high and low rail, lateral force speed with a 150-ft curve radius.

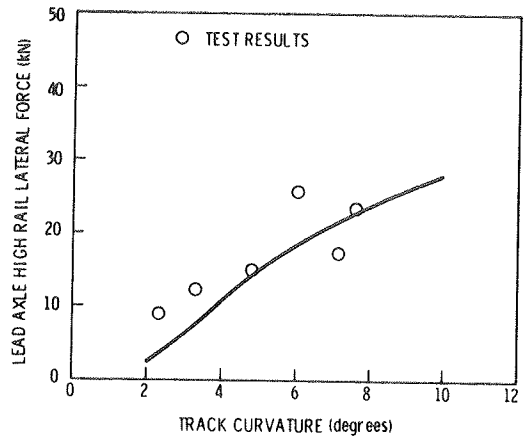

FIGURE 12 Comparison of lateral wheel/rail force predictions versus test results—cylindrical wheel, stiff suspension.

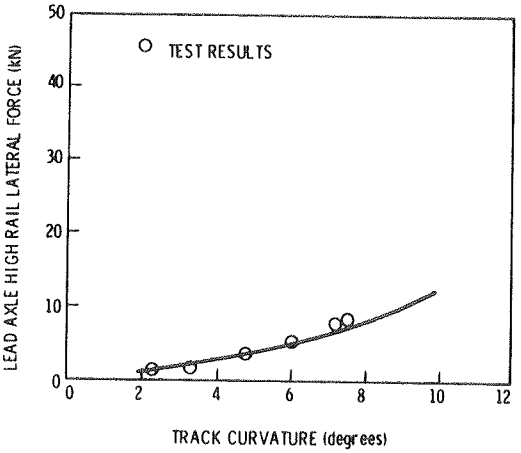

FIGURE 13 Comparison of lateral wheel/rail force predictions versus test results—tapered wheel, soft suspension.

Figure 14 shows a summary of the results from the WMATA wheel/rail force measurement made to compare tapered and cylindrical wheel profiles with the conventional stiff suspension and the experimental soft suspension. Maximum force reductions of 70 percent are observed. It is interesting to note the higher forces for curve 311 on a 1,000-ft radius curve. These forces are significantly higher for all but the tapered soft-suspension configuration because curve 311 is in the offside location from the other curves. Small-but-measurable axle misalignments ac-

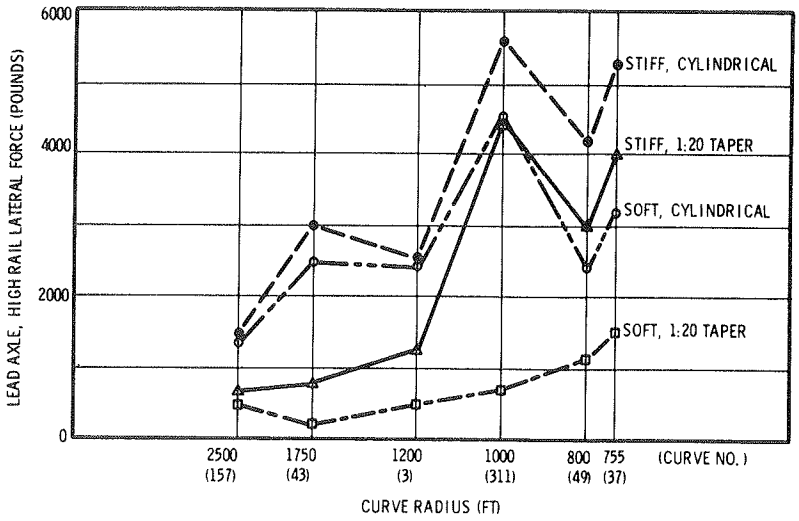

FIGURE 14 Summary of results from WMATA truck test project (for balance speed conditions).

count for a preference for the truck to curve in one direction versus the other (2,6).

Figure 15 shows a sample of actual, measured, high-rail, wheel/rail force data as a function of distance through curve 37, a 7-degree curve. The highly irregular non-steady-state force fluctuations observed are shown to correlate with the gage-face wear pattern presented above the force data. The power spectral density of each, plus their cross-spectral density, are presented at the lower left of the figure. The high correlation with a peak of approximately 41 ft is indicated. This peak is close to the welded-rail section length of 39 ft. The cause for these fluctuations has not been determined. Most likely, track geometry variations are a prime cause with truck/track dynamics emphasizing or deemphasizing the magnitude and frequency of the fluctuations.

Figure 16 shows predicted lateral wheel/rail force as a function of track curvature in degrees for a baseline conventional truck versus a self-steering truck and forced-steering truck. For the same condition, Figure 17 shows the work at the flanging wheel, which is calculated from the creep forces and the resultant creep vectors in the contact path between the wheel and the rail. This calculation of work is proposed as a wear index to relate wheel/rail force with predicted wear of wheels and rails. It is the leading outer wheel that is responsible for the

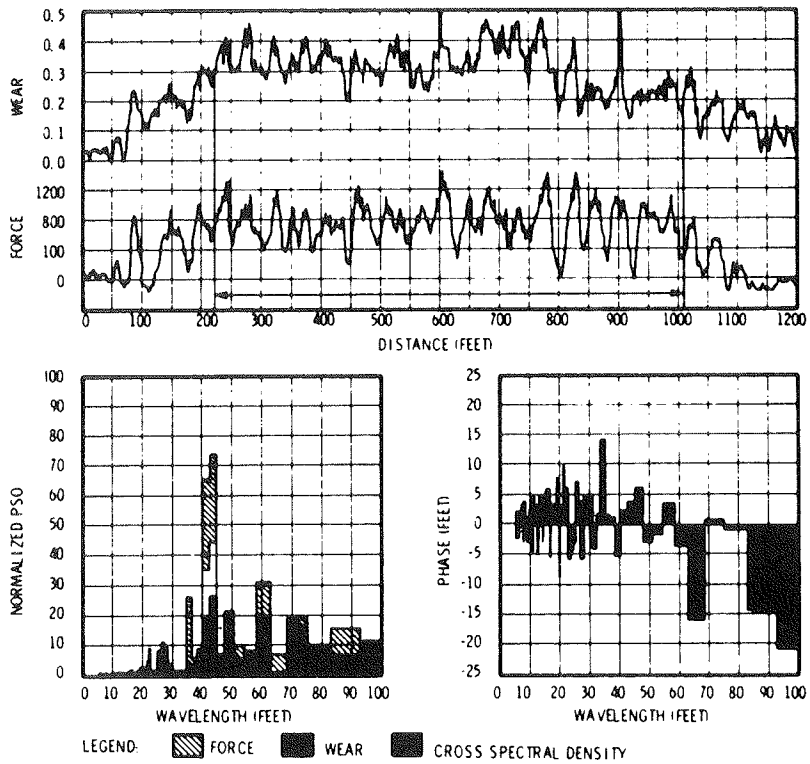

FIGURE 15 Comparison of lateral wheel/rail forces versus gage face wear—curve 37, high-rail, tapered-wheel, stiff suspension at 40 mph.

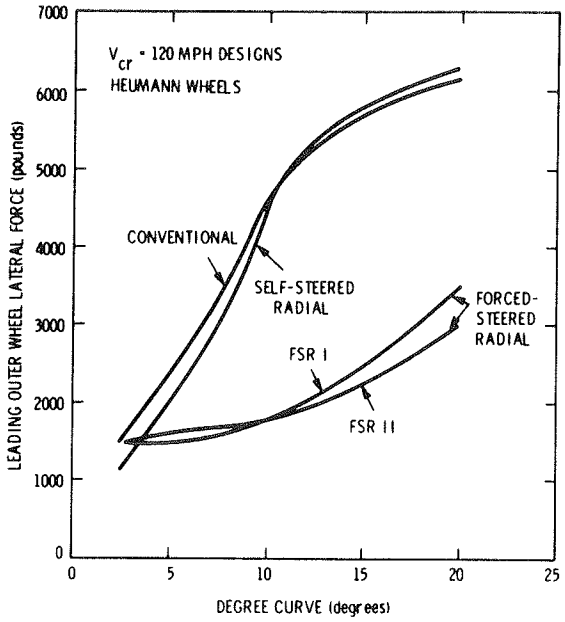

FIGURE 16 Leading outer wheel lateral force versus curvature for baseline truck designs with Heumann tapered wheels (critical speeds = 120 mph).

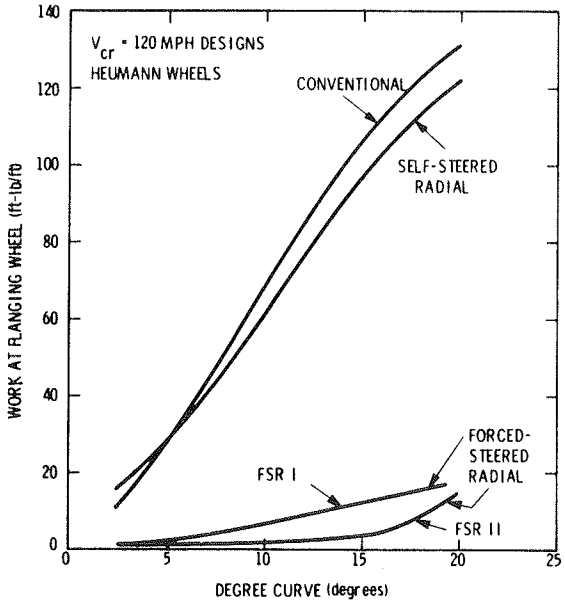

FIGURE 17 Work at flanging wheel versus curvature for baseline truck designs with Heumann tapered wheels (critical speeds = 120 mph).

vast majority of the wear that takes place on the gage face of the high rail and on the wheel flange. [Note that the predictions presented in Figures 16 and 17 are described in greater detail by Wormley et al. (1).]

Figure 18 shows data similar to Figure 15 for measurements made at the Philadelphia PATCO system (9) on a 7-degree, westbound curve comparing a conventional suspension, a soft-suspension retrofit (in revenue services), and a steerable truck (in revenue service). These measurements are given in Table 2.

The soft suspension produces a 69 percent average force reduction and the steerable truck configuration produces a 75 percent average force reduction. Measurements made on the eastbound track of the same curve did not produce significant force reductions for either the soft or the steerable configurations. This is attributed to an ascending grade eastbound versus a descending grade westbound. Application of power on the ascending grade may longitudinally compress the suspension or linkages, or both, thus preventing proper axle steering and the reduction of lateral wheel/rail forces. This phenomenon was not observed on the WMATA system tests.

A further observation of the data revealed that the steerable truck wheelset in the trailing position produced significant forces, leaving curves unlike either the conventional or soft-suspension truck configuration. Finally, it was observed that the steerable truck produced reasonably high forces when negotiating curves with restraining rail and lubrication. The kinematics and dynamics of four-point contact appear to reduce the effectiveness of the steering mechanism. Figure 19 shows a summary of the wheel/rail force measurements versus curvature of the WMATA standard and soft-suspension trucks and the PATCO standard, soft-suspension steerable truck configurations.

The Rockwell truck at WMATA had a measured primary longitudinal suspension stiffness of 460,000 lb/in. per truck for the standard configuration and 120,000 lb/in. per truck for the suspension configuration. For a 7-degree (750-ft radius) curve at WMATA, a 75 percent reduction in suspension stiffness resulted in a 65-70 percent force reduction. At PATCO, an 80 percent reduction in suspension stiffness resulted in a 50 percent force reduction on a curve of the same radius. The steerable truck produced a 70 to 75 percent force reduction under the same conditions. It is interesting to note that the slope of the steerable configuration plot is significantly less than the other plots, indicating reduced curving forces for higher degrees of curvature. The soft-suspension configuration shows reduced forces in mild curves. This may be due to its ability to adjust to the irregularities in track geometry and gage-face wear profiles in contrast to the standard and steerable truck configurations.

As a result of these measurement and analysis activities, WMATA and PATCO will each retrofit 10 car sets (80 suspensions) in the fall of 1985. Further retrofits are being prepared for Baltimore

TABLE 2 PATCO Force Measurement, Westbound 7-Degree Curve

Truck Configuration	Longitudinal Stiffness (lb-in./trucks x 10^3)	Average Force (lb x 1,000)	Maximum Force (in.)	Standard Deviation
Conventional stiff	1,180	5.3	11.6	1.6
Retrofit soft	144	1.9	7.1	1.0
Steerable	N/A	1.3	6.2	0.8

Note: NA = not applicable

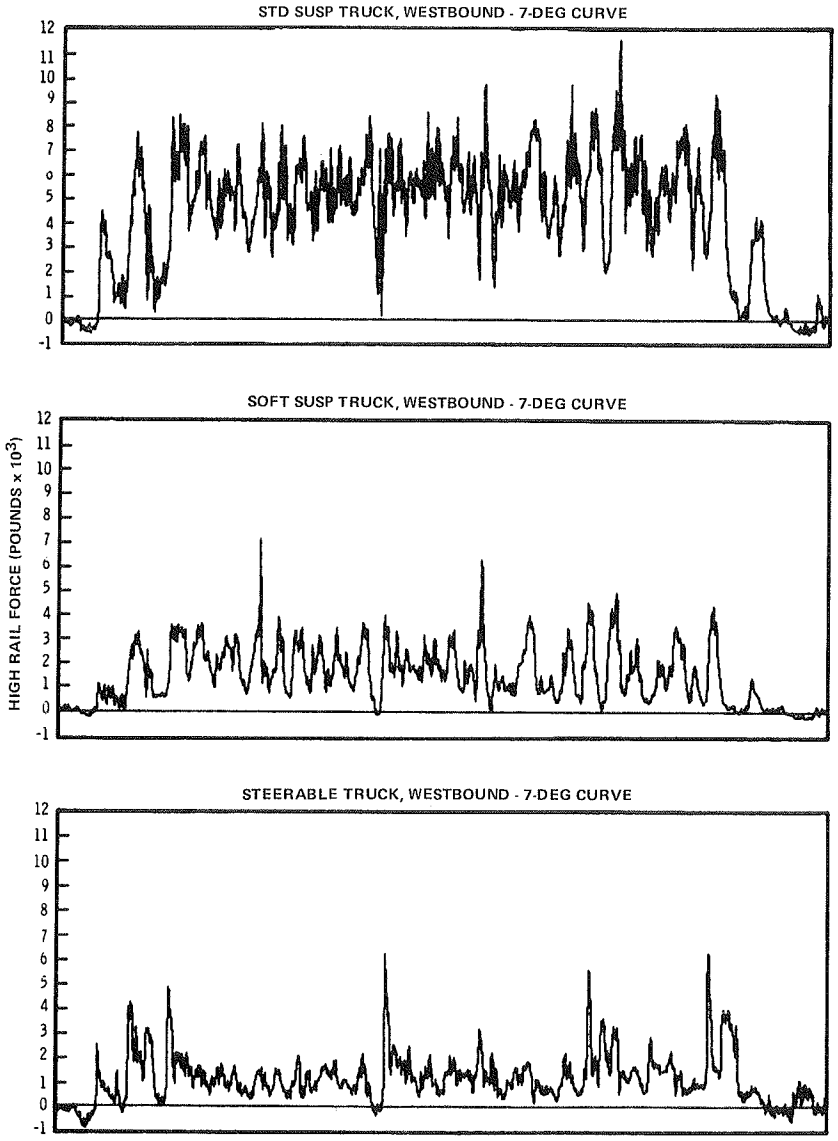

FIGURE 18 PATCO wheel/rail force measurement—standard, soft-suspension steerable configurations.

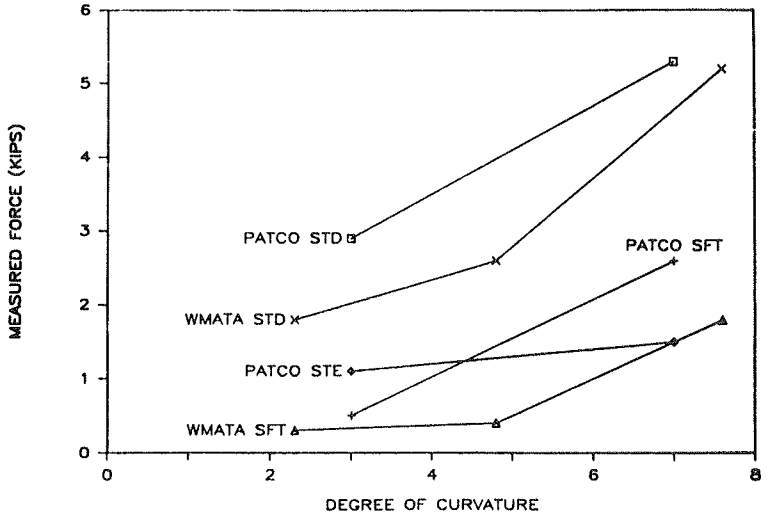

FIGURE 19 Wheel/rail force versus curvature—standard, soft-suspension steerable configurations.

and Amtrak. It is anticipated that successful fleet demonstrations will show a cost benefit if all vehicles with this type of suspension are retrofitted.

Although the steerable truck has been successfully demonstrated under revenue service at PATCO, its benefits at higher cost are not significantly better than the soft suspension configuration. No decision has been made to order more steerable trucks. It has been suggested that the true benefit of a steerable truck can best be realized on a new system specifically designed to make use of its advantages. The Vancouver/Urban Transportation Development Corporation steerable truck-equipped system should be closely monitored as an example of this condition.

REFERENCES

1. D.N. Wormley, J.K. Hedrick, and N.L. Nagurka. Stability and Curving Performance of Conventional and Advanced Rail Transit Vehicles. Report UMTA-MA-06-0025-83-10. UMTA, U.S. Department of Transportation, 1983.
2. J.A. Elkins. Wheel/Rail Force Measurements at the Washington Metropolitan Area Transit Authority--Phase II, Volume 1, Analysis Report. Report UMTA-MA-06-0025-83-1. UMTA, U.S. Department of Transportation, 1983.
3. R. Grief and H. Weinstock. Mechanics of Steady-State Curving: Relation Between Wheel-Rail Forces and Superelevation. Report 83-RT-6. ASME, New York, 1983.
4. C. Phillips, H. Weinstock, R. Grief, and W.I. Thompson. Measurement of Wheel/Rail Forces at the Washington Metropolitan Area Transit Authority--Volume 1, Analysis Report. Report UMTA-MA-06-0025-80-6. UMTA, U.S. Department of Transportation, 1980.
5. D.R. Ahlbeck, H.D. Harrison, and J.M. Trenten. Measurement of Wheel/Rail Forces at the Washington Metropolitan Area Transit Authority--Volume II, Test Report. Report UMTA-MA-06-0025-80-7. UMTA, U.S. Department of Transportation, 1980.
6. P.J. Boyd, J.P. Zaiko, and W.L. Jordon. Wheel/Rail Force Measurements at the Washington Metropolitan Area Transit Authority--Phase II, Volume II, Test Report. Report UMTA-MA-06-0025-83-2. UMTA, U.S. Department of Transportation, 1983.
7. J.A. Elkins, J. Peters, G.E. Arnold, and B.R. Raykumor. Steady State Curving and Wheel/Rail Wear Properties of a Transit Vehicle on the Tight Turn Loop. Report UMTA-CO-06-0009-83-1. UMTA, U.S. Department of Transportation, 1983.
8. J.A. Elkins and H. Weinstock. The Effect of Two Point Contact on the Curving Behavior of Railroad Vehicle. Report 82-WA/DSC-13. ASME, New York, 1982.
9. G. Mekosh. Measurement and Prediction of Wheel/Rail Forces at PATCO. Presented at 1985 Rapid Transit Conference, American Public Transit Association, Washington, D.C.

Publication of this paper sponsored by Task Force on Rail Transit System Design.

Rail Corrugation—Experience of U.S. Transit Properties

ROBERT D. HAMPTON

ABSTRACT

Rail corrugation is a common problem with all rail transit systems. Presented in this paper is information received from various U.S. transit properties in response to a questionnaire prepared on this subject and circulated in early 1985. This questionnaire requested information concerning track geometry, type of track support, and structure type where corrugation is being experienced. Information was also requested on the characteristics of rail and wheel wear as well as remedial action taken to alleviate the problem. The information received was presented at the subsequent Rail Corrugation Workshop at the June 1985 American Public Transit Association (APTA) Conference in Atlanta, Georgia. Other papers presented at this workshop discussed parameters influencing rail corrugation and current understanding of the rail corrugation phenomenon. Discussed in these papers were (a) recent studies conducted by the U.S. Department of Transportation through its Transportation Test Center at Cambridge, Massachusetts; (b) studies recently performed on the Fast Track at Pueblo, Colorado; and (c) the results of recent tests performed by the Budd Company Technical Center on the Port Authority Transit Corporation (PATCO) system at Camden, New Jersey. In summary, rail corrugation is a matter of concern for all rail properties. No rail system is immune to the corrugation problem. It was the conclusion of all participants in the rail corrugation workshop that there is a need for a more unified approach to organizing and funding a coordinated research effort to bring together the various groups currently studying the many aspects of rail wear and rail corrugation.

All operating U.S. rail transit systems have experienced problems with rail corrugation. It has been estimated that yearly maintenance dollars expended in North America for rail grinding and corrugation control exceed $1 million. Actual operation of the new rail system in Baltimore began in November 1983. It became apparent almost immediately that Baltimore was no exception because by December, rail corrugation had developed on the sharp curves in the underground section.

The immediate question was "What went wrong?" Information was requested from other rail properties and an assessment of the problem was made. (Because this assessment preceded and influenced the industry survey, the Baltimore problem will be discussed first.)

The track in the underground sections is attached to the concrete tunnel inverts by direct fixation and, in areas deemed sensitive to ground-borne vibration, by direct fixation to floating slab or Stedef two-block concrete ties, or both, supported in rubber boots. The initial corrugation was observed to develop in the sharp curves (750- to 1,000-ft radius) in the downtown section. This section contains both direct-fixation track and the Stedef two-block tie system. At that time, the corrugation was developing within the two-block tie section, but not in the adjacent direct-fixation section. This rail corrugation phenomenon has since also spread into the direct-fixation sections. Also, noticeable corrugation has developed on a section of track on a 4 percent descending grade leading inbound from the portal. This section is also located on direct-fixation track and exhibits flow of metal in the direction of travel and away from the gage-side of the track surface.

Maryland Mass Transit Administration, 300 West Lexington Street, Baltimore, Md. 21201.

Rail grinding has been employed as the only way to control the corrugation propagation in the Baltimore system. To properly control noise levels, grinding is required at frequent intervals. The criterion for grinding has been the intensity of the noise or "roar" that is developed as a train passes over a section of corrugated track. Because of restraints in scheduling grinding equipment, the frequency has been limited to three times during the 2 years of operation.

As part of the author's review of the corrugation problem in the Baltimore system, the Maryland Mass Transit Administration (MTA) prepared a questionnaire on the subject, which was sent out to 12 rail transit properties within the United States (Baltimore included). Responses were received from 11 agencies, 10 of which reported corrugation problems and associated low-frequency noise levels. One property, Boston, reported no rail corrugation problem. It is the author's understanding that some rail corrugation does occur on the Boston system. The Massachusetts Bay Transportation Authority (MBTA) does use restraining rail and rail lubrication to control rail wear, however, and this may be a factor in minimizing the rail corrugation problem.

The questionnaire requested information concerning geometry, type of track support, structure type, track gage, type of rail, and characteristics of rail and wheel wear. Information was also requested on remedial action taken. (Note that the questionnaire and a copy of all information obtained are available from the author if requested.) A summary of the responses is given in Table 1. Information was also received concerning the types and characteristics of the vehicles used on the various properties. This information requires further refinement before being incorporated into this study.

The properties did report on remedial actions taken to control rail corrugation problems. Rail

TABLE 1 Questionnaire Responses

Questionnaire Category	Number of Transit Property Responses
Track geometry (where the problem occurs)	
Tangents	6
Curves	10
Corrugation occurs on curves	
Radius under 500 ft	2
Radius under 1,200 ft	4
Radius under 2,000 ft	1
All curves	3
Low rail only	3
High rail only	1
Both rails	6
Track gage in curves	
Maximum of 4 ft 8½ in.	4
Maximum of 4 ft 8¾ in.	4
Maximum of 4 ft 9½ in.	1
Type of track support	
Wood ties on ballast	7
Concrete ties on ballast	2
Direct fixation on concrete slab	7
Dual block concrete ties on slab	3
Type of structure support	
Aerial with concrete deck	7
Aerial with open deck	5
Concrete slab on grade	7
Tie and ballast	4
Type of corrugation experienced	
Wave length <2 in.	5
Wave length 2 in. to 4 in.	2
Wave length 4 in. to 6 in.	2
Wave length >6 in.	2
Type of rail used	
100 lb	4
110 lb	1
115 lb	5
132 lb	1
Special rail in curves	
Control cooled	10
Heat treated	4
Special alloy	1
Vehicle characteristics	
Cylindrical	6
Conical	6
Significant wheel wear	6

grinding was performed by nine properties and was considered by the tenth. Frequency of grinding was from 6 to 24 months with three properties listing "occasional." Rail lubrication is utilized by all responding properties except Baltimore. Wheel modification has been employed in Washington, gage widening has been reported by San Francisco, and the use of restraining rail has been reported by Cleveland. Although many of the reported modifications were considered for other purposes, they do affect the problem of rail corrugation.

The preceding information was presented as part of a workshop on rail corrugation at the Rail Conference of the American Public Transit Association (APTA). Although it is sufficient to indicate some measure of the existing problem, it is obvious that few conclusions can be derived from these data in their present form. Three other papers were also presented for discussion at this workshop that addressed the results of other related research and recent investigation into the subject by the individual authors (1-3).

Sluz presented the results of studies performed and data collected by the Transportation Systems Center and information developed for related research studies by other investigators (1). The parameters influencing rail corrugation as defined in his paper are as follows:

- Rail hardness,
- Lubrication,
- Fastener stiffness,
- Fastener spacing,
- Truck superelevation,
- Restraining rail,
- Rail and wheel roughness, and
- Truck parameters.

In summary, the paper concludes that

> [...] it is clear that as of yet no unified hypothesis exists that can fully explain the initiation and propagation of rail corrugations although several promising theories do appear to explain at least some of the aspects of the phenomenon. In truth, there are probably a myriad of vehicle and track parameters which combine to produce corrugations. Whether corrugations appear and their severity if they do, depends upon the extent to which these parameters superimpose to exacerbate or mitigate the stresses operating on the surface of the rail.
>
> Each transit system may have its own unique conditions which lead to corrugations and in the absence of a valid general theory to help identify the particular set of parameters responsible for corrugations on its own system, may need to resort to trial and error to effect a solution. Much work has been done in this area - much more needs to be done. As a minimum, more communication among transit systems is needed to publicize what has been attempted, what has worked, and what has failed.

The research conducted by Daniels was performed at the FAST Track, in Pueblo, Colorado, and was designed to simulate the normal operation of a North American freight railroad with the objective of determining factors affecting rail corrugation growth and evaluating grinding methods to reduce corrugation growth (2). These tests have generated significant results pointing to an understanding of the corrugation phenomenon, including the effects of track vibration and wheelset/rail interaction. The report reviews specific factors such as higher-strength steel, rail lubrication, and increased wheel/rail contact areas that tend to minimize and control corrugations. Implications are discussed for track maintenance and materials.

Mekosh describes the progress being made at the Budd Company Technical Center in the area of wheel/rail dynamic simulation (3). Much of this work was started at the Technical Center during the steerable-axle truck development program and, more recently, in support of a test program that was conducted at Port Authority Transit Corporation (PATCO). The principal objectives of the recent test program were to predict and measure the wheel/rail curving forces for three distinctively different truck configurations, the standard Budd P-III truck in operation at PATCO since 1969 and referenced as the baseline for comparison, the standard P-III truck equipped with soft suspension bushings in revenue service since 1982, and the experimental steerable-axle truck also in revenue service since 1982. Budd's nonlinear rail-vehicle, dynamic simulation model is being used to simulate these force oscillations using various friction versus creepage characteristics. Listed in the paper are several preliminary conclusions that may be drawn from the present data. These conclusions are listed in part as follows:

- A lateral friction-versus-creepage characteristic that drops off after reaching a maximum value is a major contributor to computer-generated lateral force oscillations.

- The combination of the lateral stiffnesses of the track support system and the truck primary suspension affects the amplitude and frequency of the lateral force oscillations.
- Steerable-axle trucks negotiate curves essentially in the radial position, which, in turn, reduces the lateral creep force to near-zero levels.

In conclusion, rail corrugation is a matter of concern for all rail properties. Present information indicates that rail corrugation costs the American Railroad Industry an estimated $100 million annually. Annual costs to transit systems in North America for rail grinding alone exceed $1 million. No rail system is immune to the corrugation problem.

Rapid growth of rail corrugation and the demand for track maintenance are related in that both are the result of exceptionally high forces resulting from the dynamic interaction of the rail and wheels with the operation of the system. Although many factors have been identified as affecting the development of corrugation, not enough is presently understood of the interaction between these factors and the forces that create rail corrugation. Further study is needed to better understand the interaction of these many factors as a unified system so that design guidelines may be established. These guidelines will assist designers in developing criteria for the design of track systems and vehicles so that corrugation and other track wear phenomena may be minimized. This same knowledge should be beneficial in better directing maintenance action to control the problems that do develop. There is a need, however, for a more unified approach to organizing and funding a coordinated research effort to bring together the various groups currently studying the many aspects of rail wear and rail corrugation.

REFERENCES

1. A. Sluz. Short Wavelength Rail Corrugations. Transportation Systems Center, U.S. Department of Transportation, Cambridge, Mass., 1985.
2. L.E. Daniels. Overview of Factors Influencing Rail Corrugation. Transportation Test Center, Pueblo, Colo., 1985.
3. G. Mekosh. Prediction of Wheel/Rail Force Oscillations. The Budd Company Technical Center, Fort Washington, Pa., 1985.

Publication of this paper sponsored by Task Force on Rail Transit System Design.

An Assessment of Design Criteria for Continuous-Welded Rail on Elevated Transit Structures

DONALD R. AHLBECK, ANDREW KISH, and ANDREW SLUZ

ABSTRACT

For a safe, economical design, three basic problems must be addressed in the use of continuous-welded rail (CWR) on aerial structures: (a) the control of stresses in the rail caused by differential longitudinal movements between the rail and superstructure (deck, girder) attributed to temperature changes or other causes, (b) the control of rail-break gap size and the resulting loads into the superstructure caused by a pull-apart, and (c) the transfer of loads and moments from the superstructure into the substructure (i.e., columns and piers). These are conflicting design goals, however, and the ideal solution to one may worsen the problem with another. Design compromises are necessary to attain acceptable loads, component stresses, and deflections under all expected conditions. In this paper, the existing design criteria for use of CWR on elevated transit structures are reviewed and evaluated. Available literature (e.g., reports, codes, and specifications) is reviewed; and visits to five of the newer U.S. transit properties are described, discussing design philosophies, past experience, and current maintenance practices. Simple iterative computer models were developed to provide estimates of thermally induced loads into the rail and structure, and rail-gap size and loads caused by a pull-apart, as a function of nonlinear fastener characteristics and structure configuration. Results of analyses of typical transit structures employing these models are described in the paper.

As part of the technical support that the Transportation Systems Center (TSC) has provided to UMTA under the Urban Rail Rehabilitation, Construction, and Maintenance Program (UM-476), investigations have been conducted to develop safe and cost-effective means to improve the performance of elevated transit structures. The primary objectives of these investigations were to develop methods and techniques for assessing the structural integrity of transit track and elevated structures, and to determine if current design criteria, specifications, rehabilitation requirements, and maintenance practices are adequate to ensure structural integrity.

One of these investigations (1) addressed the technical and economic factors in the use of continuous-welded rail (CWR) on elevated structures. The replacement of bolted-joint rail (BJR) with CWR on elevated transit structures would reduce the maintenance and noise problems caused by wheel/rail impact loads at the rail joints. However, large variations in temperatures over daily or seasonal cycles can generate large lateral and longitudinal loads in the track because of thermal expansion or contraction. In BJR, the rail joints provide for slippage that will reduce these forces. With CWR, on the other hand, these locked-in thermal loads can damage the supporting structure if not properly handled. The older aerial track structures were not designed for CWR use, however, and the current practice of rail replacement on these older elevated structures is to continue the use of BJR. On newer elevated transit structures, CWR is more commonly used. However, the design criteria used to ensure overall structural integrity are varied, and there is a need to evaluate these criteria to determine if the resulting designs are adequate.

D.R. Ahlbeck, Battelle Columbus Division, 505 King Avenue, Columbus, Ohio 43201. A. Kish and A. Sluz, Transportation Systems Center, U.S. Department of Transportation, Kendall Square, Cambridge, Mass. 02142.

BACKGROUND

A general review of design criteria and standards for designing elevated structures for urban rail transit systems is provided in a report by Harrington (2). A major conclusion of this report was that the various criteria are similar enough that a uniform set of industry-wide standards is feasible. However, these design criteria do not explicitly address the use of CWR on elevated structures. There are no specific guidelines for rail restraint, nor established limits on the size of a rail gap that would result from a thermally induced rail break.

Current guideway design criteria also have been reviewed and compared by Dorton and Grouni (3,pp.134-144). Design methods more specific to the application of CWR to aerial transit structures are found in feasibility and design studies for the newer transit properties (4-7). Systems described in these reports range from California's Bay Area Rapid Transit (BART), the oldest of the modern U.S. transit systems (4), to the Vancouver, British Columbia, Advanced Light Rapid Transit (ALRT) system (5). A conference paper by Fox (8) discusses the design philosophy used in the Washington (D.C.) Metropolitan Area Transportation Authority (WMATA) steel bridge structures.

A recent paper prepared for the American Public Transit Association (APTA) Track Construction and Maintenance Subcommittee by Robert E. Clemons (elsewhere in this Record) specifically addresses the problems of CWR on aerial structures. In this paper (Continuous Welded Rail on BART Aerial Structures),

the concepts of direct fixation of rail to structure, the types of fasteners used, and the rail/structure interactions are discussed in detail. The three basic methods for accommodating thermally induced differential movements between rail and structure are described in this paper as follows: (a) elastic fasteners with nonslip rail clamps and rail/girder motion within the shear deflection of the fastener (used by BART); (b) elastic fasteners with controlled-slip rail clips providing elastic deformation to the longitudinal force limit of the clips [used by the Metropolitan Atlanta Rapid Transit Authority (MARTA), the Metro Dade Transportation Administration (MDTA), and the Maryland Mass Transit Administration (MTA-Baltimore)]; and (c) elastic fasteners with nonslip (or high slip-limit) rail clamps near the fixed end of each girder, and controlled-slip (low slip-limit) rail clips on the rest of the girder, where greater relative movement is expected (used by WMATA).

In summary, these reviews of current published design criteria and standards showed that the problems in the application of CWR to elevated transit structures are not specifically addressed. A review of the technical reports and design studies showed that different organizations have taken substantially different engineering approaches in handling these problems.

TRANSIT PROPERTY SITE VISITS

Five transit properties were visited during the course of this study (1) to (a) provide a firsthand look at the track and aerial structures; (b) interview system design engineers and track maintenance personnel; and (c) gather available material on design criteria, standards, and methods. These properties were as follows:

- MARTA,
- MTA-Baltimore,
- MDTA Metrorail,
- BART, and
- WMATA.

(Note that summaries of track, fastener, and aerial structure characteristics for these five systems are given in Table 1.)

The newer transit systems have followed different design philosophies in their utilization of CWR and direct-fixation (DF) fasteners on aerial structures. In an effort to control thermally induced stresses in the rail and loads into the structure, yet limit the rail-gap size in the event of a rail break, the different transit properties have used combinations of low- and high-restraint fasteners (WMATA), medium-restraint fasteners (MARTA, MDTA Metrorail, MTA-Baltimore), and high-restraint fasteners (BART).

BART has had little trouble with the high-restraint fasteners, and no evidence of excessive loads into the aerial structures. Rail gaps from the few rail breaks have been controlled to less than 1 in. WMATA, on the other hand, has experienced problems with its fasteners (9,10); and a few rail breaks have generated gap widths in excess of 6 in. Limited service experience has been accumulated on the newest systems that utilize the medium-restraint fasteners, but these fasteners have performed well to date.

EVALUATION OF CWR DESIGN CRITERIA

Three basic problems must be addressed in the design of aerial structures for use with CWR track:

1. The control of stresses in the rail attributed to differential longitudinal motions between the rail and superstructure because of temperature changes or other causes,
2. The control of rail-break gap size and resulting loads into the superstructure attributed to aerial pull-apart, and
3. The transfer of superstructure loads and moments into the substructure (e.g., piers and bents).

A solution to one of these problems may conflict with the ideal solution to another; therefore, design compromises must be made that will result in acceptable levels of component load, stress, and deflection under all expected conditions.

Longitudinal loads are developed between the CWR and the superstructure (i.e., deck and girders) of an aerial transit structure by differential movement and shear of the fasteners. Reaction loads are carried into the substructure (i.e., columns, piers, and bents) through fixed bearings and by shear or friction through expansion bearings. On curved track, lateral components of the longitudinal loads must also be reacted by the structure.

When the rail temperature drops many degrees lower than the rail neutral (stress-free) temperature, high-tensile, locked-in loads are developed. If a rail breaks, this tensile load is released. The load is distributed through rail fasteners in each direction from the point of break to points where the

TABLE 1 Track and Aerial Structure Characteristics for Representative North American Transit Systems

System	Rail Size	Rail Expansion Joints	Typical Fastener Type	Fastener Spacing (in.)	Elastomeric Pad Thickness (in.)	Rail Clip	Fastener Stiffness (kips/in.)[b] Vertical	Lateral	Longitudinal
MARTA	115 RE	None	Hixson H-10, Landis/ Pandrol, Hixson H-15 (mod)	30	3/4	Bolted clamp Spring clip Spring clip	130-300[a]	32-	10-40
MTA-Baltimore	115 RE	Special trackwork	Hixson H-15A	36	5/8	Spring clip	120-180	38-	8-50
MDTA Metrorail	115 RE	None	Landis/Pandrol	30	3/4	Spring clip	80-120	20-	10-[c]
BART	119 CF&I	None	Landis/Pandrol, Hixson	30-36	3/4	Bolted clamp	250-400[a]	24-33	18-36
WMATA	115 RE	None	Landis/Pandrol, Hixson, Lord	30	3/4	Bolted clamp	80-130	32-44	12-47

Note: PCC = precast concrete and CIPC = cast-in-place concrete; for span type: simple = single span as opposed to continuous (spans tied together) and floating = E-E/E-E bearing arrangement (see Figure 1B, righthand span); and for fastener type: nonslip = no expetted rail/fastener movement and slip = intentional (expected) rail/fastener movement.

[a] Some stiffening with age is assumed.
[b] Fastener stiffness = applied load divided by rail/baseplate relative motion in axis of load (lateral and longitudinal stiffnesses measured under vertical loading, except BART).
[c] No maximum stiffness specified.
[d] For rail stress calculations.

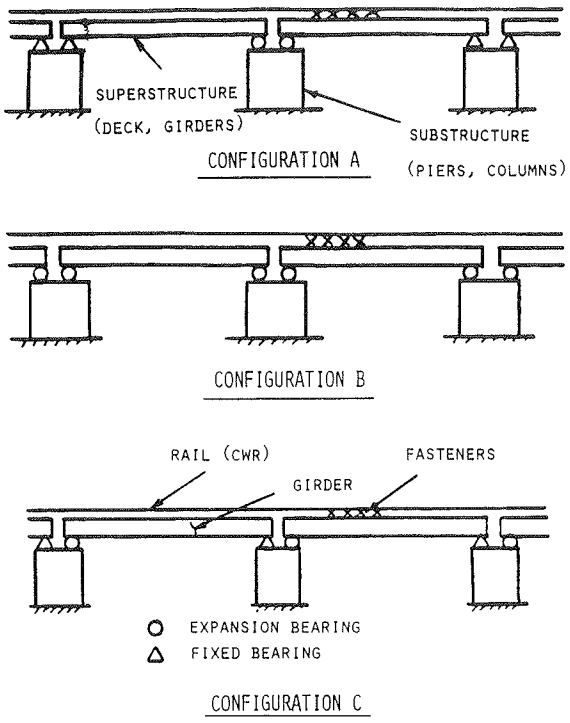

FIGURE 1 Bearing configurations for elevated structure girders.

thermal tensile load is again sustained in equilibrium.

Part of the load from a broken rail is transferred to the unbroken rail(s) of the guideway, and part is transferred to the substructure through fixed and expansion bearings. The exact magnitudes of these loads depend strongly on the substructure (bent or column) longitudinal stiffness, the structure-bearing configuration, and the rail fastener restraint characteristics.

The effects of column and girder bearing stiffnesses depend on the specific bearing configuration used in the structure. Three common configurations used with aerial transit structures are shown in Figure 1. The first of these (A) is a symmetrical arrangement common to modern transit systems such as BART. The second configuration (B), also symmetrical, is used on the level track sections of the MDTA system. The third configuration (C) is an asymmetrical arrangement commonly used on railroad and highway bridges.

Rail Stresses

An analysis of rail stresses must include contributions of vehicular and structural loads, as well as the thermally induced stresses. Current transit track design practice uses the factors recommended by the Association of American Railroads (AAR) when rail bending stress is calculated (11). Starting with the maximum bending stress under the peak expected dynamic wheel load, these factors account for contributions attributed to lateral bending, track condition, rail wear and corrosion, and unbalanced superelevation. Additional components can include

- Stress caused by acceleration or braking of vehicles,
- Stress in rail caused by bending of superstructure,
- Axial stress caused by composite-beam bending, thus inducing shear in fasteners and load into rail, and
- Stress caused by rail or structure interaction force (or both) through fasteners.

The total of these stresses plus the maximum expected temperature-induced stress is subtracted from the yield stress of the rail. This difference, reduced by a suitable factor of safety, will establish the maximum design stress resulting from differential movement between rail and superstructure. From two recent design studies (6,7), the following rail stress contributions were expected:

- Bending stress (all sources, multiplied by the factor of safety): 37 to 40 percent of yield stress;
- Thermal stress: 17 to 18 percent of yield stress; and
- Rail or structure differential movement, or both: 26 to 29 percent of yield stress.

Several methods are used to calculate the load generated in the rail by thermally induced movement of the superstructure (girders or deck). One method assumes a constant fastener restraint per unit length over the total span length. This is conservative (i.e., the calculated load is higher than the actual load), and not too inaccurate for low- to

Longitudinal Restraint Load (max., aerial, lb)		Aerial Structure Total Length	Span Length (ft)			Aerial Structure		Span Type	Rail-Laying Temperature (°F)	Expected Temperature Range (°F)	
Nonslip	Slip		Typical	Min.	Max.	Girder	Deck			Structure	Rail
10,000	2,000-3,000	4,658 (ft)	70	70	130	Steel	PCC	Floating	80		±70
–	1,200-1,600	10,500 (ft)	85	65	95	PCC unit		Simple	80		
–	1,540-2,400	20.8 (mi)	80	40	110	PCC unit		Floating	60-80	±60	±60
10,000-15,000	–	9 (mi)	70		100	PCC unit		Simple	60-80	±30	±50
7,000-10,000	250-750	3,090 (ft)	80	63	107	Steel	CIPC	Simple	55-75		-90[d]

medium-restraint fasteners. Another method assumes a linearly decreasing fastener load over the length of the span, based on fastener shear stiffness and the maximum thermal movement at the expansion end of the span. This method assumes that the fastener shear force does not exceed the slip limit force of the fastener, and is therefore accurate only for high-restraint fasteners. A much better solution is made possible by including the slip-limit force, up to the point where the linearly decreasing shear force drops below this force limit.

Over the span length of a girder, the rail is a relatively flexible element when compared with the girder itself. A small computer program was set up during this study to calculate fastener loads into the rail, assuming the rail to be a number of finite flexible elements between individual fasteners, rather than the rigid rail of the previously cited methods. An iterative solution is necessary, but the solution converges quickly (5 or 6 iterations), and the program can be run on a desk-top computer. Total loads between the rail and superstructure over one 80-ft span were calculated for three representative cases: a high-restraint fastener (BART), a medium-restraint fastener (MARTA, MDTA-Metrorail), and a low-restraint fastener (WMATA). Loads computed for a flexible rail are compared in Table 2 with loads calculated from the three cited rigid-rail methods. An important point in considering the rail flexible, however, is that the total load into the rail is distributed so that less than 70 percent of this load is reacted at the expansion end of the span at the highest-stressed point in the rail. This peak

TABLE 2 Comparison of Methods for Estimating Total Longitudinal Load Between Rail and Superstructure

	Longitudinal Loads for Different Methods (lb)			
Fastener Restraint (slip, lb)	Constant Restraint	Linearly Decreasing Shear Load	Linearly Decreasing Plus Slip	Computed (flexible rail)
High (10,000)	320,000	166,000	165,000	134,000
Medium (2,500)	80,000	166,000	70,000	67,000
Low (750)	24,000	166,000	23,000	23,000

Note: The following conditions are assumed: F--E/E--F girder bearing configuration, 60° F temperature change, and an 80-ft span length.

rail stress is a function of fastener shear stiffness: the lower the stiffness, the lower the percentage of total load (down to 50 percent) reacted by the rail at the expansion end.

Control of a Rail Break

A rail break or pull-apart will occur when the thermally induced tensile force in the rail attributed to a large drop in temperature exceeds the ultimate tensile strength of the rail. A pull-apart will most probably occur at or near an expansion joint in the superstructure (deck or girders), but the actual location of the break will be at a bad weld, rail flaw, or other weak spot.

Controlling a rail break presents two distinct problems demanding a somewhat opposite solution: (a) for safety reasons, the length of the rail-break gap must be minimized to reduce the possibility of derailment if train wheels pass over the break, and (b) the forces and moments into the superstructure attributed to the release of the locked-in thermal load must be minimized. The first requires higher fastener longitudinal restraint limits, and the second requires lower restraint limits.

The rail-break gap size is generally estimated by an equation in the form:

$$G = 2\ (X_{C1} + X_{C2} - X_{C3}) \tag{1}$$

where

$X_{C1} = P_{fns}/K_f$, the maximum longitudinal deflection of the "nonslip" fastener;
$X_{C2} = \alpha \Delta T L_s$, the nominal rail contraction;
$X_{C3} = (n_s P_{fs} + n_{ns} P_{fns}) L_s / 2 A_r E_r$, the reduction in rail contraction caused by fastener constraint;
α = coefficient of expansion, $6.5(10)^{-6}$ in./in.-°F for steel;
ΔT = temperature change, °F;
L_s = length of span (fixed to expansion point);
P_{fns} = minimum longitudinal restraint force, nonslip fastener;
P_{fs} = minimum longitudinal restraint force, controlled-slip fastener;
K_f = fastener longitudinal stiffness (lb/in.);
n_{ns} = number of nonslip fasteners in span;
n_s = number of controlled-slip fasteners in span;
A_r = cross-sectional area of rail (11.25 $in.^2$ for 115 lb/yd RE rail, the most commonly used size in U.S. systems); and
E_r = rail modulus of elasticity, $30(10)^6$ $lb/in.^2$.

A simplified form of this was used in the MDTA Metrorail design, based on a length, L, "...either side of the break over which full rail anchorage is provided...," so that

$$G = (\alpha \Delta T)^2\ A_r E_r / R_f \tag{2}$$

where R_f is the longitudinal restraint per inch of rail in pounds per inch.

To check the validity of these approximate methods, a finite-element model of the track structure was used with some typical system parameters given in Table 3. This model, called TBTRACK, has been

TABLE 3 Test Cases Run in Parameter Variation Study

Case	Stiffness (lb/in.)	Restraint (lb)	Limits (lb)	Description
1	30,000	2,500		Spring clip (MARTA, MDTA)
2	30,000	1,250		Spring clip, worn
3	10,000	1,250		Spring clip, worn
4	30,000	10,000		Bolted clamp (BART)
5	100,000	2,500		Stiff pad, spring clip
6	30,000	250	2,500	Low-slip, loose clamp
7	30,000	750	2,500	Medium slip, loose clamp
8	30,000	500	10,000	Nominal slip (WMATA)

used for several years to investigate the rail buckling phenomenon (13). The preceding equations for estimating the rail-break gap size assume linear load distributions. Results from the finite-element model, however, show the fastener load distributions to be nonlinear. Using the parameter values of Table 3, rail-break gap size for several cases as a function of temperature drops from the zero-stress (neutral) point are plotted in Figure 2.

The finite-element model is somewhat awkward and costly to run. Instead of completing the parametric study with TBTRACK, a simply iterative solution similar to that described in the previous section was developed. This model, called TRKTHRM, considers each rail element between fasteners as a spring, and

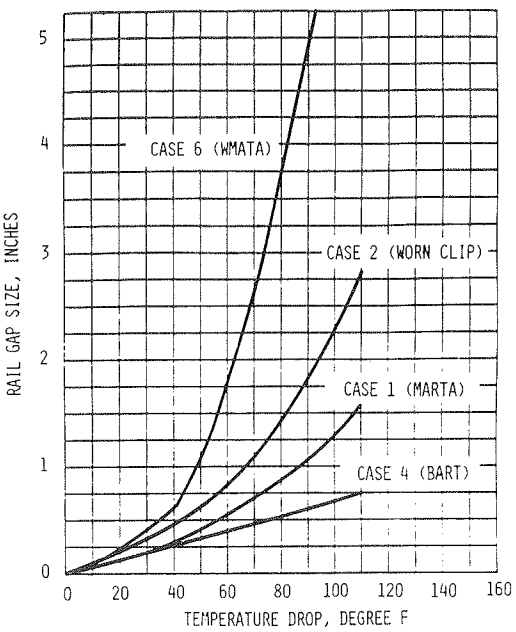

FIGURE 2 Rail-break gap size predicted by finite-element computer model.

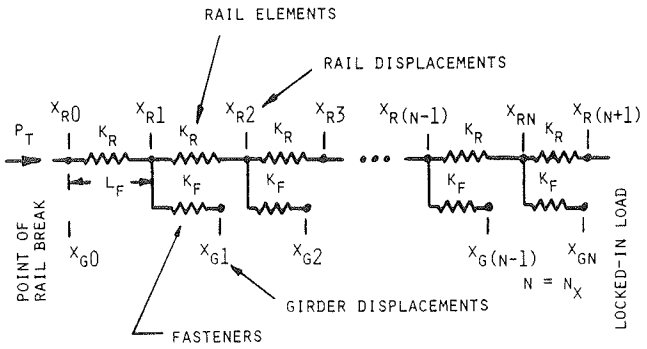

FIGURE 3 Model of broken rail on elevated transit structure.

each fastener as a bilinear spring with longitudinal slip (restraint limit). Girder displacements are inputs at one end of the fastener spring, with rail motions calculated for the other end.

Program TRKTHRM assumes that the rail breaks at the expansion joint, one spacing ahead of Fastener 1, and the locked-in thermal load must then be dissipated over an unknown number of fasteners. A first estimate of this number is calculated, just to start the iteration process. The solution moves in the appropriate direction to add or subtract fasteners until equilibrium with the locked-in load is achieved. The effects of girder contraction, which depend on the particular bearing configuration that is used (see Figure 1), are included in this model (see Figure 3).

The several methods for predicting rail-break gap size are compared in Table 4 with results from the two computer programs, TBTRACK and TRKTHRM. Note, first of all, that the finite-element model TBTRACK, with its limited number of lumped-fastener elements, tends to underestimate gap size. With medium-to-high fastener restraint, girder contraction increases gap size from 25 to 72 percent of that predicted if the girder does not contract. With low-restraint fasteners, girder contraction has little effect because movement is all in the slip zone. Equation 1 provides a reasonable estimate of gap size for medium-to-high-restraint fasteners, but badly underestimates gap size with low-restraint fasteners. Equation 2 provides a surprisingly accurate estimate in many cases, except where high-restraint fasteners are used.

Improved accuracy can be obtained with Equation 1 if the term X_{C2} is modified to use the estimated total number of fasteners over which the locked-in load is distributed so that

$$G = 2(X_{C1} + X_{C2} - X_{C3}) \quad (3)$$

where

$X_{C2} = 0.5\alpha\Delta T n_x L_s$;
$n_x = P_T/P_{fmax} = P_{fmax}K_r/2P_TK_f$;
$P_T = \alpha\Delta T A_r E_r$, the thermal load, lb;
$P_{fmax} = (n_{ns}P_{fns} + n_sP_fs)/(n_{ns} + n_s)$, the average fastener restraint limit, lb;
$K_r = A_rE_r/L_f$, the rail spring, lb/in.; and
K_f = fastener longitudinal stiffness, lb/in.

Limited data are available on rail-break gap sizes for specific fastener systems. Records of gap size and rail temperature are seldom kept. Rail breaks with high-restraint fasteners (e.g., BART and MARTA) have produced gaps of less than 1 in. The large gap sizes experienced by WMATA, on the other hand, may be induced by the dynamic stick-slip response of the rail in low-restraint fasteners.

Load Transfer Mechanisms

As discussed in the previous sections, longitudinal loads are developed between the CWR and the super-

TABLE 4 Comparison of Rail-Break Gap Size by Different Formulas

	Rail-Break Gap Size Estimates (in.)					
Case	Equation 1	Equation 2	Equation 3	TBTRACK ΔTg = 0	TRKTHRM ΔTg = 0	TRKTHRM ΔTg = 60
1	0.69	0.62	0.83	0.55	0.74	0.67
2	0.72	1.23	1.35	0.85	1.29	1.31
3	0.89	1.23	1.55	0.97	1.38	1.47
4	0.51	0.15	0.99	0.40	0.50	0.79
5	0.57	0.62	0.68		0.66	0.63
6	0.85	2.29[a]	2.47	1.77	2.39	2.68
7	0.82	1.43[a]	1.62		1.54	1.61
8	1.21	0.68	1.44		1.20	1.14

Note: ΔTg = temperature change in the girder, the girder bearing configuration = E---F/F---E/E---F, the length of the span = 80 ft, the length of the fastener = 30 in, and the temperature change in the rail = 60°F (temperature drop).

[a]Using average of Rf = $(n_sP_{fs} + n_{ns}P_{fns})/(N_s + n_{ns})$ where n_s = the number of slip fasteners, and n_{ns} = the number of nonslip fasteners.

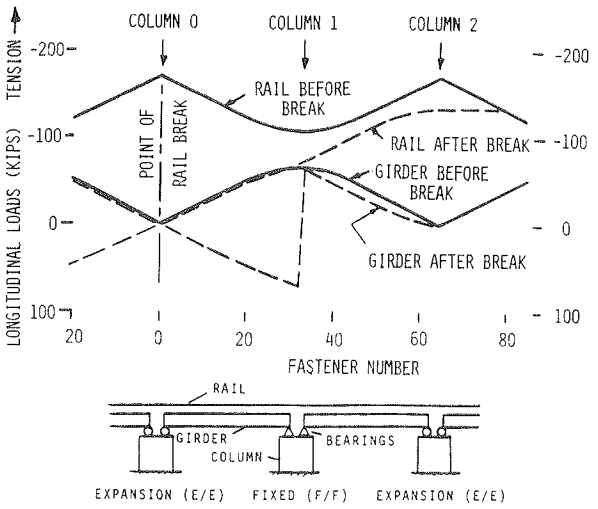

FIGURE 4 Typical force distributions on rails, girders, and columns.

structure (deck, girders) of an aerial guideway by differential movement and shear of the fasteners.

A typical axial force distribution diagram is given in Figure 4 for Case 1, the medium-restraint fastener. When a rail breaks, the substructure must then resist the unbalanced forces and moments transmitted through the girder bearings. Part of the load from the broken rail is transferred to the unbroken rail(s), and part is transferred to the substructure through fixed or expansion bearings. The exact magnitudes of these loads depend strongly on the substructure (bent or column) longitudinal stiffness, the structure bearing configuration, and the rail fastener restraint characteristics. The longitudinal stiffness of modern elevated guideway columns--depending on shape, dimensions, reinforcing steel, and, most importantly, column height--can typically range from 40,000 to 200,000 lb/in. Girder bearing stiffnesses act in series with the column stiffness, reducing the overall effective stiffness, even for fixed bearings.

An analysis of load transfer attributed to column stiffness was conducted, using an expanded version of TRKTHRM to account for the unbroken (but flexible) second rail. Results of the analysis for Case 1 (medium-restraint) and Case 4 (high-restraint) fasteners are given in Table 5. With even an effectively rigid (500,000 lb/in.) substructure, less than 40 percent of the broken-rail load on the first two girders is transferred to the column. Progressively lower loads are transferred to the columns as column stiffness decreases. Higher loads are, however, transferred to the unbroken rail, increasing the thermally induced stress in this rail and raising the possibility of a second break. Note that with high-restraint fasteners (Case 4), more load is transferred into the unbroken rail and less into the column than with medium-restraint fasteners (Case 1).

TABLE 5 Effects of Unbroken Rail and Column Longitudinal Stiffness on Loads Transferred to the Substructure

Column Stiffness (lb/in.)	Medium Restraint		High Restraint	
	Load (lb)	Gap Size (in.)	Load (lb)	Gap Size (in.)
Rigid	131,000	0.67	134,000	0.79
500,000	50,600	0.89	35,800	0.89
100,000	17,700	1.17	11,600	0.96
40,000	9,300	1.27	5,800	1.15

Note: Assuming a symmetrical girder bearing configuration of E---F/F---E/E---F, and a 60°F temperature drop.

PARAMETER VARIATION STUDIES

An analytical model was developed during this study to evaluate the more simple methods of predicting rail stresses and rail-break gap size. This program was expanded to account for structural compliances and the effects of the other, unbroken (but flexible) rails on the elevated transit structure. Basically, a relaxation method of solution is used in the model in which an initial solution based on rigid rail and structural elements is calculated, and the resulting loads are applied iteratively to the flexible elements until boundary conditions are satisfied.

An analysis of the effects of substructure (e.g., bent or column) longitudinal stiffness was conducted with the expanded model. Decreasing column stiffness was found to (a) increase rail gap size by as much as 90 percent over rigid-structure estimates, (b) increase the load transferred into the unbroken rail(s) and decrease the load transferred into the columns, and (c) increase column deflections.

A parameter variation study was then conducted to investigate the effects of different fastener stiffness and restraint characteristics using the three different girder bearing configurations of Figure 1. With unbroken rails, Configuration A (E---F/F---E/E---F) produced the highest loads into the girders and highest rail stresses, although Configuration B (E---E/E---E) produced the lowest loads and stresses. Configuration C (F---E/F---E/F---E) generally fell between the other two in load and stress magnitudes; however, because this configuration is nonsymmetrical, the girder loads are not balanced and must be reacted through the columns in bending. Reducing fastener longitudinal stiffness or slip force limit, or both, for a given configuration reduced the girder loads and rail stresses.

In the event of a rail break, girder bearing configuration was found to have little effect on the resulting rail gap size. Decreasing the fastener longitudinal stiffness or slip force limit, or both, increased the gap size, reduced load into the girder and the unbroken rail over the first girder, but increased loads transferred to subsequent girders. The asymmetric Configuration C produced the highest column bending loads on the fixed-bearing side of the rail break and these loads were substantially higher than the other two configurations for high-restraint fasteners. Configuration B, girders floating on expansion bearings, transferred the lowest loads into the columns. Configuration A transferred the least load to the girder, and more load to the unbroken rail, which was reflected in the highest unbroken rail stress of the three.

An older elevated transit structure was also modeled by the expanded computer code. This structure represented the proposed SEPTA reconstructed Frankford line with concrete deck, direct-fixation fasteners, and CWR track. The salient feature of the line is 231-ft-long girders supported on four rather compliant bent/column substructures. The proposed system will utilize high-restraint fasteners on one girder midway on a (maximum) 3,300-ft CWR string, with low-restraint fasteners used on the rest of the superstructure.

Results of this study show that the low-restraint fasteners do not adequately control the rail-break gap size. In addition, computer results showed that although rail stresses were increased as the low-restraint-fastener, slip-force limit was increased,

maximum girder longitudinal deflections were reduced, thus decreasing the loads into the columns. A medium-restraint fastener (2,500-lb slip-force limit) throughout the track structure could control the rail-break gap size and eliminate the need for rail expansion joints without producing exceptional rail stresses.

CONCLUSIONS

Current guideway design criteria were reviewed and compared in this study to assess their application to the use of CWR on elevated transit structures. The status of current design criteria and standards can be summarized as follows:

1. No specific criteria exist that govern the thermal interaction with CWR structures.
2. No technically justifiable guidelines exist for limiting the rail-gap size for rail breaks at low ambient temperatures.
3. Large variations exist in structural design methods from one transit system to another, leading to the conclusion that some systems may be overdesigned (hence cost inefficient), although others may have a lower factor of safety or (more likely) develop maintenance problems early in their lives.
4. Current methods of analysis range from simple formulas to complex finite-element models. The simpler methods are, for the most part, unreliable in predicting stresses and structural behavior critical to several major CWR-related design elements. These include (a) the control of stresses in rails attributed to thermally induced differential movements between rail and supporting structure, (b) the control of rail-break gap size and resulting loads into structures during low-temperature rail pull-apart failures, and (c) the transfer of thermally induced loads from the superstructure (deck and girder) through expansion bearings or fixed joints into the substructure (columns, piers, and foundations).
5. Decisions concerning CWR can have significant cost impacts on system construction. Based on a cost of $12 million/mi of elevated structure without CWR and thermal effects considered in the system design, the most conservative approach to design for CWR and thermal effects could increase structure costs by 23 percent. The least costly (though probably inadequate) design encountered increased structural costs by only 1 percent. Hence, a clear understanding of CWR behavior and of its implication on design criteria can substantially influence cost savings and performance.

The success of an operating system with aerial structures, DF fasteners, and CWR track is, to a large degree, a tribute to the successful application of particular design criteria. This success can be predicated to at least some degree, however, on component manufacturer, field construction and fabrication skills, and, eventually, maintenance practices. In this context, the BART track system (4) has been highly successful, and the system design criteria are therefore proven to be effective. In some features, however, the design may be overly conservative. The newer systems, such as MARTA and MDTA Metrorail, will hopefully prove to be equally as trouble-free.

ACKNOWLEDGMENTS

The authors wish to acknowledge the valuable contributions to this study by Henry G. Russell of Construction Technology Laboratories, Portland Cement Association, and Jeffrey A. Hadden of the Columbus Division, Battelle Northwest Laboratory. Thanks also to Karl Frese of Lee Wan Associates, Ed Jensen of Kaiser Transit Group, and Bertie Jackson of the Dade County Transportation Administration, as well as to the personnel of the five transit systems, for their generous assistance in this study.

REFERENCES

1. D.R. Ahlbeck, J.A. Hadden, H.G. Russell, A. Kish, and A. Sluz. CWR Design Criteria Assessment for Transit Structures. Final Report. Technical Task Directive 15. U.S. Department of Transportation, Jan. 1985.
2. B.W. Harrington, Jr. Investigation of Design Standards for Urban Rail Transit Elevated Structures. Report UMTA-GA-06-0010-81-1. UMTA, U.S. Department of Transportation, June 1981.
3. R.A. Dorton and H.N. Grouni. Review of Guideway Design Criteria in Existing Transit System Codes. ACI Journal, April 1978.
4. Rail-Structure Interaction Studies for Aerial Structures. Tudor Engineering Company, San Francisco, Calif., Nov. 1970.
5. Feasibility of Direct Track Fixation on Unballasted Structures, Appendix A: Interaction Between Rail and Structure on Unballasted Aerial Structures. De Leuw Cather and Company, Washington, D.C., March 1974.
6. Metropolitan Dade County Transportation Improvement Program Compendium of Design Criteria, Volume III--Guideways Design Criteria. Kaiser Transit Group, Miami, Fla., June 1978.
7. CWR/Aerial Structure Interface Report for Intermediate Capacity Transit Systems Vancouver ALRT Project. Parsons Brinckerhoff Centec, Vancouver, British Columbia, Canada, July 1982.
8. G.F. Fox. Design of Steel Bridges for Rapid Transit Systems. Presented at the 1982 Canadian Structural Engineering Conference.
9. P.W. Witkiewicz. A Survey of Direct Fixation Fastening Systems in North America: Existing Types and Associated Problems. Presented at 1983 Direct Fixation Fastener Workshop, Transportation Systems Center, U.S. Department of Transportation, Cambridge, Mass.
10. De Leuw, Cather and Company. Track Fasteners on the WMATA Metrorail System. Presented at 1983 Direct Fixation Fastener Workshop, Transportation Systems Center, U.S. Department of Transportation, Cambridge, Mass.
11. G.M. Magee. Calculation of Rail Bending Stress for 125 Ton Tank Car. Association of American Railroads Research Center, Chicago, Ill., April 1965.
12. W. So and G.C. Martin. Finite Element Track Buckling Model. Report T7-/RT-S. American Society of Mechanical Engineers, New York, April 1977.

Publication of this paper sponsored by Task Force on Rail Transit System Design.

Segmental Aerial Structures for Atlanta's Rail Transit System

DOUGLAS J. MANSFIELD

ABSTRACT

The typical superstructure of the aerial structure of the Metropolitan Atlanta Rapid Transit Authority (MARTA) rail transit system is a rectangular box girder supporting a concrete deck for the two parallel tracks. Alternative designs permit a steel box girder with either a precast or cast-in-place deck or a monolithic girder and deck of cast-in-place concrete. Segmental construction of the monolithic superstructure is permitted. Precast monolithic superstructure is not practical, however, because of highway load limits. On two separate projects constructed from 1982 to 1984, the contractor elected to build the monolithic superstructure by the segmental method and gained approval for a value engineering proposal to change the girder cross section from rectangular to trapezoidal and to increase its width and depth. One of the projects (on MARTA's South Line) included 65 spans with a total superstructure length of 5,231 ft and the other project (on MARTA's North Line) included 20 spans with a total length of 1,880 ft. Some property that had been acquired for the proposed parking lot for MARTA's Oakland City Station afforded the contractor a convenient site for a casting yard (within 1 mi of the centroid of the South Line aerial structure). Although the same yard was used for casting segments for the North Line aerial structure, those segments had to be hauled more than 10 mi to the erection site. The completed structures have been in service since late 1984 and represent what is believed to be the first employment of segmental construction methods for rail transit aerial structures in the United States.

Early route location studies for Atlanta's rail transit system placed considerable portions of the system in corridors occupied by existing transportation facilities such as railroads or streets, or both. In most locations, the corridor was too narrow to accommodate the rail transit system either at-grade or on conventional aerial structure.

STRUCTURE CONCEPT

The solution to the constricted corridor was an aerial structure with single-shaft piers and a single box-girder superstructure supporting a 2-track deck slab. This concept permitted the transit system to be fitted in a ground-level strip only 8 ft wide. Another advantage was that it enabled the use of a minimum-height aerial structure as follows: by supporting the tracks on the cantilevered portion of the deck slab, the transit system track profile could be set as little as 2 1/2 ft above the ceiling of the clearance envelope of the underlying street or railroad. Certainly the concept exemplified the adage that form follows function.

EARLY SUPERSTRUCTURE DESIGNS

When the design of the standard aerial structure was undertaken in 1973, the intent was to provide a single type of superstructure: a steel box girder acting compositely with deck slabs of precast, transversely pretensioned concrete. The goal of providing a family of standard designs for span lengths up to 100 ft was satisfied with a box girder that was 7 ft wide and nominally 4 ft deep. To facilitate steel fabrication, a rectangular girder cross section was chosen. Deck slab width was 30 ft 3 in. with a depth varying from 13 in. over the girder to 8 in. at the outboard edges. Composite action between the girder and the deck slabs was achieved by shear studs (or lugs) and bolted hold-downs in slab block-outs along the top flanges of the girders. Deck slabs were nominally 10 ft long, keyed together at transverse joints.

Although the single type of superstructure afforded a market for both steel and concrete, the concrete industry was not satisfied with its share. In response to its requests, alternative designs were developed as follows: (a) a cast-in-place deck slab, transversely post-tensioned; (b) precast, prestressed (pretensioned or post-tensioned), concrete box girders with precast or cast-in-place deck slabs; (c) a monolithic girder and deck of cast-in-place, post-tensioned concrete; and (d) although no design was presented, the prescription of requirements to be met if the contractor elected to build the superstructure segmentally. All alternatives preserved the superstructure cross section that was initially established to optimize the steel-and-concrete design.

EARLY SUPERSTRUCTURE CONSTRUCTION

On Projects CE125, CE130, CW560, and CW565, which were the first four construction projects to include the standard aerial structure, the contractor elected to use steel box girders and precast, pretensioned deck slabs. The box girders for all four projects were fabricated in Japan. The results would perhaps

Parsons Brinckerhoff/Tudor, P.O. Box 469, Atlanta, Ga. 30301.

have been different had current "Buy America" provisions (Federal Public Transportation Act of 1982, P.L. 97-424) been in effect, but those contracts were awarded in the mid-1970s, when American steel was rapidly increasing in price and was, at times, available only with long lead times.

DESIGN REFINEMENTS

It became evident during the late 1970s that all the design alternatives being offered were not practical. The Department of Transportation of the State of Georgia made clear that it intended to enforce the highway load limits, which restrict gross vehicular weights on the state highway system to 75 tons. As a result, the portfolio of designs was reduced by eliminating the precast concrete girder alternatives. There was some degree of discomfort with those alternatives anyway as the degree of composite action between the precast concrete girders and the precast deck slabs was based on design assumptions whose validity was made questionable by tests conducted by the Construction Technology Laboratories of the Portland Cement Association.

MONOLITHIC SUPERSTRUCTURE

Project CS310 and CS350, started in 1979, utilized a superstructure in which the girder and deck were of cast-in-place concrete, the girders post-tensioned longitudinally and the deck slabs post-tensioned transversely. Project CS520, which was started in 1984, was constructed in the same manner.

SEGMENTAL STRUCTURE

It was on two projects in the early 1980s that the segmental method was proposed for construction of the aerial structure for Atlanta's rail transit system. The two projects had some common characteristics and some differences. The most relevant common characteristics were that the two projects were to be built during the same period and that the same contractor, J. Rich Steers, Inc., was the low bidder for each. This commonality had the obvious advantage of enabling the contractor to spread over two projects the design and mobilization costs of pioneering the segmental construction method for MARTA aerial structures. Bid documents for both projects presented the design, among others, of a monolithic girder and deck of cast-in-place, post-tensioned concrete and permitted the contractor to build that structure segmentally provided that he develop and gain the engineer's approval of the segmental design and preserve the dimensions of the superstructure cross-section.

PROJECT CS360

Bids for MARTA Project CS360 were opened in August 1981. The project, which was designed by Parsons Brinckerhoff/Tudor, included the construction of 65 spans of aerial structure with span lengths between 70 and 100 ft. All spans were simply supported with expansion bearings at both ends. The total length of the superstructure is 5,231.1 ft. The aerial structure extends south from a pier, built under an earlier contract, near the intersection of West Whitehall Street and Lee Street to an abutment near the intersection of Oakland Lane and Lee Street. Its narrow corridor, bounded on the west by Lee Street and on the east by the tracks of the Atlanta & West Point Railroad, roughly parallels those two facilities. The elevation difference between finished grade and the soffit of the girders is typically about 20 ft.

The contractor retained Figg and Muller Engineers, Inc., for the preparation of the segmental design. The contractor proposed, as a value engineering change proposal, increasing the girder depth and width and sloping the girder webs 60 degrees from horizontal. The proposal was accepted, although, obviously, the girder cross section was changed. What appeared from the ground to be a 4-ft-deep by 7-ft-wide rectangle was instead a 6-ft-deep trapezoid with a bottom width of 8 ft and a top width of 14 ft 11 in. The cross section offered obvious advantages such as greater torsional stiffness, lower prestressing requirements, lower cantilever moments in the deck slab, less differential deflection of the deck slabs at girder ends, and the ability to span greater distances (the original cross section limited the span of the steel girder to 100 ft and the span of the cast-in-place monolithic concrete girder to 96 ft).

On acceptance, in principle, of the contractor's proposal, Figg and Muller proceeded with redesign. The typical interior segment was 10 ft long. The segment at each end of each span was 5 ft long, and the length of the next segment was between 2.5 ft and 7.5 ft as required to achieve the span length. Longitudinal post-tensioning tendons were encased in ducts run in the girder voids and were held down in interior segments by deviation blocks cast into the top of the bottom flange at its juncture with the girder webs. The steel sleeves in the deviation blocks and the subsequent grouting of the tendons with portland cement grout achieved bonding of the tendons to the concrete only at the locations of the deviation blocks. For purposes of determining ultimate moment capacity, the structure could therefore not be considered fully bonded. The joints between segments had multiple shear keys.

MARTA made the property acquired for the proposed parking lot for its Oakland City Station available to the contractor for use as a casting yard. Segment casting was thereby made possible within 1 mi of the erection site. Segments were match-cast by the long-line method. (Note: match-casting is the use of the end of a previously cast segment as the end form for the abutting segment; long-line casting is the use of a single bed for the sequential casting of all the segments making up one girder.) Transverse prestressing of the deck slab was achieved by pretensioning strands in a portable steel frame and then supporting the frame in position while placing the deck slab concrete. The project required 643 segments.

Segments were hauled to the erection site individually on modified dump trucks and set by crane on a pair of erection trusses temporarily supported by brackets on the aerial structure piers. The trusses, triangular in cross-section with the apex up, supported each segment by its wings. Shims and rollers between the top chord of the erection truss and the underside of the deck slab facilitated erection; the rollers enabled the segments to be set at one end of the span and winched longitudinally to their final position; the shims made it possible to adjust the vertical position of the segments preparatory to their being longitudinally post-tensioned. After post-tensioning, the girders were lowered onto their bearings and around their anchor bolts by means of hydraulic jacks between the trusses and the truss support brackets. Tendon grouting followed. When lowered, the rear of the truss was supported, through a C-frame, by a rubber wheel that ran on the top of the deck. The front of the truss was then supported

by crane, and the truss was advanced to the next pier. The contractor achieved maximum erection rates of 1 span per day and 4 spans per week.

PROJECT CN480

Bids for MARTA Project CN480 were opened in January 1982. The project, designed by Anderson-Nichols & Company, Inc., included the construction of 20 spans of aerial structure with span lengths between 75.2 and 142.7 ft. Twelve simply supported spans were under 92 ft long and therefore could have been either steel box girders with concrete deck slabs or monolithic girders and decks of cast-in-place concrete; four other simply supported spans were nominally 115 ft long and were designed as 7-ft-wide by 8-ft-deep steel box girders with cast-in-place concrete deck slabs. The four longest spans were comprised of two 2-span, continuous steel box girders with cast-in-place concrete deck slabs; box girders were 8-ft wide and 6-ft deep. The total length of superstructure is 1,879.8 ft. The aerial structure extends north from an abutment near the intersection of Burke and Canterbury Roads, runs alongside and east of the tracks of the Southern Railway, crosses over the tracks, then runs alongside and west of the tracks of the Southern Railway to an abutment near the intersection of Lenox Square Parkway and East Paces Ferry Road. The elevation difference between the existing ground line and the soffit of the girders varied widely but averaged about 30 ft.

Figg and Muller served as the contractor's engineer for preparing the segmental design for this project also. The contractor's value engineering change proposal included more than just changing the cross section of the 4-ft by 7-ft box girders, however. The contractor proposed using the section developed for Project CS360 for the entire superstructure and also proposed a reconfiguration of the continuity of the spans. As designed by the Anderson & Nichols Company, Spans 8 and 9 were a 2-span continuous girder, Spans 10 and 11 were a 2-span continuous girder, and Span 12, as well as the other 15 spans, were simply supported. The contractor proposed to build Spans 9-12 as a 4-span continuous girder and Span 8, as well as the other 15 spans, as a simply supported girder.

On acceptance, in principle, of the contractor's proposal, Figg and Muller proceeded with redesign. Much of the design done for the simple spans of Project CS360 was reusable. Like Project CS360, typical interior segments were 10-ft long, and the segment at the end of each simple span was 5-ft long. The length of the precast segment next to the end segment was between 4.4 and 7.6 ft, as required, to achieve the span length.

The 4-span continuous girder, with a total length of nearly 448 ft, necessitated additional original design effort, including consideration of the long-term moment redistribution due to creep. On top of each of the three interior piers of the 4-span, continuous structure, a 10-ft-long pier segment was created by placing a 2-ft 6-in.-long, cast-in-place segment between the 3-ft 9-in.-long end segments of the two spans. To provide a construction tolerance, a 6-in. cast-in-place closure pour was placed at each side of the three pier segments and between the first and second segments at the simply supported end of Span 9. To resist the negative moment over the interior supports, longitudinal post-tensioning tendons for the 4-span continuous girder were overlapped through the tops of the 10-ft-long pier segments at those supports.

The 223 segments for this project were cast at the yard developed by the contractor for Project CS360. The location of the erection site required that the segments be hauled more than 10 mi. The erection trusses from Project CS360 were reused although the greater span lengths necessitated intermediate supports for the trusses. The overlapping of prestressing tendons between adjacent spans of the 4-span continuous girders necessitated that the segments for those spans be erected at their final elevation rather than be lowered into place after being post-tensioned together.

PRECAST SEGMENTAL VERSUS CAST-IN-PLACE

Compared with casting the superstructure in place, the segmental construction method had the following several advantages:

1. Precasting enabled better control of the quality of both the concrete and its finish; steam curing was used, as were steel forms.
2. The requirements for falsework and elevated formwork were eliminated for Project CS360 and for the majority of the spans of Project CN480.
3. Traffic disruption in Project CS360 was reduced because of shorter occupancy times of the curb lane of Lee Street.
4. Except for the pier segments and closure pours of Project CN480, cure time for field-placed concrete did not delay post-tensioning.

No construction method is completely problem-free, however, and minor difficulties were encountered such as

1. Prediction of segment lengths required to achieve the specified girder length in the post-tensioned structure was not always accurate. As a result, slotted holes in the girder sole plates did not always align with the anchor bolts, and the width of the transverse joint in the deck between girders was not uniform.
2. Provisions were inadequate for moving the post-tensioned girders longitudinally to achieve centering over design bearing locations.
3. Minor spalling of concrete occurred at the match-cast joints during handling in the yard, transportation, and erection. Some also occurred during post-tensioning, presumably due to imperfect alignment of the segments on the erection trusses.

Available cost data for these projects in Atlanta do not make it possible to determine the cost advantage, if there is any, of building transit aerial structures by the segmental method. The MARTA contractor benefited from (a) being able to set up his casting yard on a site near one of the erection locations and (b) being the contractor for two projects built at the same time. It is the author's opinion that the cost advantages of segmental construction are not fully realized for typical transit aerial structures in an urban/suburban environment (i.e., for short spans built from 20 to 30 ft off the ground in accessible areas).

CONCLUSION

The two projects including aerial structure constructed by the segmental method were incorporated into MARTA's operating rail transit system on December 15, 1984, when the system was extended by five stations and 8.8 mi. The structures are believed to represent the first employment of this construction method for rail transit aerial structures in the United States. Subsequent utilization will therefore not be a "first" but a mere application of a technique whose practicality has been proven by the joint efforts of the MARTA, Parsons Brinckerhoff/Tudor, Figg and Muller Engineers, Inc., and J. Rich Steers, Inc.

Publication of this paper sponsored by Task Force on Rail Transit System Design.

Continuous-Welded Rail on BART Aerial Structures

ROBERT E. CLEMONS

ABSTRACT

A review and description are presented of the design approach and development of materials needed to directly attach continuous-welded rail (CWR) to prestressed concrete aerial structures on the San Francisco Bay Area Rapid Transit (BART) Project. The methods used to calculate the interaction forces and movements between the CWR and aerial structure are defined and the results are illustrated. Special designs for track crossovers and anchor abutments are described. BART's construction of 24 route miles of aerial track was the first large-scale installation of CWR directly affixed to concrete girders in North America. The design concepts and hardware developed for BART established a basis for the design of all subsequent new transit projects.

The San Francisco Bay Area Rapid Transit (BART) Project, which was authorized in 1962 and placed in systemwide operation in 1974, has been the subject of articles and discussions describing the many interesting engineering and construction issues. Few of these papers have covered issues relating to trackwork, although significant work was accomplished in such areas as direct-fixation rail fasteners, concrete cross ties, and the installation of continuous-welded rail (CWR) on aerial structures. The latter issue is (a) of continuing importance in the transit field and (b) of growing importance to railroads. It is, therefore, the subject of this paper.

Early on in the Project's design, the following three basic decisions were made that controlled track and structure design:

1. CWR would be used to the maximum extent possible to reduce track maintenance costs and to minimize noise and vibration.
2. Aerial structures would be simple-span prestressed or post-tensioned concrete girders supported on T-shaped concrete piers. A standard design would be used systemwide for (a) single grade separations longer than 200 ft (61.00 m) and (b) long viaduct-type structures, the longest of which is 10 mi (16.1 km). Ballast deck bridges would be used for all grade separations shorter than 200 ft.
3. Track construction on aerial structures would be by direct attachment of rail to concrete girders to minimize dead load, thus contributing to the aesthetics of minimium girder depth and pier diameter. In addition, the rail fastener design would incorporate sound and vibration absorption, electrical insulation, and a means for adjusting the line and grade of the track.

Individually, these requirements did not break new ground in engineering design. Knowledge and experience were available in the railroad applications of CWR, in post-tensioned concrete bridges, and in rapid-transit applications of direct-rail fastening. However, the combination of these requirements presented a challenge that few engineers had ever faced before on a domestic railroad or rapid transit project. How this challenge was met is the subject of the following sections, each of which describes a component or aspect of the track-aerial structure system.

Bechtel Civil & Minerals, Inc., P.O. Box 3965, San Francisco, Calif. 94119.

BART AERIAL STRUCTURE

The standard BART aerial structure consists of two lines of precast, post-tensioned, concrete box girders, spaced 14 ft (4.27 m) apart, and supported on 5 ft (1.525 m) hexagonal concrete T-shaped piers (1). Simple support is used for spans up to 100 ft (30.5 m) and continuous supports or composite steel girders with cast-in-place concrete deck, or both, are used for longer spans.

The standard box girder is trapezoid-shaped, 4 ft (1.22 m) deep with an overhanging deck-slab 11 ft 8 in. (3.556 m) wide to support the 5-ft 6-in. (1.6775-m) gage track. Figure 1 shows a typical girder in the casting yard. The aerial girder deck provides a

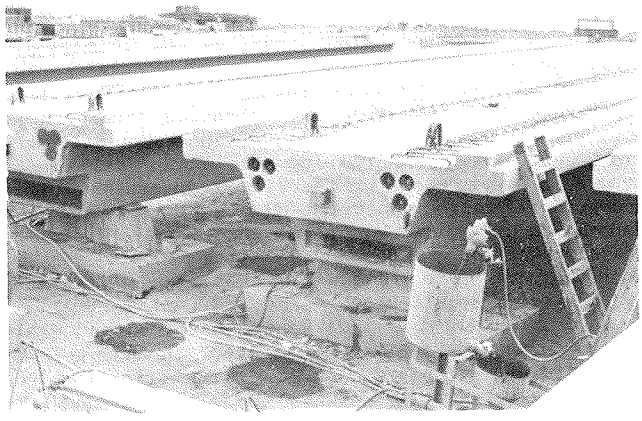

FIGURE 1 Aerial girder in casting yard in Richmond, California.

continuous, 31-in. (78.7-cm) wide by 3-in. (7.6-cm) deep block-out under each rail to receive a second pour of reinforced concrete to support the rail fasteners. Stirrups project up into each block-out on 10 in. (25.4 cm) centers to anchor the second pour concrete to the girder.

The design of aerial structure was controlled by stringent criteria covering expected loadings in the Bay area, aesthetic considerations, and BART operat-

ing requirements. Of these requirements, the following are of particular interest to the track engineer:

1. Longitudinal thermal interaction forces between the CWR and the simple-span structures were mathematically simulated and found to be significant on the first three piers from an abutment or the end of an aerial crossover. Design interaction loads of 17,000 lb (75 650 N) per rail were applied to each of these piers.
2. Girder lengths were controlled and a uniform pattern of girder fixed or free (or both) end support was adopted to minimize the relative thermal movement between the rail and structure. These requirements, along with rail fastener requirements, avoided the use of such special devices as rail-free fasteners and rail expansion joints.
3. Transverse loading due to CWR of 11,000/radius lb/ft (1 604 918 N/m) of rail was applied to all curved structures.
4. All girders were cambered to compensate for deflections due to dead and live load including impact. Actual camber values were subject to wide variations; however, the typical 70-ft (21.35-m) girder was designed for initial midspan camber of 0.23 in. (5.8 mm), which would grow to 0.56 in. (14.2 mm) over the long term. Designed live load plus impact deflection on the same girder was 0.34 in. (8.6 mm). The top of the rail was installed at the profile grade, without regard to the camber of each girder.
5. All girders were designed with notch ends to minimize the distance from the bearing surface to the top of the rail. This feature increased the stability of the girder under lateral loads and reduced the relative longitudinal push-pull movement between rail and girder due to girder end rotation produced by live-load deflection. This push-pull movement produced fatigue loading on the rail fastener and was introduced as a laboratory test requirement during the fastener development program.

RAIL FASTENER DEVELOPMENT

A BART rail fastener development program, initiated in January 1966, by the AAR Research Center, consisted of (a) a detailed investigation of existing rail fasteners to attach rail to concrete, (b) mechanical and fatigue testing of selected rail fasteners, and (c) sound and vibration studies (2). Concurrent with the effort, seven supplier firms were working on the development of new rail fasteners to meet the BART service requirements. This cooperative effort between the engineers and the suppliers provided an excellent climate for the development of rail fasteners that could (a) be manufactured at a reasonable cost and (b) satisfy BART service requirements.

All input to this program was gathered and evaluated during the first half of 1967. In August 1967, BART issued a performance-type specification for direct-fixation rail fasteners that included the following principal requirements:

1. General requirements:
   (a) Single design for all concrete trackbeds.
   (b) One-man installation.
   (c) Transverse adjustment of plus or minus 1 in. (2.5 cm) in 1/8-in. (3.2-mm) increments.
   (d) Maximum thickness of 1 1/2 in. (3.81 cm).
2. Rubber component tests in a hostile environment.
3. Laboratory test requirements:
   (a) Static longitudinal load versus deflection. The load at 0.1-in. (2.5-mm) deflection must be between 1,800 and 3,600 lb (8,000 and 16,020 N).
   (b) Static lateral versus deflection. The deflection at a lateral load of 3,000 lb (13,350 N) must not exceed 0.33 in. (8.47 mm).
   (c) Minimum direct current resistance of 100 megohms.
   (d) Minimum alternating current impedance of 10,000 ohms to frequencies between 20 Hz and 10 kHz.
   (e) Repetitive push-pull test of plus and minus 1/8 in. (3.2 mm) for 1.5 million cycles.
   (f) Repetitive tie-wear tests of a 14,500-lb (64,525-N) vertical load with a lateral load that varied from 5,000 lb (22,250 N) on the gage side to 2,600 lb (11,750 N) on the field side applied to the railhead for 3 million cycles.
   (g) Heat aging at 212°F for 70 hr before longitudinal and lateral static tests.
4. Qualification--laboratory test reports were required before production to prove conformance.
5. Quality control--additional laboratory tests were conducted at random during production to ensure quality.

Three bids were received in December 1967 ranging from $9.05 to $10.90 per fastener. However, these bids were rejected and the responsibility of furnishing rail fasteners was transferred to the track installation contractors. Using this method, the contractor would select the fastener with the lowest total cost for furnishing and installation.

The first trackwork contract was awarded in April 1968 to Dravo Corporation. The contractor elected to furnish and install the Landis fastener. This fastener was also furnished in the four subsequent trackwork contracts that were split between Dravo Corporation and the William A. Smith Contracting Company, Inc. Figure 2 shows a Landis rail fastener installed on a BART aerial structure.

The rail fastener is a sandwich-type pad consisting of a 1/4-in. (6.4-mm) thick, steel lower plate and a 1/2-in. (12.7-mm) thick, steel upper plate bonded together by a 3/4-in. (19.1-mm) thick elastomer pad. The rail is clamped to the upper plate with cast steel clips and high-strength bolts and the lower plate is anchored to the concrete deck by two 7/8-in. (22.2-mm) diameter high-strength bolts threaded into embedded inserts in the concrete. The elastometer provides electrical resistance, vertical elasticity to dampen sound and vibration, and longi-

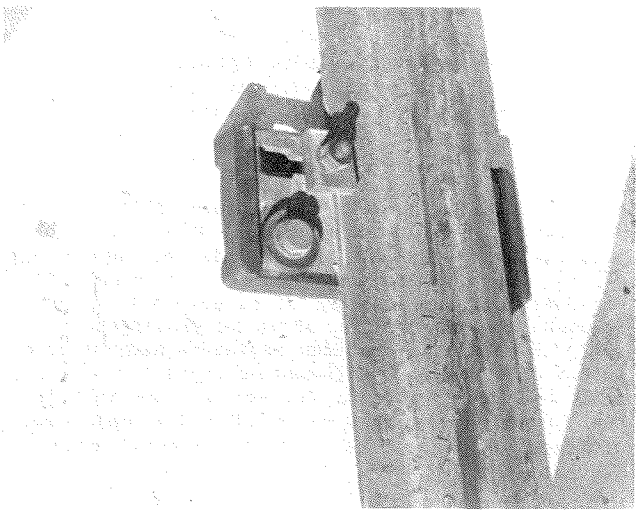

FIGURE 2 Landis rail fastener installed on BART aerial structure.

tudinal elasticity to accommodate rail structure interaction movements. Transverse elasticity is restricted because of the design of the pad. The elasticity constants of the fabricated fasteners are as follows:

1. Vertical--421 kips/in. (735,827 N/cm).
2. Longitudinal (new)--23 to 36 kips/in. (40,295 to 63,071 N/cm).
3. Longitudinal (worn)--28 kips/in. (49,055 N/cm). This spring rate is almost constant to the point of rail slip, which varies between 5 and 7 kips (22,250 and 31,150 N) of longitudinal load. These are laboratory values determined on a single fastener.
4. Maximum allowable longitudinal shear movement--1/3 in. (8.4 mm) limited by the elastomer.

AERIAL TRACK DESIGN

The concept of BART aerial track was set by two decisions described previously (i.e., the use of CWR and the direct attachment of rail to the concrete deck of simple-span, concrete girders).

Aerial track consists of three components: rails, rail fasteners, and the direct connection details. They are as follows:

1. Rails for the BART mainline are 119 lb/yd (59.24 kg/m) American Railway Engineering Association (AREA) section.
2. Rail fastener development and the selected rail fastener were described in a previous section. The adjustment features were of particular importance for rail fasteners on aerial structures. Vertical and horizontal adjustment capacity were required during construction to compensate for errors and structural tolerances, and during operation to compensate for rail wear, long-term creep in the concrete girders, and for differential settlement of the supporting piers. The rail fastener provided for lateral horizontal adjustment by moveable rail clips on a serrated base plate. Vertical adjustment was obtained by varying the 3/8-in. (9.5-mm) nominal thickness polyethylene shim installed between the rail fastener and track concrete.
3. Direct connection detail was a second pour of track concrete placed in the continuous block-outs of the aerial girders. The function of this track concrete was to transmit wheel forces to the girder; to support the rail fastener in proper elevation, cant, and superelevation; to embed the threaded anchor bolt inserts in the proper positions; and to allow for girder construction tolerances. The track concrete varied in thickness from 3.5 in. (8.9 cm) to 8.5 in. (21.6 cm) depending on the girder construction tolerances and the positive camber of the girder. The track concrete was reinforced for temperature and load distribution with three longitudinal No. 5 bars and No. 5 transverse hook bars at 12-in. (30.5-cm) centers. The specified concrete mix was similar to that used for thin precast slabs using small aggregate (-.5 in.) (-12.7 mm), high-cement content (6.5 sacks per yd^3), 3-in. (7.6-cm) average slump, and moist curing. The mix provided strength and workability for the difficult placement around forms, rail fasteners, embedded inserts, and reinforcing bars. The surface between the track concrete and the girder deck was considered a construction joint and therefore required surface preparation by sand blasting or other means. Curing by water or membrane methods was required to protect against drying on the exposed aerial girders. Figure 3 shows the jig used to form the track concrete.

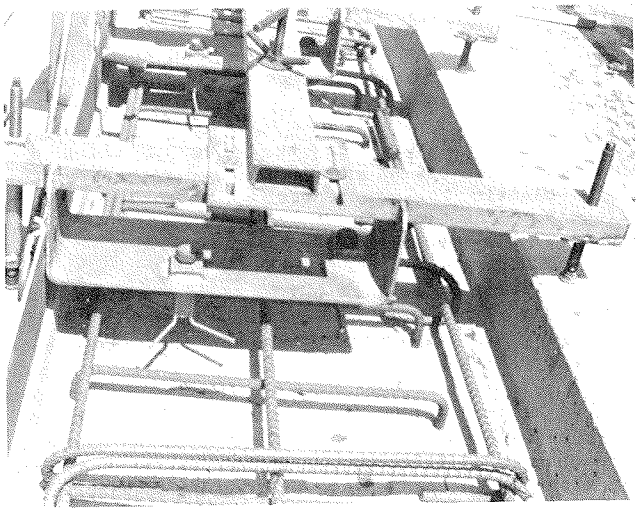

FIGURE 3 Jig used to form the track concrete.

The fastening of CWR was controlled by the specification to prevent the build-up of excess rail-structure interaction forces produced by temperature change. Rail fastener advance on each rail was staggered five girder lengths from any other rail on the same structure during periods of rapid temperature change or if the fastening operation was interrupted for 3 hr or more. No restrictions applied during a uniform rate of advance and a constant rail temperature.

The specifications required the actual rail temperature at zero thermal stress to be within ± 10°F of a temperature 10°F below the median of the long-term temperature extremes of the region. This requirement was set to protect the thermit-type rail welds from pull-apart failure, while recognizing that high-temperature sun kinks were almost impossible on aerial structures. Rail was normally laid at a temperature lower than the required range and then stretched by hydraulic rams (before field welding and fastening down) to shift the actual zero stress temperature to within the allowable range. Field records of the rail temperature and the amount stretched were used to calculate the theoretical zero stress temperature. Figure 4 shows the completed aerial track.

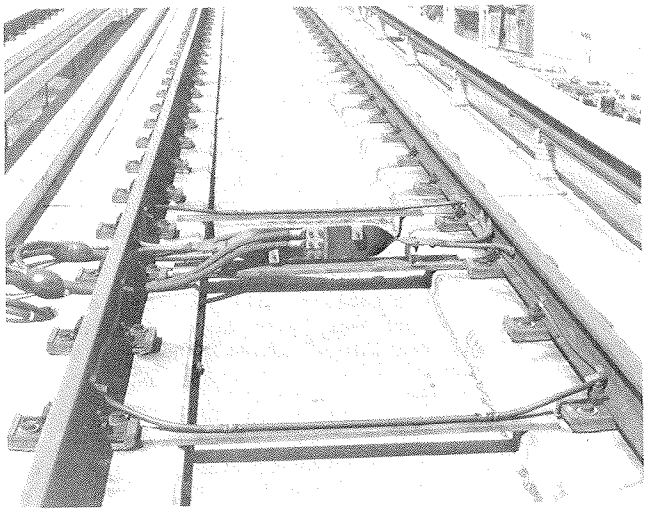

FIGURE 4 Completed aerial track.

RAIL-STRUCTURE INTERACTION

A structural system is formed when CWR track is installed on an aerial structure. The major components of this system are

1. Long, elastic CWR, the ends of which are anchored in the ballasted track beyond the abutments.
2. Elastic rail fasteners to attach the rails directly to the girders.
3. Simple-span elastic girders.
4. Elastic bearing pads.
5. Elastic piers anchored to rigid foundations.

Forces and movements between the components (called rail-structure interaction) are produced when the system is subjected to loads from its own weight, moving trains, and temperature changes. The largest loads on the system are induced by temperature changes of the components. In the San Francisco Bay area, these changes amount to plus or minus 30°F from the no-load temperature of concrete structures, and plus or minus 50°F from the no-load temperature of the rails.

Temperature changes affect the system in two ways. First, a uniform internal force is developed in the end-restrained rail in direct proportion to the temperature change. For a 50°F change in 119-lb/yd (59.24-kg/m) rail, a force of 113,200 lb (503,740 N) is developed. If the end restraint is sufficient to resist this force, the rail will not move. Note that this force exceeds the nominal 100,000-lb (445,000-N) capacity of a bolted rail joint.

Second, the change in temperature causes longitudinal expansion or contraction in each girder. This movement produces moments in the elastic rail fasteners, which, in turn, create the following:

1. A longitudinal shear movement in the elastomer of each rail fastener.
2. Longitudinal forces on the rails that produce local stretching or compressing. This situation can be demonstrated with a rubber band that is stretched to simulate the uniform internal thermal force in a rail. If a series of opposing longitudinal forces is applied to the rubber band, the original tension is locally reduced or increased depending on the placement and direction of the applied forces.
3. Longitudinal reaction forces acting on the girder are transmitted to a pier through the fixed-girder connections.

Because the major components are elastic members, the structural system can be analyzed and the interactions determined for specific loadings. The complete analysis was complex because of the large number of members, and required a high-capacity computer and program such as ICES-STRUDL.

Interaction studies on the typical BART aerial structure of 70-ft (21.35-m), simple-span concrete girders were conducted throughout the design phase. Early studies defined the basic approach to be followed throughout the structure and track design. (This approach is shown in Figure 5 with plots of relative rail and fastener forces.) Further studies were conducted to establish rail fastener criteria and to determine maximum loads and deflections in the system (2). Results of these studies are summarized as follows:

1. Longitudinal elasticity of rail fastener. The maximum modulus was set at 36,000 lb/in. (63,071 N/cm) to limit the interaction forces acting in the CWR and on the piers. The minimum modulus was set at 18,000 lb/in. (31,535 N/cm) to limit rail break gap to a target value of 1 in. (2.54 cm).

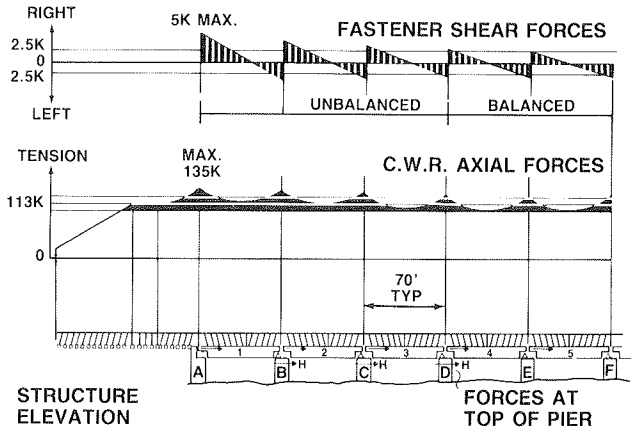

FIGURE 5 Standard aerial structure.

2. Longitudinal shear movement of rail fastener. Studies indicated that shear movements up to 0.15 in. (3.8 mm) would occur on typical systems [50-ft (21.35-m) spans] and up to 0.25 in. (6.4 mm) on special long span systems [170-ft (51.85-m) maximum spans].
3. Spacing of rail fasteners. The 36-in. (91.4-cm) spacing was determined by analysis of rail bending stresses, interaction forces on the rail and rail fasteners, and the amount of pull-apart at a weld failure. The light static wheel loads (12,500 lb) and the stiff rail (the moment of inertia is 71.4 in.^{4}) contributed to the relatively large spacing.
4. Total axial rail stress. The studies indicated locations of peak rail stress. Field welding by thermit methods was prohibited at these locations of high rail stress.
5. Interaction forces on abutments and piers. The three piers nearest an abutment and an aerial crossover were designed to withstand a longitudinal interaction force of 17,000 lb (75,650 N) per rail applied at the top of the pier. Interaction forces were not applied to standard abutments because girders were not fixed to the abutments. Exact solutions at the abutments cannot be computed because the end restraint of the CWR in crosstie and ballast track is neither elastic nor rigid and is subject to variation as a result of maintenance practices.

Additional interaction studies were conducted throughout the design phase to check special structures such as long-span girders, high piers, changes in girder support patterns, aerial crossovers, and CWR anchor abutments. As valuable as these studies were to the design of BART's structures and track, the identification and location of high-stress components is equally valuable to the BART operating staff.

AERIAL CROSSOVERS

BART operating criteria required main line crossovers to be located throughout the system to facilitate single-track operation during maintenance and emergency situations. These crossovers normally consist of two, single No. 10 crossovers between main tracks that are 14 ft (4.27 m) apart. The special work included No. 10 rail-bound manganese frogs and 19-ft 6-in. (5.948-m) curved switches. All rails and special trackwork items were connected with American Railway Engineering Association (AREA) bolted joints for ease of replacement. Five of these crossover locations are on aerial structures.

Two special problems were encountered during the

design of these aerial crossovers. The first was the method of attachment of the frog and switch to the concrete girders. Direct attachment, which was similar to the standard aerial track, was a possibility; however, this was discarded because of the lack of available hardware and service experience. Short timber ties embedded in concrete and supporting standard turn-out hardware were selected.

Special flat top girders were designed to support the crossovers. These girders were set 6 in. (15.24 cm) lower than the adjacent standard girders to accommodate the concrete-embedded short ties. In addition, a poured-in-place closure deck was constructed between each pair of girders to support the crossover track. The structural layout was designed to minimize the girder thermal movement under the switch and all bolted rail joints. Each single crossover was supported by three 76.4-ft (23.302-m) pier spans or four 57.3-ft (17.477-m) pier spans depending on local conditions.

The second special problem was how to avoid excessive rail-structure interaction forces caused by the interruption of CWR at the crossovers. Previous studies indicated that the CWR thermal and interaction forces can exceed the capacity of AREA bolted rail joints. In addition, the interruption of two or more CWR at one location caused by joint failure could overstress the aerial structure under normal Bay-area temperature changes.

The initial approach was to avoid any rail joints by welding in reinforced frogs and stock rail and by designing a structural load transfer member between the curved stock rail and the straight closure rail. This has been done successfully on British Railways (3). However, this approach was rejected because of the lack of domestic hardware and service experience.

The alternative was to solve the rail-structure interaction problem within the design of the aerial structure and avoid the use of the track components as structural members. This allowed the use of standard track hardware including bolted rail joints. This alternative was selected and the BART "tie bar" was developed.

The concept of the tie bar is quite simple. The CWR is a interrupted at the crossover and the rail ends are attached as rigidly as possible to special "AXO" girders adjacent to the outer ends of the pair of single crossovers. (The AXO girders are similar to standard girders except for the addition of embedded steel plate for the welded attachment of the tie bar.) The tie bar, a structural steel member of cross section that is equal to two rails, is located on the centerline of each track and is welded to the embedded plates on the centerline of the two AXO girders. The tie bar is approximately 550 ft (167.75 m) long and rests on Teflon bearing pads directly on the concrete deck. Figure 6 shows a tie bar installed on an aerial crossover.

During a temperature change, the thermal force built up at the end of each pair of CWR strings is transferred to an AXO girder through a group of 20 standard rail fasteners spaced at 20 in. on centers. An equal and opposite thermal force is developed in the tie bar and transferred to the AXO girder through a welded connection. Therefore, the net longitudinal thermal force on the AXO girder is zero. The CWR thermal force is directed through the tie bar instead of down into the piers where structural damage could result or into the jointed special work where track bolt damage could result.

The tie bar presented many design challenges. The location of the tie bar in the girder drainage channel required the use of rust-resistant ASTM A441 steel. The 2- by 24-in. (5.08- by 60.96-cm) cross section and the long length required many heavy butt field welds during fabrication. The operation of the tie bar in compression as well as tension, required the placement of hold-down devices every 4 ft (1.22 m) to prevent buckling during hot weather. Ideally, the tie bar should be completely free of the supporting crossover girders; therefore, low-friction Teflon bearing pads were used on all contact surfaces. Train control designers required insulated joints at each end of the tie bar to minimize interference with the control system. Finally, the 6-in. (15.24-cm) step between the deck of the AXO girder and the crossover girder required an eccentric connection.

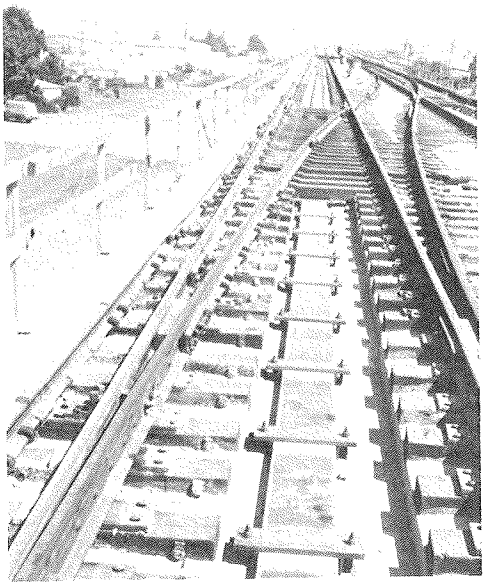

FIGURE 6 Tie bar on aerial crossover.

CONCLUSION

In summary, the BART design and construction of CWR on aerial structure has provided the following benefits:

1. A concrete aerial structure design that does not induce unacceptable local stresses in the rail.
2. A single-rail fastener design that is elastic enough to allow for relative movement between rail and structures for standard spans up to 100 ft (30.5 m) and special spans up to 160 ft (48.80 m). In addition, the fastener conforms to a number of other mechanical, electrical, and vibration absorption requirements.
3. Aerial track design, which proved to be constructible and substantial enough to withstand and distribute the imposed loads.
4. Structural crossover tie bar details that are sufficient to transmit interaction loads around the track special work and avoid overstressing the bolted rail joints.
5. Special anchor abutments that are able to withstand the full thermal and interaction loads that can be developed in the rail.

In operation for 13 years, the rail-structure system has functioned as expected and without any adverse incidents. A BART Rail Fastener Report issued in 1983 (4) indicated no failure in 10 years of service, and no deterioration of physical properties of the fasteners after 5 years of service. The latter conclusion was based on a repeat set of laboratory

qualification tests and a comparison of results between used and unused fasteners. BART's conclusion was

> ...the useful life of a BART fastener will in all likelihood not be a factor of the loads on the rail system under normal services conditions and may well depend on other conditions, such as environmental deterioration, heat, ozone, sunlight, or some unknown type of failure. However, from visual inspection and from the electrical tests, none of these factors has caused significant harm to these fasteners to date.

In conclusion, the BART challenge to install CWR on aerial structures was successfully met by a practical design that has been confirmed by 13 years of experience.

REFERENCES

1. L.W. Riggs. 27 Miles of BART Aerial Structure. Railway Track and Structures, July 1966, pp. 17-21.
2. Report of Rail-Structure Interaction Studies for Aerial Structures. Tudor Engineering Company, Nov. 1970.
3. A. Paterson. Preparing British Railways Track for High Speed Running. The Railway Gazette, June 7, 1968, pp. 413-416.
4. V.P. Mahon. BART's Experience with Direct Fixation Fasteners. Presented at the UMTA Direct Fixation Fastener Workshop, Boston, Mass., Feb. 1983.

Publication of this paper sponsored by Task Force on Rail Transit System Design.

Manufacturing, Reclamation, and Explosive Depth Hardening of Rail-Bound and Self-Guarded Manganese Frogs on the Chessie System

D. R. BATES, C. L. GOODMAN, and J. W. WINGER

ABSTRACT

Rail-bound and self-guarded manganese frogs have been used on the Chessie System for many years. For the past half-century, they have been manufactured or reclaimed at shops operated by the railroad. In May 1961, explosive depth hardening was initiated and the policy established whereby this process was applied to all rail-bound manganese frogs, self-guarded frogs, and one-piece manganese guard rails manufactured or reclaimed by the railroad. This amounts to approximately 90 percent of the systems requirements. In addition, any of these components purchased complete from outside suppliers are sent to the Chessie System and are explosive depth hardened before being put into service. Tests indicate that this process extends the service life of products manufactured from austenitic manganese steel and also acts as a quality control check on the integrity of the products exposed to this process.

In the case of rail-bound manganese frogs, the components are acquired from various sources and the finished products put together at the Chessie System plants in Martinsburg and Barboursville, West Virginia. Although the word "manufacturing" is more commonly used to describe the activity, "assembling" would be a more accurate term.

Chessie Systems Railroads, 801 Madison Avenue, P.O. Box 1800, Huntington, W. Va. 25718.

MANUFACTURING FROGS

Rail-bound manganese frogs are used primarily on heavy density lines where traffic is approximately equal on both sides of the frog. Figure 1 shows the names of detail parts of a rail-bound manganese frog per American Railway Engineering Association (AREA) Plan 690-52 in the Portfolio of Trackwork Plans. The major components are the manganese insert, wing rails, leg rails, filler blocks, and necessary high-grade bolts of sundry lengths. The inserts are purchased from various sources. Head and toe filler blocks and necessary bolts are likewise obtained

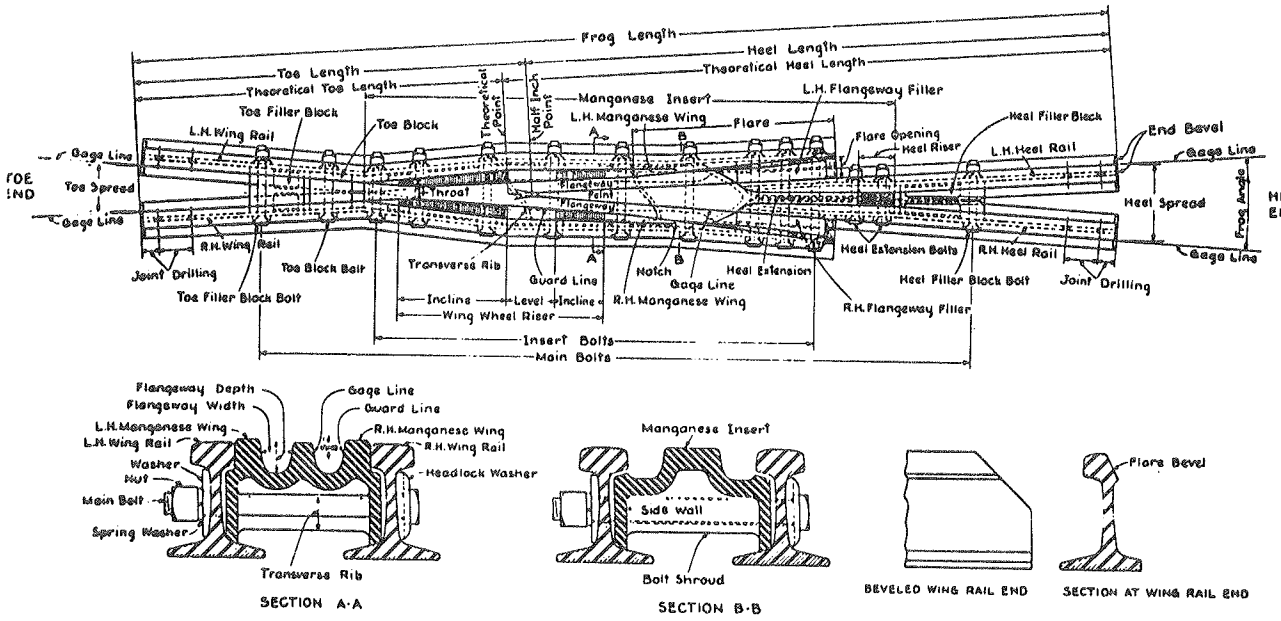

FIGURE 1 Preferred names of parts for rail-bound manganese steel frogs.

from outside sources. Wing and leg rails are manufactured from standard stock rail received from various rail rolling mills. They are cut to length, planed, drilled, heated, and bent at the shops to conform to the type of frog being made. The necessary components are brought together and assembled to form a finished frog. Tests are being conducted concerning the use of various types of fasteners. Also, epoxy glues have been used to bond the wing rails to the casting. These tests are being analyzed to determine whether the service life of the frog is extended sufficiently to justify the additional cost involved. To date, the data assembled are inconclusive. To demonstrate the magnitude of this operation, the two plants manufactured 462 new frogs in 1985.

RECLAIMED FROGS AND GUARD RAIL

As with many metallic trackwork materials, certain portions of a rail-bound manganese frog experience considerable wear while others are only slightly affected. Because of this fact, many parts of a scrapped frog are salvaged and used to produce a secondhand frog that is as good as a new one, with no limitations regarding where it may be installed.

Used frogs are shipped to the plants and inspected to ascertain their condition. Those found to have usable parts are moved into the shop for disassembly. Castings are inspected for wear and cracks. Those found sound and worthy of reuse are welded to conform to a preestablished acceptable profile. Either new or reclaimed components are used to assemble a secondhand frog. The criteria used to determine whether new or repair components are used depend on the availability of salvageable parts. Should there be a sufficient quantity of repaired or repairable parts, then reclaimed frogs will be built using such items. However, if used parts are not available, new and used components are intermingled. After assembly, the frogs are moved to a finishing location in the shops where they are ground to final tolerances and inspected for conformance with specifications.

Approximately 350 rail-bound manganese frogs are reclaimed annually. Recent economic studies indicate that this practice results in the production of a frog that has unrestricted usage for about 42 percent of the cost of a new one. (Note that there is no significant difference in service life between reclaimed and new frogs.)

Manganese Self-Guarded Frogs

Self-guarded frogs are not manufactured at the Chessie System plants. They are, however, explosive depth hardened and reconditioned. All new self-guarded frogs are given a one-shot explosive-hardening treatment before installation in the track. When a frog becomes worn beyond acceptable limits, it is removed from the track and shipped to one of the plants where its condition is inspected and a determination is made as to whether it is repairable. Usually, the worn areas are built up by welding and the missing components are replaced.

Various welding electrodes with a variety of chemical compositions are used for rebuilding. It has been determined that an electrode with an alloy content of approximately 40 percent (consisting of chromium, manganese, nickel, silicone, and carbon) will provide the best welding properties with minimum plastic deformation. Such an electrode produces tensile properties of about 130,000 psi with a 2-in. elongation of approximately 33 percent.

Surface preparation using air carbon arc or grinding, or both, is employed. When actually welding, care should be taken to minimize overheating the manganese casting. Good practice calls for applying a 500° to 600°F tempelstik to the casting adjacent to the area to be welded. When the tempelstik begins to melt, it indicates that the casting has absorbed excessive heat and the welding should be stopped until the metal cools off at that location. To continue welding the casting when the temperature exceeds these limits will result in an inferior weld that will not fuse with the parent metal and will result in premature failure.

Each used frog is evaluated and if the estimates indicate that repairing it would require in excess of 60 lb of electrode, the casting is scrapped. This is based on the fact that the cost involved exceeds the benefits. Any usable components are salvaged for use in other frogs. This is only a guideline and not a rule because other extenuating factors are given consideration.

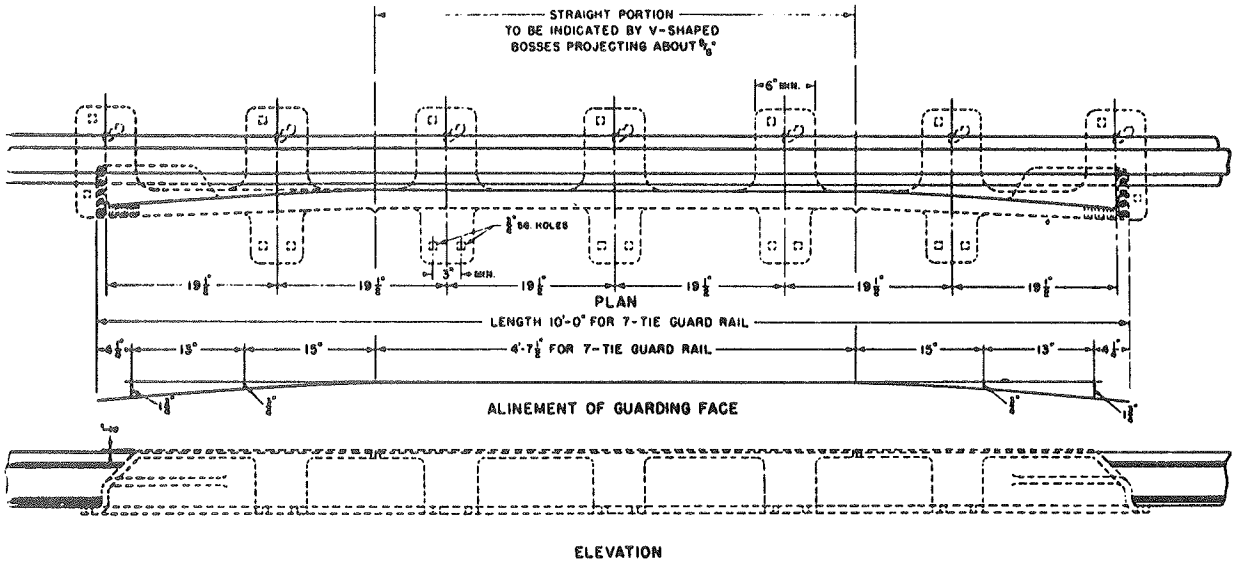

FIGURE 2 Manganese steel one-piece guard rail in accordance with AREA Plan 510-40.

Manganese One-Piece Guard Rail

Manganese one-piece guard rails are standard on the Chessie System. They are purchased from various suppliers on the basis of plans and specifications that accord with AREA Plan 510-40 (see Figure 2). The guard rail is exactly 10 ft overall and incorporates fixed tie plates, which requires spiking seven ties. As was the case with frogs, the primary wear on these components is on the guarding face. Chessie System standards dictate that new guard rail be installed with a 1 7/8-in. flange-way opening. The Guard Check Gage and Guard Face Gage allowable limits are based on the class of track involved. When the wear on the guarding face reaches the point at which it is impossible to maintain the permissible tolerances, the guard rail is removed from the track and shipped to a reclamation shop. Each item is inspected with regard to structural integrity and measurements are taken regarding physical wear. If an item is determined to be sound, the guard rail is checked for alignment and straightened if necessary and the guard face and rail seats are built up by welding. They are then ground to approximate an original "new" contour. Reclaimed guard rails are not restricted with regard to future installation. Service life is equal to that of the original product. Cost comparisons indicate that a one-piece manganese guard rail can be reconditioned to as-good-as-new condition for less than 10 percent of the initial new cost.

Manganese Crossings

Except in emergency situations, the Chessie System purchases all railroad crossings from outside sources. The corners are explosive depth hardened (two shots) at Martinsburg before installation. When rail crossings wear beyond the economical point of field welding, they are replaced and the various segments are inspected to determine if reclamation is feasible. Several factors determine whether a crossing will be repaired. The extent of wear and the characteristics of the traffic passing over the crossing are the primary factors used in making this decision. Because of the customized features of each individual crossing, few are interchangeable. Heavy-tonnage high-speed crossings are seldom reclaimed. Those in minor traffic territories are rebuilt if conditions warrant it.

Manganese steel is an extremely tough nonmagnetic alloy in which the usual hardening transformation has been suppressed by a combination of high manganese content and rapid cooling from a high temperature. The resultant steel is characterized by high tensile strength, high ductility, and superior wear resistance. It is particularly suited to railway track work components, such as frogs and crossings that are subjected to severe service of combined abrasion and heavy impact loading. Manganese steel is produced in various chemical combinations varying from 1.0 to 1.4 percent carbon and 10 to 14 percent manganese; however, Chessie System castings are purchased according to AREA specifications for special track work that conform to ASTM A-128, Standard Specification for Austenitic Manganese Steel Castings, except that the chemical properties may be modified to satisfy special situations. Manganese steel's unique ability to "work-harden" under impact loading is an extreme advantage to railway users. Hardnesses in the 550 Brinell Hardness Number range have been achieved, but because of the low yield strength of manganese steel, plastic deformation or flow will occur in isolated areas as a result of impact before surface hardening. To minimize metal flow and the resulting problems, however, it is necessary to preharden manganese steel castings before their installation. Such prehardening will retard the plastic deformation and thus provide increased service life.

EXPLOSIVE DEPTH HARDENING

Prehardening can be accomplished by hammering, pressing, or explosive depth hardening (EDH). The Chessie System has used EDH since 1961 and is convinced that it is a beneficial process. In 1956, a new type of detonating explosive was developed in the form of a flexible sheet of uniform thickness. It was safe to handle, easy to cut to any pattern to fit complex shapes, and could be attached to castings using an adhesive, thus making it adaptable to track work components.

The high-velocity hardening technique is based on an entirely different principle than the plastic deformation of cold metal using the hammering or pressing concept. The manganese steel is subjected to shock waves with extremely thin interfaces that travel through the casting at high velocities. The pressure waves set up the slip or strain lines within

the manganese steel that characterize the cold working process. Velocity impact-hardening can be carried out on practically all of the casting surfaces providing that the explosive sheet can be cut to, and shaped to fit, irregular and nonflat surfaces such as fillets and radii.

After numerous tests, it was determined that the most practical and economical procedure to follow in using this process is as follows:

One shot using a flexible plastic explosive having 0.083-in. uniform thickness and 2.0-g/in.^{2} weight. This increased the hardness of the areas subjected to the hardening to approximately 325 Brinell Hardness Number (BHN).

Others have experimented with two and three applications, which increases the hardness of the parent metal to between 350 and 390 BHN. Laboratory and field tests have shown that no more than three shots should be made on a casting. Additional attempts to further increase the hardness could result in surface fatigue in the form of microcracks and thereby defeat the benefits of the process.

An additional benefit of EDH is that as well as extending the surface life of manganese castings, it aids in locating casting defects and, as such, acts as a quality control measure.

EDH on the Chessie System is performed at Martinsburg, West Virginia. The shooting bed was fashioned from a retired building foundation in a remote location about 7 mi from the city. The pit is 15 by 40 by 8 ft deep. A 39-in. frame sits on top of the wall and supports a curtain of 1-in. rubber belting, which dampens the shock waves. The bottom of the pit has a 24-in. bed of river sand. Frogs to be shot are placed into the shooting bed using a 5-ton capacity crane mounted on a truck. The frogs are positioned on the floor of the bed so that the rail ends are free and not resting on the sand. This helps to prevent bending of the frog when detonation occurs. Next, each frog is cleaned to remove oil, grease, protective coatings, and so forth. This is accomplished by using a solvent and wire-brushing the areas involved. Moisture is removed from the frog using a propane torch. When the frog is thoroughly clean and dry, an adhesive is applied with a paintbrush.

Flexible-sheet explosives 0.083 in. thick and weighing 2.0 g/in.^{2} come in 20-in., 20-lb rolls. They are precut using templates that conform to the frog areas to be shot. The precut explosive pieces are placed on the adhesive and smoothed out so that no air bubbles exist. Also, the explosive material is extended below the top of the wear surface by at least 1 in. The entire surface to be hardened is covered with explosive material. A blasting cap is affixed in the vicinity of the point and connected to underground wires that terminate at the shooting building approximately 350 ft from the blast site. After detonation, each item that was explosive-hardened is inspected for defects, checked for hardness, and stamped to indicate the month and year the item was hardened before it is shipped and used. Extreme care is taken to ensure that all of the shooting operations are performed safely. The sheet explosive is stored in an approved magazine and a daily perpetual inventory is maintained. Detonating caps are kept separate from the explosives and stored in a bunker away from the blasting pit and explosives. Only qualified persons are permitted to perform the EDH process. They must be familiar and comply with the rules and regulations of the state of West Virginia and U.S. Bureau of Explosives.

A WORD OF CAUTION

For the past 5 years, local residents, the news media, county commissioners, and the Governor's Office have applied pressure to force relocation of the Chessie System's shooting facilities. It is a "no-win" situation. Anyone planning an explosive-hardening operation should conduct an extensive environmental impact study and obtain the necessary permits to carry out the operation before investing the required funds. The environmental aspects of the operation are becoming critical. Although seismographic measurements taken at distances of 1,500 to 3,000 ft from the shooting site indicate that the resulting vibrations and noise levels are well within safe ranges, the nuisance factor exists and must be given consideration.

TEST RESULTS

Based on previous studies, the average vertical wear in the vicinity of the point of a frog is 0.0006 ft/million gross tons (MGT) for EDH frogs and 0.002 in./MGT for nonhardened frogs. Chessie System Engineering Department Maintenance Rule 1429 requires that a slow order be placed on main-track frogs with vertical wear at the point in excess of 3/8 in. The frog should be built up by welding before the slow order is lifted. When the wear exceeds 0.5 in., the frog is taken out of service and replaced or repaired, whichever is the most practical and economical. Using the preceding figure as a basis, EDH frogs should accommodate 625 MGT before reaching the slow-order status and 833 MGT before removal. Nonhardened frogs will only sustain 187 MGT before reaching slow-order limits and 250 MGT before removal. These are only average figures and could vary considerably depending on the physical characteristics of the turn-out and maintenance practices.

CONCLUSIONS

EDH costs an average of $410 per frog. Based on an average cost of $3,000 per frog, the process increases the cost of the item by 12 percent while extending the service life from 2 to 3 times that of nonhardened frogs. It can be proven beyond a doubt that EDH is a justifiable process. For a 12 percent increase in the cost of a frog, the service life is extended 2 to 3 times, producing a 44 to 63 percent annual savings in frogs only. Other maintenance functions such as welding, surfacing, adjustment to bolts, and so forth, are likewise minimized. A reduction in the cost enhances the justification of the process, but, for this paper, it has been quantified.

There is some controversy regarding the number of shots a manganese casting should receive. Tests on the Chessie System indicate that one shot produces the desired results. Each shot adds approximately $400 to the cost of the end product. As can be seen from Figure 3, the relationship between the number of explosive applications and the wear hardness is not a straight line function. Wear occurs rapidly during the first 3 to 4 MGT. Beyond this point, the rate of wear is much less. A series of tests indicates that after 20 MGT, one-shot frogs have reached approximately 350 BHN hardness.

These results are a combination of EDH and work hardening of the wheels over the frog. Wheel work hardening is a noncost process. If manganese castings are artificially hardened to 350 BHN or greater, the work-hardening process is less efficient and the additional cost questionable.

GLOSSARY (1)

Frog--A track structure used at the intersection of two running rails to provide support for wheels and

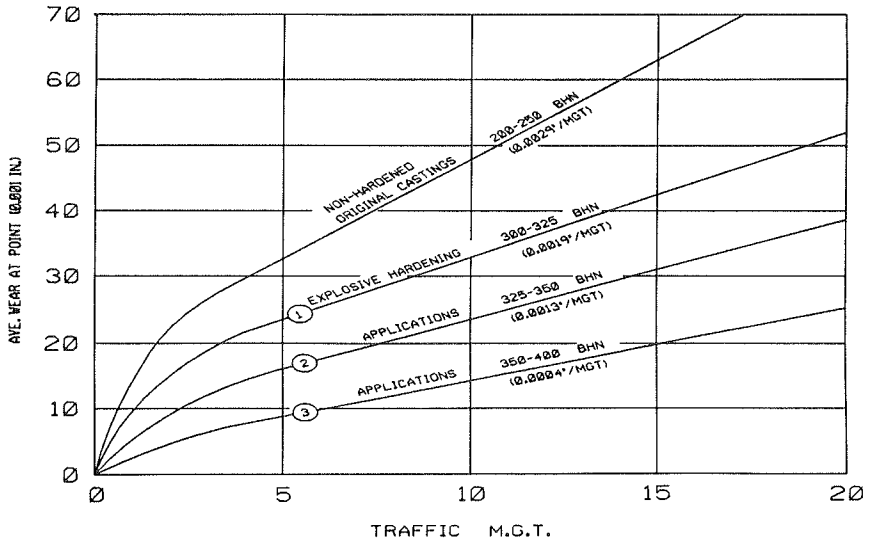

FIGURE 3 EDH/work hardening versus wear/service life.

passageways for their flanges, thus permitting the transfer of wheels from one rail to the other.

Rail-Bound Manganese Frog--A frog consisting of a cast manganese insert that is fitted into and between properly bent rolled rails and held together with bolts.

Self-Guarded Frog--A single manganese steel casting frog with guides or flanges above its running surface that contact the thread or rims of wheels for the purpose of guiding their flanges correctly past the point of the frog.

Heel End (Frog)--That end of a frog that is the farthest from the switch; or the end that has both point rails or other running surfaces between the gage lines.

Toe end (Frog)--That end of a frog that is nearer the switch or the end that has both gage lines between the wing rails or other running surfaces.

Frog Point (Frog)--That part of a frog lying between the gage lines extending from their intersection toward the toe end.

Half Inch--A point located at a distance from the theoretical point toward the heel.

Guard Check Gage--The distance between the gage line of a frog to the guard line of its guard rail or guarding face, measured across the track at right angles to the gage line at a point 5/8 in. below the top of the head of the running rail.

Guard Face Gage--The distance between guard lines measured across the track at right angles to the gage line.

Guard Rail--A rail or other structure laid parallel with the running rails of a track to hold wheels in correct alignment to prevent their flanges from striking the points of turnouts, or crossing frogs, or the points of switches.

Alloy Steel--Steel containing more than 1.65 percent manganese or more than 0.60 percent silicon or other elements added for the purpose of modifying or improving the mechanical or physical properties normally possessed by plain carbon steel.

REFERENCE

1. The Track Cyclopedia. Simmons-Boardman Publishing Co., Omaha, Neb., 1985.

Publication of this paper sponsored by Committee on Railroad Track Structure System Design.

Manganese Steel Castings: New Technology for Welding Frogs to Rail

M. BARTOLI and M. DIGIOIA

ABSTRACT

Manganese steel frogs are normally connected to rails with the use of bolted fishplates because of the inability to weld the frog directly to the rail (as is normally done when connecting rails to each other). Described in this paper is a new process that makes the frog-to-rail connection possible by inserting an adapter casting that is flash-butt welded, first to the frog and then to the carbon-steel rail, thus eliminating the mechanical discontinuity between the parts to be connected. The chemical composition of the adapter casting is such that it can withstand, without embrittlement, the welding thermal cycle of the austenitic manganese steel of the frog and that of the carbon steel of the rail. In addition, it can undergo work hardening either before or after the installation, with a hardness between that of the frog and that of the rail. Unlike previously proposed techniques, this new process does away with the local deformation of the rail where the adapter is installed, which is a source of problems to the track and rolling equipment. Test sections of the proposed material have been flash-butt welded to both frog and rail ends with highly successful results.

Austenitic manganese steel has the well-known property of work hardening under repeated impact or other mechanical loading. Surface hardnesses of from 500 to 550 Brinell Hardness Number (BNH), depending on the carbon content, may be achieved while maintaining the typical toughness of the austenitic structure in areas away from the surface. For these reasons, austenitic manganese steel is widely employed as wear-resistant material under heavy-impact loading conditions.

Frogs for railway switches are often provided as austenitic manganese steel castings with a solution heat treatment. This heat treatment is necessary to eliminate embrittled precipitated carbides in the grain boundaries and the acicular carbides within the grains that developed during the slow cooling through the critical range of 800°C to 300°C following the pouring of the casting. A general relationship of the increase in brittleness of austenitic manganese steel versus the time-at-temperature is shown in Figure 1.

It is for this reason that manganese steel is not employed in services for which temperatures over 260°C are expected. Welding, therefore, is usually considered to be a hazardous operation with manganese steel and particularly so when extreme precautions are not taken to maintain a cold-welding procedure (1).

As a result, austenitic manganese steel frogs are normally connected to rails by the use of bolted fishplates for the preceding reasons. This causes a discontinuity at the frog-rail interface, which, in turn, results in increased wear of both the track and car wheels, especially on high speed railways.

The direct weld connection between manganese frogs and carbon steel rails cannot be carried out with the usual welding processes (e.g., thermit welding, shielded manual arc welding, etc.) nor with relatively modern processes such as flash-butt welding, which is widely employed in railway track applications.

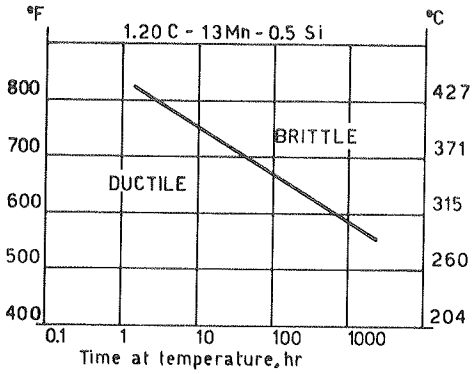

FIGURE 1 Time-temperature relationship for embrittlement of austenitic maganese steel.

This is due to the metallurgical incompatibility of the two steels. Rail carbon steel requires a slow cooling from the welding temperature to avoid brittle microstructures, while a slow cooling would produce serious amounts of carbide precipitation in austenitic manganese steel. Numerous unsuccessful methods, including other adapter designs, have been proposed to resolve the problem of joining the dissimilar steel components together. They all differ, however, as to the technique to be used to connect the adapter to the frog and rail, and as to the size and structure of the adapter itself. The following considerations should be taken into account in order to obtain the most reliable connection:

1. Material for the Adapter
   - The adapter must be of a quality that will enable it not to embrittle after welding, whether cooled rapidly or slowly.

Breda Fucine Meridionali, Via T. Columbo 7, 70100 Bari, Italy.

• It must be able to work harden under repeated impact loading, so as to present a hardness intermediate between the materials it connects.

2. Dimensions and Shape of the Adapter

• Because the material components of the adapter are the most costly of all those under consideration, owing to their special properties, the adapter must be as short as possible. However, it must be long enough to ensure that neither of the two welds will have any thermal effect on the other.

• Because the frog/adapter/rail connection is essentially subjected to fatigue loading in service, the transverse cross section should have a profile similar to that of the rail to avoid stress concentrations resulting from sudden changes in shape.

3. Welding Characteristics

• Flash-butt welding is the most suitable procedure for this kind of application because of its rapidity, quality, reliability, and consistency, as well as the capability it offers to control the supply of heat and limit it to a restricted area.

• The utilization of this procedure permits butt welds without special and costly preparations on the end faces to be welded. For all the foregoing reasons, flash-butt welding is widely used in the railway industry to connect rails to each other.

PROPOSED TECHNOLOGY

In accordance with the preceding considerations, the technology that the authors propose for connecting frogs to rails involves the following steps:

1. The redesign of the frog end to obtain a transverse section with a profile similar to that of the rail so that it can be flash-butt welded to the adapter. It should be noted in this regard that frogs designed by Breda Fucine Meridionali and used on the Italian railway network already have end sections with a profile that is similar to that of a rail, as shown in Figure 2. In order to be able to use the proposed technology for the "self-guarded" frogs designed in accordance with the American Railway Engineering Association (AREA) rules, it may be necessary to make some design changes, as schematically shown in Figures 3 and 4.

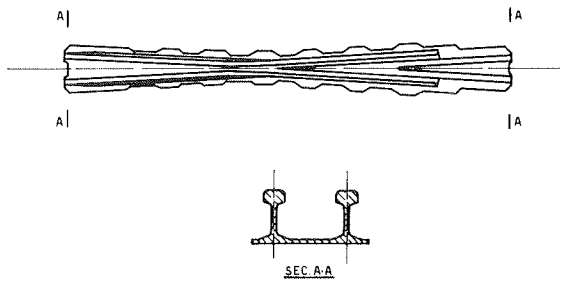

FIGURE 2 Italian railway frog.

FIGURE 3 Self-guarded frog in accordance with AREA rules.

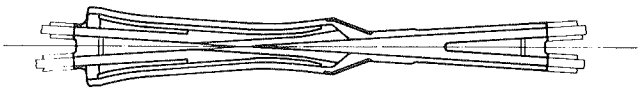

FIGURE 4 "Modified" self-guarded frog.

2. The production of an adapter, also with a profile similar to that of a rail, and with a length of between 100 and 200 mm. This length represents, in fact, a compromise between the two diverging requirements as to limiting the cost of the materials and allowing for sufficient distance between the two welds to avoid thermal effects of one weld on the other.

3. The use of the flash-butt welding technique for the joining of the adapters to the frog ends and rail ends. This will successively allow one to employ technology and equipment now used by the railroads.

4. The control of heat input, flash fumes, and quenching rate are important for successful frog-to-adapter welds as is the controlled cooling rate following the welding of the adapter-to-rail joint.

EXPERIMENTAL RESULTS

To verify the validity of the proposed technology, a set of test samples and rail pieces, outlined in accordance with Union Internationale des Chemins de Fer 60 (UIC60), was prepared for the following materials:

1. Austenitic manganese cast steel, in the solution heat-treated condition, representative of the manganese frog;
2. Carbon steel for the rails, in an as-rolled condition;
3. High-alloy cast steel for the adapter, in a solution heat-treated condition.

All these samples have been flash-butt welded to each other under different conditions, with results that can be described as follows:

1. Base Material Properties. In Table 1, the main physical, chemical, metallurgical, and mechanical properties are summarized for the three types of materials. These properties have been obtained from samples A and C in a solution heat-treated condition with water cooling from 1100°C, and in an as-rolled condition for the rail, steel sample B.

2. Properties of the Weld Between A and C. For the purposes of determining the properties of this weld, samples were used that had square cross sections with 22 mm per side. These were flash-butt welded and cooled with water.

Bend tests, as identified by ASTM specification A 128, were made using a load perpendicular to the weld. In addition, impact tests on Masnager K-type specimens with a 2-mm U-notch on the fusion line as well as tensile tests of round specimens with welds at the center of the gage length were used for the evaluation. The results of the tests are given in Table 2 and are from specimens in an as-welded condition.

With respect to the base materials, the tensile test confirms that the weld does not diminish these mechanical properties. In fact, the tensile test fractures occurred in the C-type material at slightly higher ultimate values than were obtained from the unwelded C material without affecting the weld itself. The impact test values in the fusion zone were lower than those of the two base materials (A and C)

TABLE 1 Base Material Properties at Room Temperature

Material	Chemical Composition (%)		Mechanical Properties: Yield Strength [0.2% offset, in MPa (Ksi)]	Tensile Strength [MPa (Ksi)]	Elongation (%)	Impact K [J/cm^2 (ft lb)]	Bend (α°)	Hardness (BHN)
Type A (frog)	C	1.20						
	Mn	13.00	360	730	40	230	180	215
	Si	0.40	(52.2)	(105.8)		(136)		
Type B (rail)	C	0.45						
	Mn	1.00	540	780	18	35	80	220
	Si	0.20	(78.4)	(113.0)		(20.7)		
Type C (adapter)	C	0.15						
	Mn	6.00	295	575	50	150	180	190
	Si	1.80	(42.8)	(83.3)		(88.5)		
	Cr	23.00						
	Ni	13.00						

Note: C = carbon, Mn = manganese, Si = silicon, Cr = chromium, and Ni = nickel.

TABLE 2 Mechanical Properties at Room Temperature

Weld Type	Tensile Test: Yield Strength [0.2% offset, in MPa (Ksi)]	Tensile Strength [MPa (Ksi)]	Elongation (%)	Failure Location	Impact K [J/cm^2 (ft lb)]	Bend (α°)
A-C	310 (44.9)	580 (84.0)	42	Failed in C material	80 (47.2)	80
B-C	290 (42.1)	580 (84.0)	38	Failed in C material	30 (17.7)	80

connected together; however, the results were still significantly higher than those of the base rail material. The bend test, however, during which the first cracks appeared at approximately 80 degrees, showed that the fracture presented totally ductile features.

Rotating fatigue tests were also carried out in accordance with (DIN) Specification 50113. The results indicated a fatigue limit exceeding 220 N/mm^2. All specimens had the weld at the center of their gage length and broke in the C-type material at distances greater than 10 mm from the fusion line, thus indicating that the weld performed well when subjected to fatigue.

The research was completed with a microscopic examination that showed a negligible amount of carbide precipitation at the grain boundaries and within the grains of the austenitic manganese steel. An increase in carbide precipitation occurred on the C material side of the weld between the A and the C materials (Figure 5). This latter precipitation is the result of the significant difference between the carbon contents of the two materials, and, as the results of the tests clearly demonstrate, does not cause a reduction in the property values of the weld. On the contrary, a series of tests performed on specimens that were solution heat-treated after welding showed a drop in the impact properties, with average values of only 4 J/cm^2, notwithstanding the microscopic study, which showed an absence of the carbide precipitation line.

3. Properties of the Weld Between B and C. Similar to the tests performed on the weld joining materials A and C, a second series of tests was carried out on specimens obtained by flash-butt welding material B with material C and controlling the post-weld cooling by sending current impulses through the joint. The results of these tests are summarized in Table 2.

This weld also shows mechanical properties comparable to those of the materials welded: the bend and impact test values are influenced by the carbon steel properties of the rail. During the course of the bend test, the fracture of the B-C joint started after approximately 80 degrees and involved only material B, without affecting the fusion area.

The rotating bend fatigue tests confirmed the results obtained on the weld linking materials A and C. The microscopic study revealed an absence of brittle structures on the carbon steel rail side of the weld.

4. Weld between Rail Specimens with an Outline in Accordance with UIC60 and Materials A, B, and C.

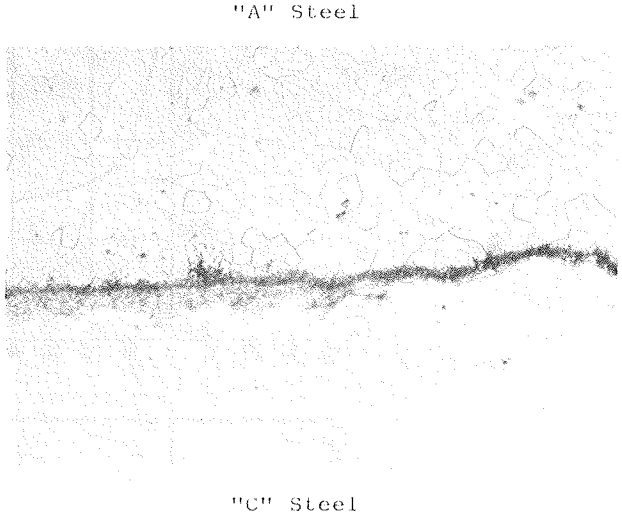

FIGURE 5 Micrography of A-C welding (75x).

For the purposes of verifying the effectiveness of the technology proposed in the present paper, studies on the small samples were followed with tests on welds connecting specimens of rail having an outline conforming with UIC60.

Bend Tests

These bend tests were performed in accordance with the provisions of the Italian Railway Rules to verify the quality of the flash-butt weld between the rails. The values of the resulting deflection, measured over a length of 1 m and obtained before cracks began to appear on the flange, were (a) weld between A and C materials: $\geq$ 60 mm; and (b) weld between B and C materials: $\geq$ 40 mm. (It must be noted, however, that the minimum deflection value required for the acceptance of flash-butt welds between rails is 25 mm.)

Plain Pulsating Bending Fatigue Tests

Two plain pulsating bending fatigue tests were performed in accordance with the loading configuration reproduced in Figure 6, using a load varying from 30 to 300 kN to verify the manner in which the proposed procedure reacted to fatigue.

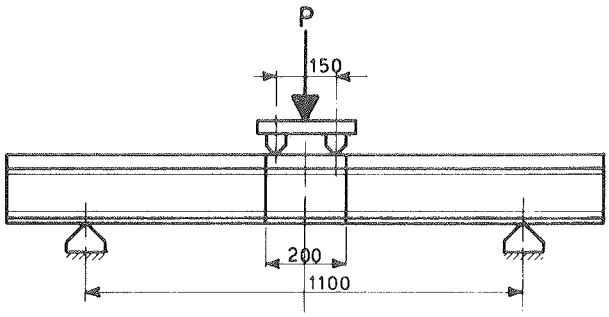

FIGURE 6 Fatigue test configuration.

The two joints presented a fracture initiation after 1.5×10^6 and 2.5×10^6 cycles, respectively; in both cases, the fracture occurred at approximately 10 mm from the fusion line of the A-type material, which simulated the frog cast in manganese steel.

This result, considering also the rotating bending fatigue tests carried out on specimens and previously described, leads the authors to attribute the cause of the fracture to defects already existing in the manganese steel, and not to weakness factors induced by the weld itself. This was also confirmed by the results of a fractometric and microscopic study done on the fracture face. The propagation of the fracture occurred slowly, an indication of the toughness of the joint structure.

Verification of the Size Effect

Samples were taken from the weld zone of actual rail specimens for tensile, impact, bending, and rotating bending tests. The results of these tests confirmed the data obtained from the tests described previously.

Verification of the Work Hardening of Material C

As stated earlier, a primary goal of the proposed technology lies in the ability of the adapter to harden on impact loading, or to undergo prework hardening before installation when subjected to one of the techniques usually adopted for austenitic manganese steel. Also, it is necessary for the adapter to have a hardness intermediate between that of the cross-frog and that of the rail.

TABLE 3 Surface Hardness After Explosion

Material	No Shot (BHN)	One Shot (BHN)	Two Shots (BHN)	Three Shots (BHN)
Type A	215	315	352	388
Type C	190	225	245	265

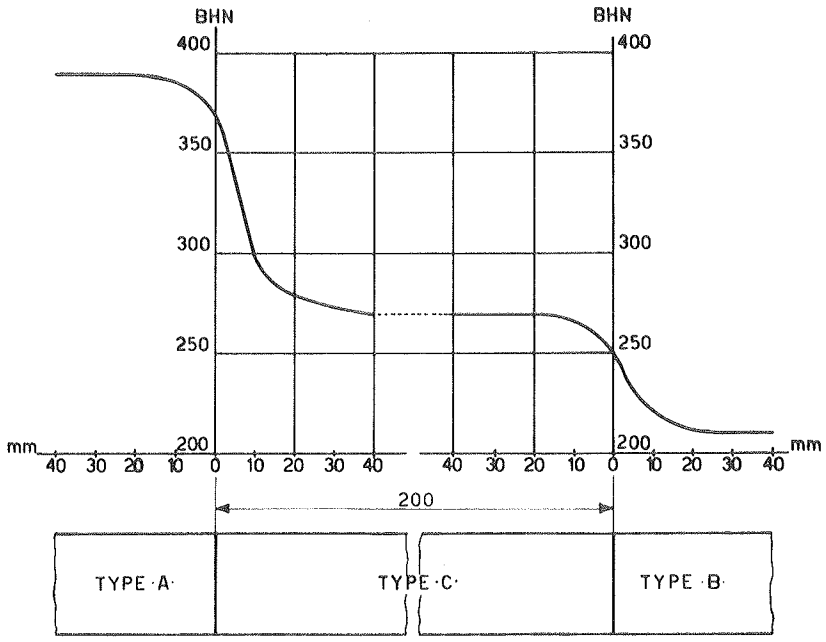

FIGURE 7 Hardness trend after explosion hardening.

Because data relative to parts already in service were not available, explosion hardening tests were performed to verify the soundness of the preceding affirmations. The results obtained on the A- and C-type steels are summarized in Table 3.

The extent to which the C material of the adapter will harden varies from 190 BHN for the solution heat-treated material to 265 BHN after three explosions. As expected, it thus presents a hardness that is intermediate between the hardened cross-frog and that of the rail.

Figure 7 schematically shows the hardness trend close to the two welds and along the adapter.

It must be noted that a special microscopic study showed that the hardening of the adapter must be traced back not so much to sliding planes, as occurs in austenitic manganese steel, but to the fragmentation of large austenite grains into smaller and more numerous ones.

CONCLUSIONS

A new technology has been presented in this paper that permits the connection of the manganese frog to the rail without mechanical discontinuities, and that overcomes limitations arising from other similar proposals. In addition, a series of successful results has been presented from tests performed at Breda Fucine Meridionali on flash-butt welds between experimental samples and between specimens of actual track materials.

The results obtained allow the authors to affirm that the proposed process is extremely reliable and has met all of the initial objectives. Other materials, also patented in Italy, are presently being tested at the authors' plant in Bari.

REFERENCE

1. M. Bartoli. Welding Filler Metal (Materiale d'apporto nella saldatura). Il Gionale dell'Officina, No. 3, Milan, Italy, March 1985.

Publication of this paper sponsored by Committee on Railroad Track Structure System Design.

Evolution of the Rail-Bound Manganese Frog

E. E. FRANK

ABSTRACT

During the 19th century, the railroad frog was fabricated from standard carbon steel rail. During this period, there were many designs for the rigid frog from riveted plate frogs to the current AREA standard rigid frog. In the late 1800s, however, R.A. Hadfield of England developed "Hadfield Manganese Steel." The unusual properties of this manganese steel, as well as its toughness and ability to withstand severe impacts, made it most suitable for railroad service. The first manganese steel castings were made for street railway frogs. The success of manganese steel in the street railway castings led to its use in steam railway special work frogs, crossings, and switches. By the first decade of the 20th century, the rail-bound frog was introduced to the American railroads. Since then, the rail-bound manganese frog has progressed through many design improvements. Currently, there are new designs being developed to meet the needs of the heavy-haul railroad.

The rail-bound manganese frog evolved from the need to greatly improve the life of the rail-built frog, which was the standard frog used during the 19th century. During this period, the rail-built frog was manufactured from Bessemer steel in a variety of designs (i.e., riveted plate rigid frogs, clamp-type rigid frogs, bolted rigid frogs with cast iron fillers, and, in later years, with rolled steel fillers).

Abex Corporation, Railroad Products Group, Trackwork Division, 200 South Michigan Avenue, Chicago, Ill. 60604.

MANGANESE STEEL IN SPECIAL TRACKWORK

During this era, Bessemer rail-built frogs installed in severe locations would last on the average of 3 months. The industry recognized that the Bessemer rail-built frog was a high-maintenance, high-cost track component, and that a product having both

longer life and improved economics was required. At the present time, the rail-built frog is still being manufactured and installed in accordance with AREA recommended practice in yards and industry tracks where traffic is light.

In the late 1800s R.A. Hadfield of Sheffield, England, developed "Hadfield Manganese Steel." The unusual properties of this manganese steel, toughness, hardness, and ability to withstand severe impacts, made it most suitable for railroad service.

The Taylor Iron and Steel Company of High Bridge, New Jersey, in cooperation with Hadfield secured this new development for use in the United States. Hadfield manganese steel was first introduced in the 1890s for use in manufacturing car wheels.

It was not long, however, before it was realized that manganese steel was not suited for this application. When manganese wheels were used in railroad service, the wheel tread developed corrugations and excessive flow was experienced during the work-hardening period. Shortly thereafter, it was learned that manganese steel, which was a failure for steam railroad car wheels, was a great success for special trackwork over which the car wheels ran.

When the street railways supplanted the horse-drawn cars with electric cars, the heavier wheel loads proved to be quite destructive to frogs and crossings then in use. The necessity to improve the designs in the areas of greater wear in trackwork components became evident. It was apparent that the structures would have to be renewable, or durable, or both.

The manufacturers of special trackwork components worked on a solution to this problem. The solution seemed to be a replaceable manganese insert casting known at the time as "Hard Center Work." Designs for the application of a manganese insert casting were developed and a frog with a manganese steel center plate was manufactured and installed on the Atlantic Avenue Railroad in Brooklyn, New York, in 1894. The design furnished is shown in Figure 1. This design utilized lugs cast on the underside of the cast center plate for locking the insert in the frog body.

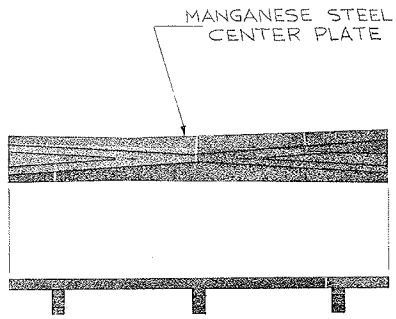

FIGURE 1 First manganese steel insert casting used in special trackwork—installed in 1894.

That year several installations were made on electric railways using manganese steel for various trackwork components. The expectations for the superiority of manganese steel for special trackwork castings were more than fulfilled by the results received from these test installations. Shortly thereafter, special trackwork components using manganese steel were developed for the electric railways (e.g., frogs, tongue switches, and mates) in both hard center designs and solid construction. The typical hard center frog design used by the electric railways throughout the United States and Canada during the 20th century is shown in Figure 2.

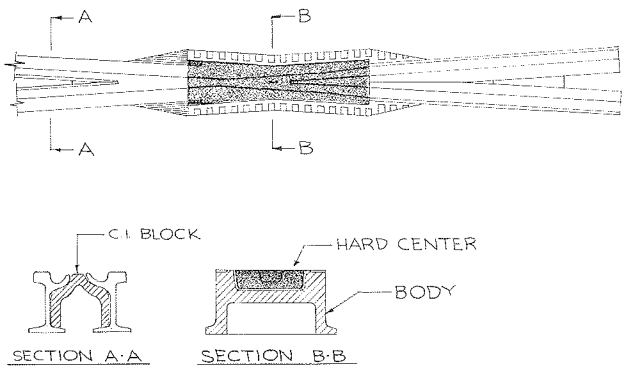

FIGURE 2 Typical manganese steel insert design frog used by electric railways throughout the United States and Canada.

The first solid construction frog used by the electric railways is shown in Figure 3, and was furnished to the Delaware County Passenger Railway Company of Philadelphia, Pennsylvania, in 1895.

In 1899, the first manganese steel crossing was designed for the Union Traction Company of Philadelphia and is shown in Figure 4. The crossing was to be installed at a location where the electric street railway crossed a steam railway. The solid manganese steel rail of heavy box section was to be for the steam railway track and the Bessemer rail for the electric railway track.

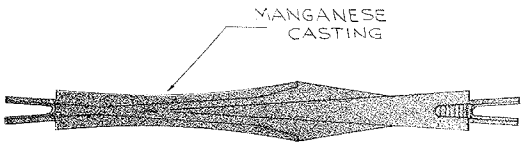

FIGURE 3 First solid manganese frog used in special trackwork—installed in 1895.

During the same year, a solid manganese frog as shown in Figure 5 was designed for the Pennsylvania Railroad to be installed in Philadelphia. This was the first solid manganese frog installed on a steam railroad. The frog was installed in 1900 replacing a Bessemer rail-built frog. The Bessemer rail-built frog was lasting on an average of 3 months whereas the solid manganese frog that replaced it lasted 17 times as long. The solid manganese frog was removed from track once for regrinding to good surface. The frog was then replaced in track in the same location, and was finally removed after a total service life equal to the life of 25 Bessemer rail-built frogs. The results of this test installation's service life did not change the misgivings of the steam railroad engineers. The steam railroad engineers were concerned with the possible breakage of the casting in high-speed locations. To overcome this objection and the objection raised relative to the necessarily short length of the solid manganese frog, the rail-bound manganese frog was designed (Figure 6). The first rail-bound manganese frog was installed in the Baltimore Terminal on the Pennsylvania Railroad in 1900. After 2 years of successful service, the rail-bound manganese frog gained the confidence of the steam railroad engineers and its use in high speed service was established. During

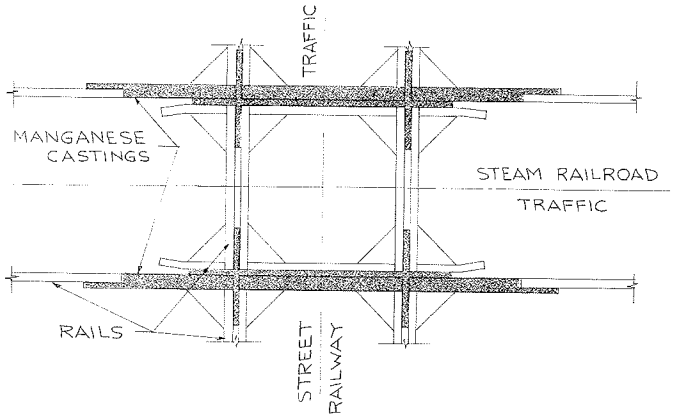

FIGURE 4 First manganese steel crossing installed in track (stream railway crossing electric railway)—installed in 1899.

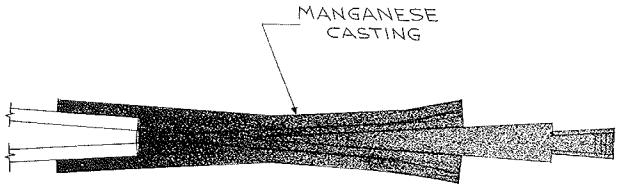

FIGURE 5 First solid manganese frog installed in steam railway track—installed in 1900.

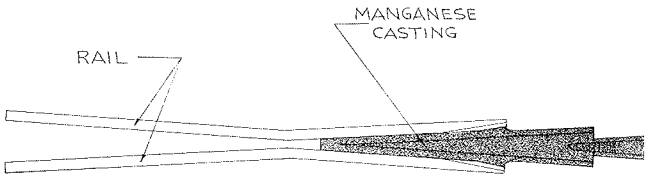

FIGURE 6 First rail-bound manganese steel frog—installed in 1900 on the Pennsylvania Railroad.

the period from 1900 to 1910, the use of manganese steel was extended to

- Solid manganese crossings,
- Rail-bound manganese crossings,
- Solid manganese guard rails,
- Manganese steel-faced guard rails,
- Rail-bound manganese spring frogs,
- Manganese steel-pointed split switches,
- Cast manganese steel rail, and
- Rolled manganese steel rail.

With the use of manganese steel in special trackwork having been firmly established and the economic benefits obtained in severe service widely recognized, the eastern railroads began extensive use of the unique metal for special trackwork components.

The Europeans were closely watching the results being obtained in the United States and when manganese steel was finally introduced in Europe for application to special trackwork, it was apparently received with less skepticism than in the United States.

DEVELOPMENT OF THE RAIL-BOUND MANGANESE FROG

After the successful service of the first rail-bound manganese frog installation at the Baltimore Terminal in 1900, the railroad engineers gained confidence, and, in 1902, a rail-bound manganese frog was installed in high-speed service on the Pennsylvania Railroad. The success of this installation established the use of manganese steel in special trackwork. The eastern railroads recognized the economic benefits of manganese steel in special trackwork and began extensive use of this unique metal, commonly referred to as "the metal par excellence for the purpose."

During the succeeding years, there have been many attempts to develop a metal superior to manganese steel; however, to date, none has been found. From 1900 to the 1920s, there were many designs for special trackwork components developed and tested by the steam railroads, resulting in improved designs and service life to meet the demands of the ever-increasing wheel loads and higher speeds.

The first rail-bound manganese frog design shown in Figure 6 was introduced with modifications by the Pennsylvania Railroad in the 1940s. This design was successful but as the wheel loads increased, the short heel length created wear problems resulting in the heel joint becoming loose, thus increasing the need for maintenance. A new design rail-bound manganese frog was introduced by the Ramapo Iron Works in 1905, as shown in Figure 7. There were two basic variations to this design, one as shown in Figure 7 with extended fillers and the other design without extended fillers.

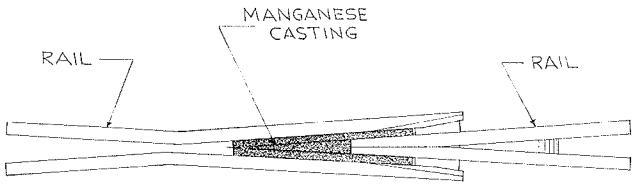

FIGURE 7 Typical rail-bound manganese frog introduced in 1905 and used extensively by steam railroads.

The frog design in Figure 7 was used extensively in the new Grand Central Terminal, which was being constructed from 1906 to 1911. Other eastern railroads made extensive use of this newly designed rail-bound manganese frog. A modification of the design shown in Figure 7 is still in use today and is shown in Figure 8. (Note: the frog shown in Figure 8 has manganese wings that were introduced about

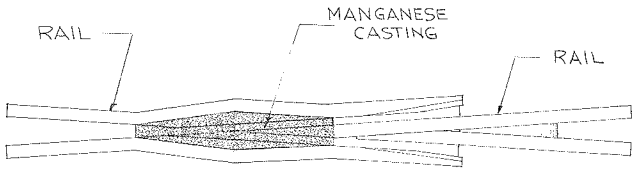

FIGURE 8 Frog design currently in use based on the design in Figure 7.

1915.) As the wheel load increased, the false flange (in wheel terms hollow tread) developed, causing crushing and wear on the receiving guard line or gage line in the area where the false flange traverses the flangeway.

To overcome this problem, in 1915 manganese wings were added to the basic design to provide a wearing surface in this area. The manganese provided a surface that work hardened, thus reducing wear and maintenance. This modified design as shown in Figure 9 has the manganese wings fitted to a milled recess in the wing rail. To improve the heel-rail connection, a heel extension was added to provide a means of attaching the heel rails to the manganese insert casting. The manganese recess at the toe end provided a continuous line on the gage line, which was desirable, but as wear occurred, the manganese flowed resulting in chipping and, in some instances, breakage of the manganese guard. During this same period, integrally cast manganese wear surfaces were added to the rail-bound manganese center frog casting at the bend in the guard rail as shown in Figure 10. This wear strip was discontinued in the second decade of the century as new designs became available. By the mid-1920s, the rail-bound manganese frog design shown in Figure 11 was developed and became the AREA

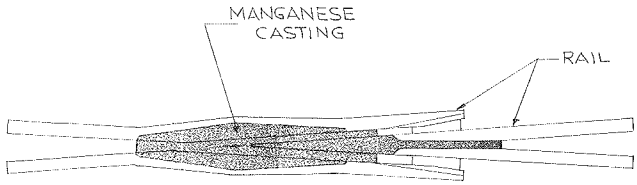

FIGURE 9 Improved frog design introduced in 1915.

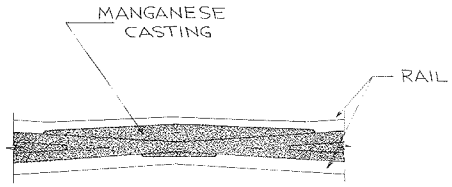

FIGURE 10 Application of integrally cast manganese wear surfaces to special trackwork components.

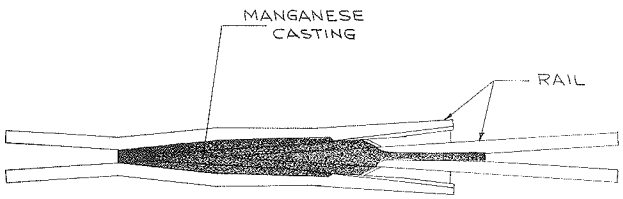

FIGURE 11 AREA rail-bound manganese frog design introduced in the 1920s.

standard rail-bound manganese frog referred to as the AREA 600 design.

This design was in universal use until 1946 when the current AREA 621-design rail-bound manganese frog shown in Figure 12 was introduced. As the wheel loads increased, it became evident that a heavier frog was required. The main deficiency in the 600-design rail-bound manganese frog was the weak section where the heel extension connected to the body of the frog, resulting in breakage at this location. The new AREA 621-design frog had heavier walls and the section where the heel extension connects to the body of the frog was improved; in addition, the notch in the wing rail was eliminated. To (a) improve the 621-design rail-bound frog and (b) reduce maintenance, the depressed heel shown in Figure 13 was adopted in 1971. The depressed heel permits the wheel

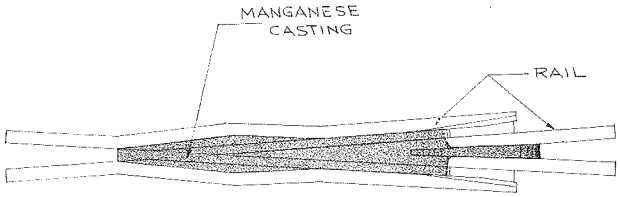

FIGURE 12 AREA rail-bound manganese frog design introduced in 1947.

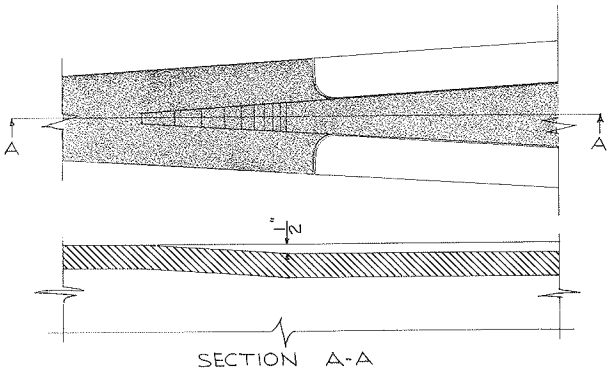

FIGURE 13 Depressed heel for AREA 616- and 621-design rail-bound manganese frogs introduced in 1971.

load to be carried by the wheel tread on the heel rail and manganese insert, gradually transferring the wheel load from the wheel tread to the false flange when the false flange engages the ramp that is located inside the body of the casting where there is a stronger section. The normal plastic flow and resulting chipping experienced by the original AREA 621-design rail-bound manganese frog required grinding in the heel extension area to control the metal flow and eliminate chipping. The depressed heel has since been adopted as a standard by the AREA for the 621-design (heavy-wall) and the 616-design (medium-wall) rail-bound manganese frogs.

During this same period, the integral base-design frog was introduced using the same design criteria as the AREA 600- and 621-design rail-bound manganese frogs except with the sections as shown in Figure 14. This frog design has been used with success in heavy-haul locations.

During the last decade, the number of heavy-haul lines and unit trains consisting of 100-ton cars has greatly increased. This increase in high-tonnage cars has developed the need for an improved rail-bound manganese frog.

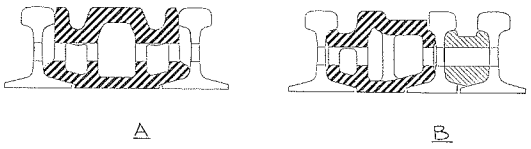

FIGURE 14 Sections for integral base design frogs.

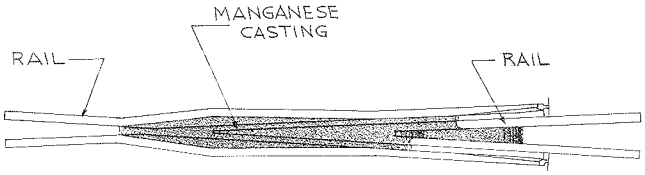

FIGURE 15 Improved rail-bound manganese frog designed for heavy-haul railroads introduced in 1980.

In 1980, a new design rail-bound manganese frog was introduced to meet these demands. This new design rail-bound manganese frog is shown in Figure 15 and typical sections are shown in Figure 14.

To overcome the failure of the heel extension on the current rail-bound manganese frogs, the new design has the joints where the heel rails connect to the manganese casting staggered rather than opposite as the existing design requires. The staggered joints provide improved sections in the heel area that are stronger than the existing design. In addition, the casting section is improved.

MANGANESE IN EUROPE

After the use of manganese steel for special trackwork was firmly established in the United States, it was introduced in Europe with great success. The results obtained in the United States with manganese steel in the application of special trackwork had been closely monitored by the Europeans. The Europeans began using solid manganese frogs and crossings and experienced the same results as the U.S. railroads--longer life and economic returns.

It was reported that one installation on the Central London Line at the British Museum Station was in use 14 to 15 years handling approximately 700 million gross tons (MGT) of traffic whereas the rail-built crossings previously had a life of 6 to 8 weeks.

The Europeans still use solid manganese construction and, to date, have not used rail-bound manganese construction. A typical frog currently in use in Europe is shown in Figure 16.

CURRENT NEW FROG DEVELOPMENTS

The preponderance of 100-ton cars and unit trains in the last decade has developed the need for frogs that will withstand the impacts delivered as the wheels cross over the flangeway from the point to the guard (or wing) surface or conversely from the guard to the point. Currently, frogs have the receiving guard line or gage line crushed by the false flange, which requires maintenance.

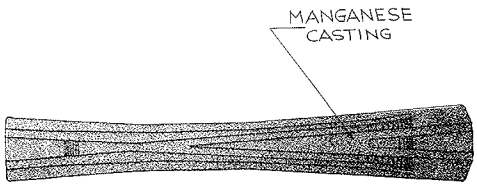

FIGURE 16 Typical European Monobloc frog.

To improve the dynamics of the turnout, the welded/epoxy-bonded turnout was designed and tested in 1972 on the Penn Central Railroad. The tests proved successful, and, with the elimination of bolted joints, switch heel joints, and short frog arms, the dynamics of the turnout were greatly improved. The long switch-point rail and long frog arms permitted the natural track wave to propagate through the switch and frog providing a smoother ride. The welded turnout also included long guard rails with the guard rail flare opposite the frog flare. This greatly reduced the lateral movement of the frog, which reduced stresses in the casting and frog bolts.

In 1984, a spring frog for welded or epoxy-bonded turnouts was introduced and tested on Amtrak in the Northeast Corridor. The tests have been successful in providing a continuous surface for the wheel tread to traverse. The long frog arms dampen the vertical movement of the spring wing and provide additional force biasing the spring force. It is to be noted that a spring frog should only be used in a location where 80 percent or more of the traffic is on the main line and 20 percent or less is for the turnout run. Further improvements are being sought and a new generation of frogs is being developed, specifically, movable wing and point frogs. These designs provide a continuous surface for the wheel tread to traverse thus eliminating the impact delivered by the wheel crossing a flangeway. These frogs are still in the testing stage and results are to be evaluated. The main drawback, however, is economic because an extra machine is required for the frog and more circuitry is necessary to have the switch and frog thrown in correspondence.

CONCLUSION

Today, manganese steel in special trackwork is extensively used throughout the world and still remains "the metal par excellence for the purpose" and, since its introduction, nothing has been found superior to it.

GLOSSARY

Crossing (track)--A structure used where one track crosses another at grade, and consisting of four connected frogs.

Electric Railway (track)--A track whereon is to be operated rolling stock, the wheels of which have smaller flanges or narrower treads (or both) than those of AAR standard wheels, the motive power being immaterial (according to AREA Portfolio of Trackwork Plans).

Frog--A track structure used at the intersection of two running rails to provide support for wheels and passageways for their flanges, thus permitting wheels on either rail to cross the other.

Joint, Rail (manganese)--A fastening designed to unite the abutting ends of a manganese casting and rail.

Special Trackwork--All rails, track structure, and fittings, other than plain unguarded track that is neither curved nor fabricated before laying.

Bolted Rigid Frog--A frog built essentially of rolled rails with fillers between the rails, and held together with bolts.

Rail-bound Manganese Steel Frog--A frog consisting

essentially of manganese steel body casting fitted into and between rolled rails and held together with bolts.

Solid Manganese Steel Frog--A frog consisting essentially of a single manganese steel casting.

Heel End of Frog--That end of a frog that is the farthest from the switch; or, the end that has both point rails or other running surfaces between the gage lines.

Toe End of Frog--That end of a frog that is nearer the switch; or, the end that has both gage lines between the wing rails or other running surfaces.

Publication of this paper sponsored by Committee on Railroad Track Structure System Design.

Development Work on Switches and Crossings by British Rail

C. LOCKWOOD and P. J. THORNTON

ABSTRACT

To meet the increased demands imposed on switch and crossing installations by higher train speeds and higher axle loads, British Rail has a continuing program of development work. This program's purposes are to (a) provide junctions for higher speeds and (b) reduce track maintenance costs by improving track layout geometry and component design as well as materials and the support structure. Recent work in these areas includes design of high-speed junctions suitable for speeds up to 125 mph (200 km/hr), and studies of the paths of wheels through junctions, with particular emphasis on entry into switches. Computer simulations have been developed to predict wheel/rail forces. Measurements of actual forces by means of load-measuring wheelsets have confirmed predictions. Theoretical vertical wheel trajectories through a variety of crossings have been considered in detail, leading to proposals for changes in local railhead geometry to reduce impact forces. (Large vertical impact forces measured at crossings are illustrated.) Improved steels have been developed for use in crossings that can be welded into track, thereby eliminating troublesome bolted joints. Better support for switch and crossing work (in the form of prestressed concrete bearers) is being evaluated.

The railways in Britain link conurbations that, in many cases, are less than 40 km apart so railways have to compete with the motorway network with its speed limits of 113 km/hr. Some of the longer journeys are up to 650 km from end to end and have to compete for business travel with internal air routes. With these types of competition, it is important that the speed of passenger trains should not be unduly restricted at junctions, in order to maintain the highest average speed possible between station stops.

C. Lockwood, British Railways Board, Civil Engineering Department, Departure Side Offices, Paddington Station, London W2 1FT, England. P.J. Thornton, British Railways Board, Research Division, Railway Technical Centre, London Road, Derby DE2 8UP, England.

JUNCTIONS FOR HIGHER SPEEDS

Historically, the geometry of switches has been designed on the basis of a maximum-allowable cant deficiency at the switch tip. This was based on the amount of discomfort tolerable to passengers as assessed from running trials. The effective radius at the switch tip on a diverging route is calculated from the versine on a 12.2-m chord centered at the switch tip (1). The short-lived cant deficiency on that radius of curve must not exceed 125 mm (5 in.), and the sustained cant deficiency on the turnout curve is limited to 90 mm (3.5 in.).

These rules are still applied in British Rail (1). As speed requirements increased, switchblade geometry was gradually refined, and straight planing gave way in the 1950s to curved planing, which provides a narrower entry angle and improved travel from planed rail to full-switch rail (Figure 1). This was further improved in the late 1960s by making

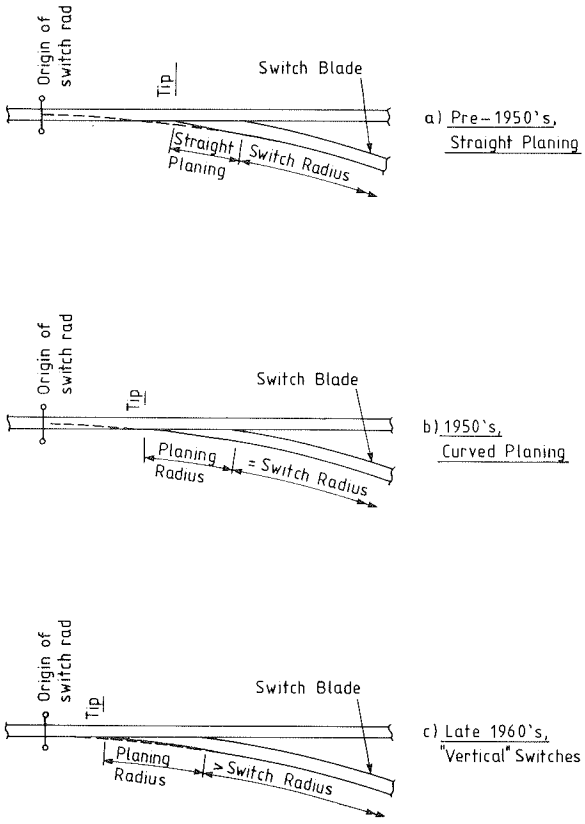

FIGURE 1 Development of British Rail switch design.

the switch curve tangential to the plain rail ahead of the switches, but with the switchblade planing at a slightly larger radius still intersecting the straight to maintain a sufficiently robust tip (Figure 1). The range of standard turnouts was rationalized to be in accordance with operating requirements. A further development at this stage was to make all rails of switch and crossing layouts vertical instead of inclined at 1 in 20 as most were hitherto. This led to a considerable reduction in the number of different baseplates required for this so-called "vertical" design.

All switch rails are flexible and have a fixed heel. Turnouts that incorporate such switches and that are suitable for speeds up to 70 mph (113 km/hr) are widely used (Figure 1 and Table 1). Crossovers incorporating these turnouts are subject to reduced speed limits, because of the rules for the rate of change of cant deficiency (maximum 80 mm/sec or 3.25 in./sec), to ensure passenger comfort (1). Use of spiral-transition turnout curves with flatter crossing angles and a portion of straight track between the two crossings enables the speed potential of the switches to be realized in crossover situations.

In response to a recent operating requirement of 125 mph (200 km/hr) as the running speed on the East Coast Main Line of British Rail, switches suitable for this speed when laid "split" symmetrically [or for speeds of 90 mph (145 km/hr) out of straight] were designed and put into service in 1983 (Figure 2) (2,p.149).

A REAPPRAISAL OF SWITCH DESIGN

Requirements for higher speed through junctions have prompted British Rail to closely examine the way vehicles are affected by their passage through switches and crossings, aided by the greater knowledge of vehicle behavior that now exists. Large lateral wheel/rail forces are known to occur and theoretical assessment of switch designs by computer modeling is an important part of the current work, aimed at reducing those forces.

The Tangential Switch

This switch configuration has been proposed in the light of current knowledge of wheelset curving behavior with the aim of reducing the angle of attack of the wheel on the switchblade and, hence, the impact forces, while still adhering to the cant deficiency criteria.

On British Rail, there commonly is a 6-mm nominal clearance between the wheel flange and the rail on straight track. A wheelset running centrally approaches a set of switches in a straight line until one wheel flange contacts the diverging switch rail where this is approximately 6 mm thick, when all the flangeway clearance is used up. In the current, curved, planed switches, this contact is made at an angle of attack slightly larger than the planing angle at the tip of the switch (Figure 3).

To improve the situation, the switch (and turnout) curve would ideally continue forward to its tangent with the stock rail, but the resultant, extremely thin switch tip would be unsatisfactory. However, if the wheel does not normally contact the switch rail until the latter is 6-mm thick, then the switch rail in front of that point can be made straight, thus giving a finite angle at the tip of the switch and still providing the desired reduction in angle of attack. If a wheel is hugging the stock rail on the closed turnout switch side, the impact angle will be the same as for the 6-mm position, as will be the exit angle for the reverse direction of travel. The length of straight provided is short and will barely affect the running of a vehicle onto or off the switch curve. (Note: This design approach is shown in Figure 4 and is known as the tangential switch.)

TABLE 1 Current Range of Switch Types

Switch Type	Planing Length (m)	Planing Radius (m)	Switch and Turnout Radius (m)	Natural Angle (℄measure)	Maximum Speed (km/hr)	Speed Restriction (mph)
AV	2 900	197	141	7	30	15
BV	3 500	231	184	8	35	20
CV	4 250	287	246	9.250	45	25
DV	5 200	367	332	10.750	50	30
EV	7 000	740	645	15	70	40
FV	8 550	1137	981	18.500	85	50
SGV	10 150	1399	1264	21	100	60
GV	11 600	1826	1650	24	115	70
HV	16 500	3188	3001	32.365	150	90

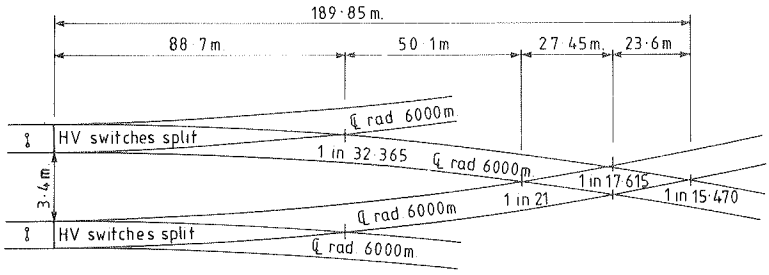

FIGURE 2 High speed junction for 125 mph (200 km/hr).

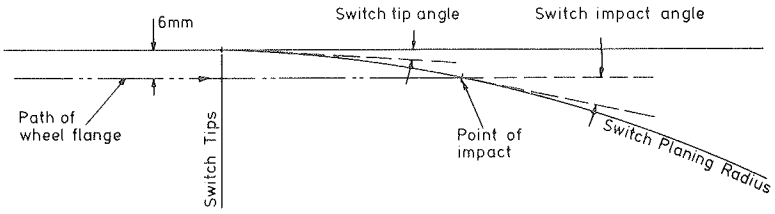

FIGURE 3 Switch tip angle and impact angle compared.

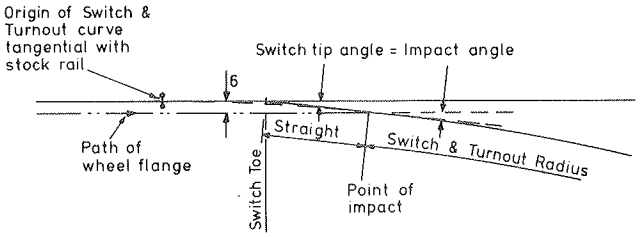

FIGURE 4 Design of tangential switch.

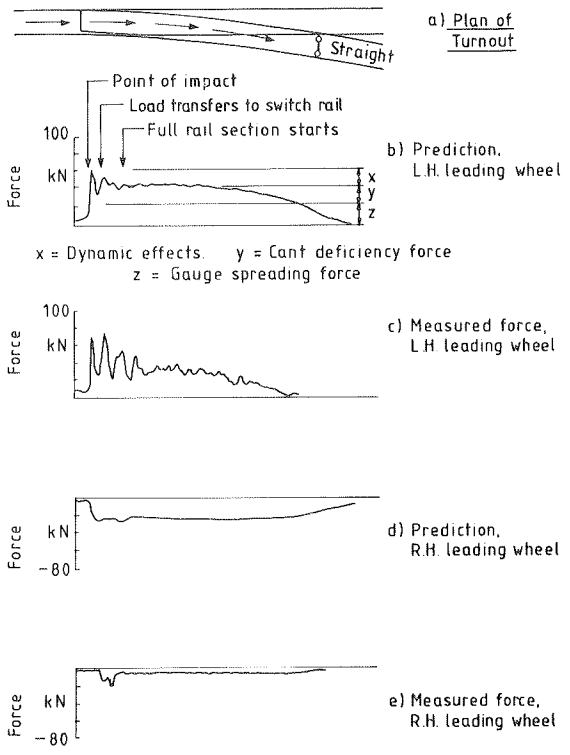

NOTE — Vehicle in all cases is a diesel freight locomotive

FIGURE 5 Comparison of predicted and measured lateral forces in a turnout.

Lateral Forces

Although the calculation of cant deficiency at switch tips will give a reasonable indication of the lurch that will be experienced by a passenger, the study of the track forces applied by the wheels of vehicles gives a much more scientific approach to the assessment of likely wear and tear on the components. The Research Division of British Rail has studied the forces generated by a wheelset negotiating track alignment irregularities. The lateral force at the impact position on switches can be likened to that generated at such an irregularity. The levels of the forces experienced by conventionally designed switches have been predicted by a computer model and these have proved to be close to those recorded on track by load-measuring wheels fitted to a locomotive and to a freight vehicle (Figure 5). This information has been used to investigate the lateral impact force generated by the wheelset striking a diverging switch rail. Shown in Figure 6 are comparisons of predicted impact forces, which indicate that significant improvements can be made by adopting a tangential design, especially for facing-direction traffic. The horizontal forces would be the same in the facing and trailing directions for this design.

When compared with the current design of switches, the new tangential design can be expected to give a reduction of about 55 percent in the dynamic horizontal forces on a switch with a locomotive traveling through the turnout in a facing direction. In the trailing direction, the forces could be reduced by about 25 percent. The improvements would be achieved at the expense of an increase in planing length of about 12.5 percent.

Measurements of wear and monitoring of the integrity of components will show whether the increased cost of the tangential switch is outweighed by the increase in life expected as a result of the lower force levels.

VERTICAL WHEEL TRAJECTORIES THROUGH CROSSINGS

The discontinuity of the running surface at a crossing has always presented a challenge to the Permanent Way Engineer. Under traffic, large vertical impact

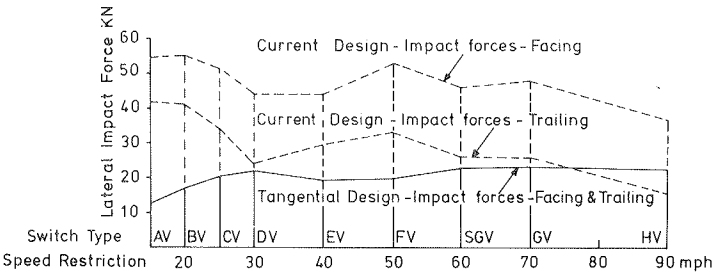

FIGURE 6 Predicted impact forces on switches (laterally unsprung mass of 2.39t).

forces can occur that can cause severe deformation and, perhaps, damage to the railhead, and can sometimes lead to fatigue failure. Rail fastenings and timbers are affected and accompanying deterioration of the track support hastens these processes. At higher speeds, the vertical trajectory of a coned wheel passing over a crossing is an important factor governing the magnitudes of the wheel/rail forces generated, which are similar in general shape to the irregularities presented by dipped joints or welds and by wheelflats (3), and a knowledge of this geometry is essential to the crossing designer. The problem of how to provide the best possible support for the wheel is compounded by the wide range of tire profiles likely to traverse the track--from a variety of brand new ones to those that are due for reprofiling--each one producing its own resultant wheel trajectory. Wear of the rails further complicates the issue.

The customary means of assessing the wheel's vertical path has been by the laborious drawing of wheel and rail profiles larger than full size and superimposing them on one another, for close spacings along the track. The wheel's height relative to a datum could then be scaled and plotted. This is a slow process and is probably a prime reason why the wheel/rail interaction at crossings has not been given as much attention as the materials from which the crossings are made.

However, the advent of powerful computerized drawing facilities has brought the possibility of carrying out such work much more quickly and accurately and has encouraged detailed assessment of trajectories. British Rail's Research Division has carried out some preliminary analysis work on existing crossing designs and will extend this to a consideration of modified designs. The effects of different tire profiles, new and worn, in different lateral positions can quickly be analyzed, once the basic crossing and tire data are filed. Such an assessment offers a quick means of comparing the likely results of modifications without the expense of service trials, and also of identifying undesirable features not otherwise apparent.

The working process is the same as for the manual method but the information provided is much more accurate than hitherto and professional-standard drawings are readily available. Having examined an existing crossing, the engineer can quickly test design changes and assess their benefits.

Theoretical Trajectories

The combination of tire coning and railhead geometry (the latter both vertical and horizontal) through the heart of a crossing leads to an irregular wheel path in the vertical plane, often of an undesirable shape and magnitude.

The wheel has, in effect, a series of ramps to negotiate and may even meet small steps. The results of a computer-aided analysis of a new, coned tire profile, type P.1 (Figure 7), traveling through a 1 in 9.25 angle common crossing fabricated from rolled rail are shown in Figure 8. This tire profile, which has a 1 in 20 tread coning, has been widely used by British Rail for many years, although other types of profile are becoming more numerous. This is shown superimposed on the nose area of the crossing in Figure 7. The three tire positions (A, B, and C) correspond to those of a centralized wheelset (B)

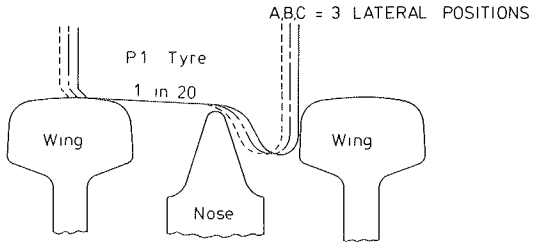

FIGURE 7 New P.1 tire at nose of rolled rail crossing.

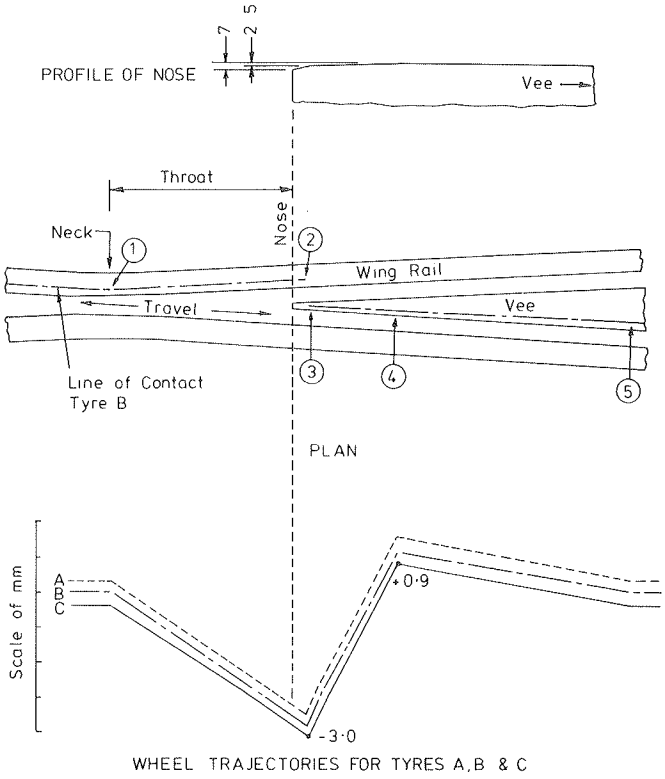

FIGURE 8 Vertical wheel trajectories for new P.1 tire/rolled rails.

and wheelsets near their two lateral extremes (A and C). The plan view in Figure 8 shows the running surfaces in the throat and nose areas of the crossing, irrelevant detail being omitted. The derived wheel/rail contact line for tire B is marked.

The path plotted in Figure 8 shows clearly that as the left-hand wing rail departs from the running direction along 1-2, a right-traveling (i.e., facing direction) wheel descends by some 3 mm until contact transfers to the vee at 3, behind the nose. The sloping shape here (Figure 8) presents an upward ramp to the wheel, 3-4, to a height of 1 mm above the general railhead level, from where the descent is made to the latter level at 5. A wheel traveling from right to left will follow the same path in reverse.

This case, although easy to visualize and capable of analysis by calculation, has been described in some detail as an introduction to more complex cases where the tire tread is worn and needs to be drawn accurately.

The ramped shape, 1-2, 3-4, is well known, but the rise above the railhead level to 4, due to the machined railhead shape locally, is not so obvious until analyzed in the manner described. The paths of a centralized wheelset and wheelsets near their two lateral extremes are almost identical (Figure 8). This will usually be the case for a new P.1 tire but will not be so for a worn example or for any other tire design whose profile is curved from new.

Figure 9 shows that a moderately worn tire will have a different path from a new one, running with the outer part of its tread on the wing rail and giving a less severe ramp angle at the bottom of its deviation from a level path. The path of a heavily worn P.1 tire is shown in Figure 10 and again is seen to be somewhat less severe than that of a brand new tire except at 1, where the abrupt step is worse for wheels traveling right to left (i.e., trailing direction).

The preceding discussion concerns a crossing that has rolled rails. The use of castings gives the designer more freedom in choice of running surface shape to improve the wheel's path. One such shape widely used by British Rail is shown in Figure 11. It has a 1-in-20 cross slope to match the P.1 tire, and the resultant wheel trajectories are shown in Figure 12 for new and Figure 13 for worn tires. Clearly, there is an improvement for these two over the rolled rail crossing; however, the heavily worn tire's path (Figure 14) does not compare so well, particularly in respect of transfer of contact from vee to wing at 1 in the trailing direction of travel. A slight modification to the outer part of the wing

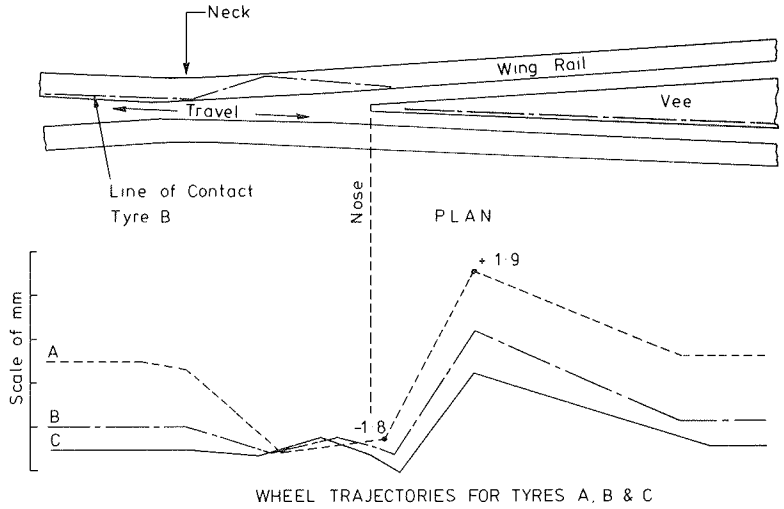

FIGURE 9 Vertical wheel trajectories for worn P.1 tire/rolled rails.

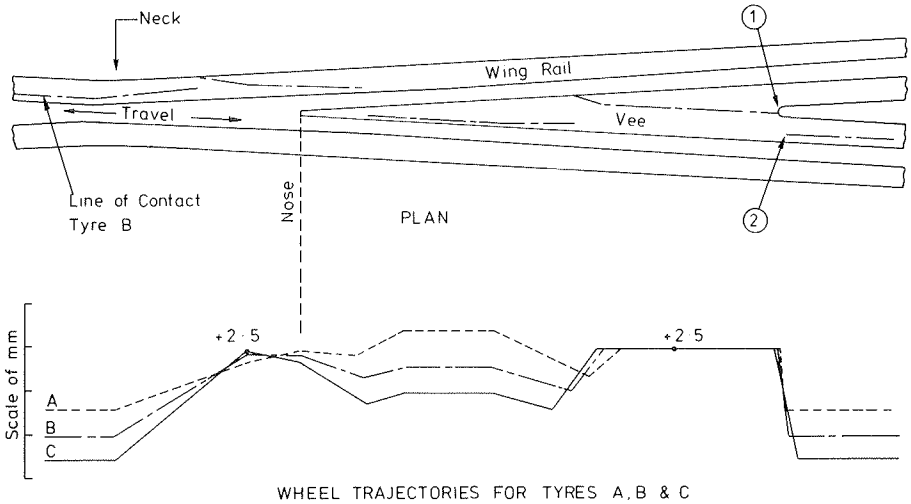

FIGURE 10 Vertical wheel trajectories for heavily worn P.1 tire/rolled rails.

rail surface could ease this, although it is difficult to satisfy the requirements for the smooth passage of all the possible tire shapes.

The irregular wheel paths discussed previously have been derived using as-designed railhead shapes, with no attempt made to relate them to real conditions in track. Wear of the running surfaces will lead to modification of the paths.

Battering of the rails will quickly smooth out small irregularities, which may not therefore be important. Larger, abrupt changes cannot be ignored, but may be amenable to redesign in the light of theoretical analysis. Generally, the wheels will act to smooth out the path and the use of designed rail shapes in analysis will tend to be pessimistic.

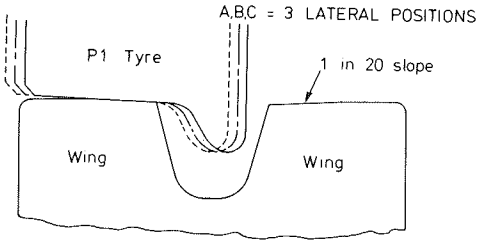

FIGURE 11 New P.1 tire at neck of cast crossing.

FORCES

As already noted, the wheel trajectories resemble those resulting from plain rail joint irregularities although the ramp angles to be negotiated in crossings can be more severe. Dynamic models used to predict wheel/rail forces for ramp irregularities in plain rails are well developed and have been validated experimentally. Extension of this work to crossings would be of great value to the designer.

The following table gives values of theoretical ramp angle for a new P.1 tire traversing a variety of crossings, compared with a severely dipped plain rail joint.

	Description	Trajectory (millirads)
1	Severely dipped plain rail joint	20
2	Part-welded common crossing	18
3	AMS cast crossing	13.5
4	Switch diamond crossing	19
5	Fixed obtuse crossing	16

Other tire/crossing combinations can give much larger angles, perhaps as much as double those quoted. The forces generated will depend on this geometry and on the effective mass and stiffness of the track structure and of the vehicles and can thus vary considerably in practice.

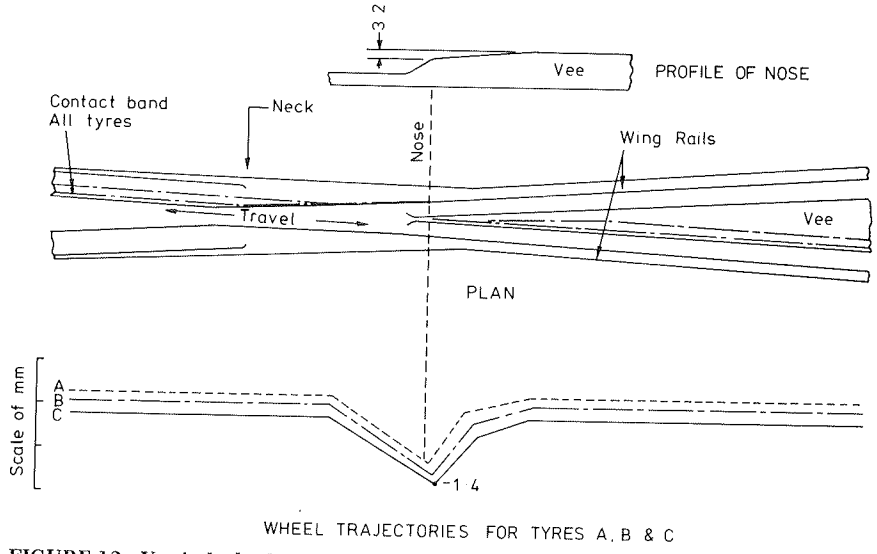

FIGURE 12 Vertical wheel trajectories for new P.1 tire/cast crossing.

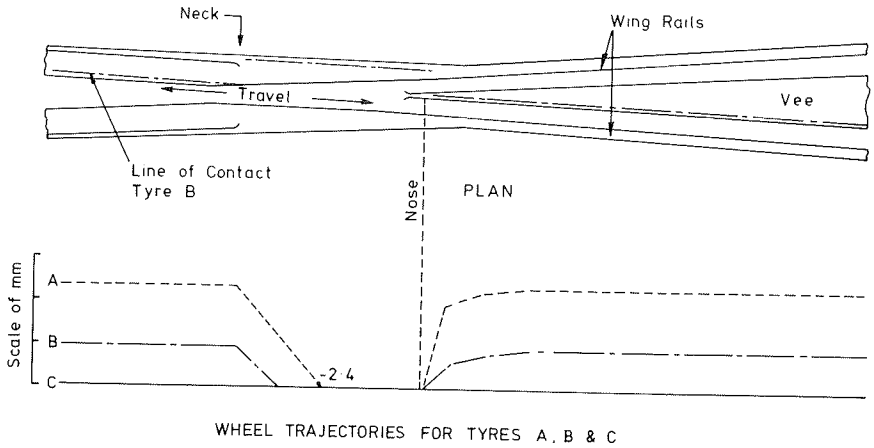

FIGURE 13 Vertical wheel trajectories for worn P.1 tire/cast crossing.

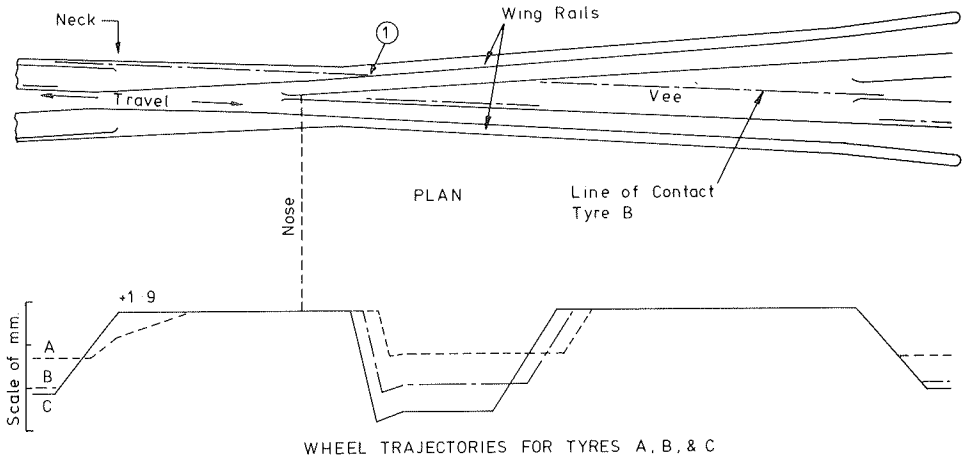

FIGURE 14 Vertical wheel trajectories for heavily worn P.1 tire/cast crossing.

Figure 15 shows examples of forces recorded at crossings, with plain rail joint responses for comparison. The forces are large and wheel trajectory analysis should play an important part in reducing them, thus prolonging crossing life and reducing maintenance costs.

IMPROVED MATERIALS FOR CROSSINGS

British Rail has evaluated new materials for crossings, seeking higher strength steels and harder welding consumables for the part-welded type of crossing, and an alloy steel for cast crossings, which combines good casting properties with good weldability and mechanical properties. Improved materials for use in part-welded crossings of the type shown in Figure 16 have been developed by British Rail in collaboration with T.W. Ward Ltd. (railway engineers).

Commercially available grades of rail steel and welding consumables have been subjected to laboratory assessment and selected combinations used in service trials. That using 90 kg/mm² ultimate tensile strength (UTS) pearlitic steel rail with A33 welding wire has been adopted as standard. This combination gives a high resistance to deformation, can be welded into track, and can be weld-repaired in situ.

A considerable drawback to austenitic manganese steel (AMS) is the difficulty of welding it into track. At present, there is no economically attractive alternative to troublesome bolted joints. To avoid the problem, a bainitic alloy steel has been developed as an alternative to AMS, which not only has excellent casting and mechanical properties, but is readily weldable to pearlitic steels. Collaborative work with Edgar Allen Engineering Ltd. had led to trials of cast center crossings (Figure 17) and performance so far is encouraging.

CONCRETE BEARERS FOR SWITCHES AND CROSSINGS

The support for British Rail's switches and crossings has received much less investigative attention than that for plain track. High-speed main routes are now largely equipped with plain rails on prestressed concrete sleepers employing spring rail fastening clips and rail pads, but owing to the variety of rail-fastening positions in switch and crossing layouts, timber bearers have continued to be used for these with gray cast-iron baseplates and spring rail fastening clips.

Softwood bearers were used for many years, but their service life was insufficient and Jarrah hardwood has been used in recent years. When the rails of older types of switch and crossing assemblies needed replacement, there was often little life left in the softwood, but improved designs of steelwork were found to outlast the bearers. Hardwood has helped to restore the balance but the need to im-

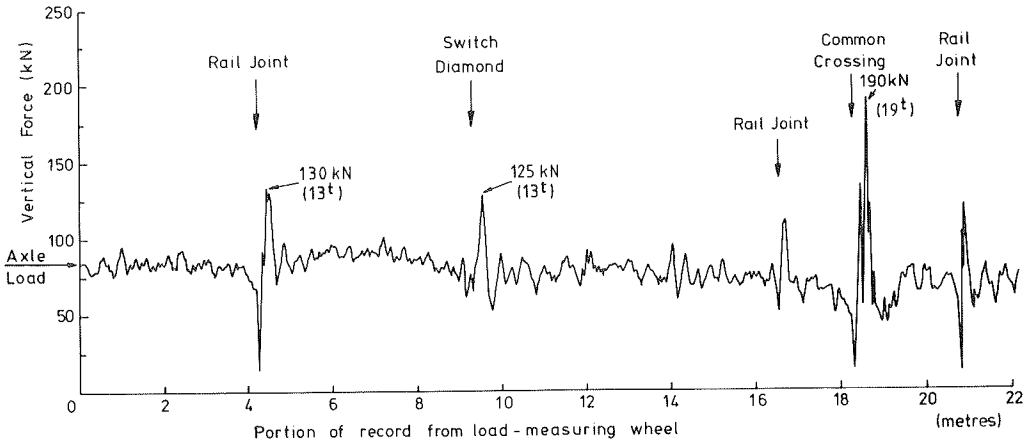

FIGURE 15 Comparison of wheel/rail forces measured at track irregularities.

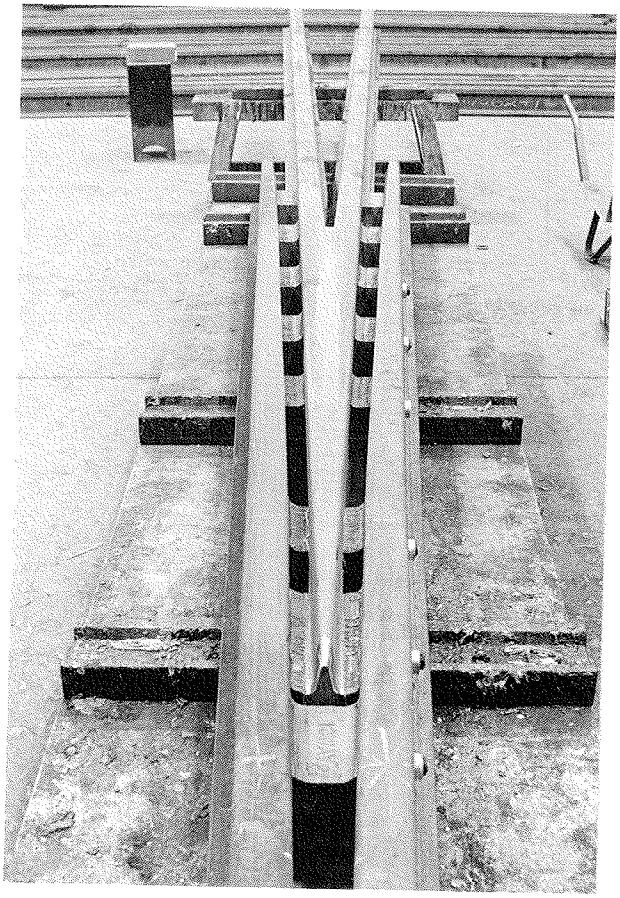

FIGURE 16 Part-welded crossing in BS.11 grade steel (90 kg/mm^2).

prove the retention of track geometry, and reduce maintenance costs and reliance on imported timber, has resulted in the development of prestressed concrete bearers. This is seen as a logical move to follow plain track practice, and concrete bearers are expected to last at least twice as long as the steelwork and result in more economic renewal cycles.

A few trial layouts had been laid as early as 1967 (one turnout) and 1972-1973 (six turnouts), in minor lines. They took advantage of the then new "vertical" switch and crossing designs, which required baseplates only for the switch slides. The concrete bearers were laid out as timber ones would be, with the steelwork laid on top as a template, enabling holes for the malleable iron spring clip housings (Figure 18) to be drilled in the concrete. A resin adhesive was used to glue in the housings. Stud bolts were resin-bonded into the concrete for holding down fabricated steel slide baseplates.

The service performance of these layouts encouraged installation of three further ones in 1981, incorporating improvements. Earlier problems with bowing of the longer bearers due to uneven drying shrinkage leading to track cross-level errors were overcome by casting them on their sides so that any bowing took place in plan. Standard gray cast-iron switch slide baseplates were adopted, and the the bearers here are correspondingly shallower to maintain uniform construction depth. In these three installations, the holes for spring clip housings were percussion drilled, either as described previously or using jigs for location. The latter proved to be the more expensive. Also, cost studies showed that if the labor costs associated with the fixing of rail clip housings could be reduced by casting them

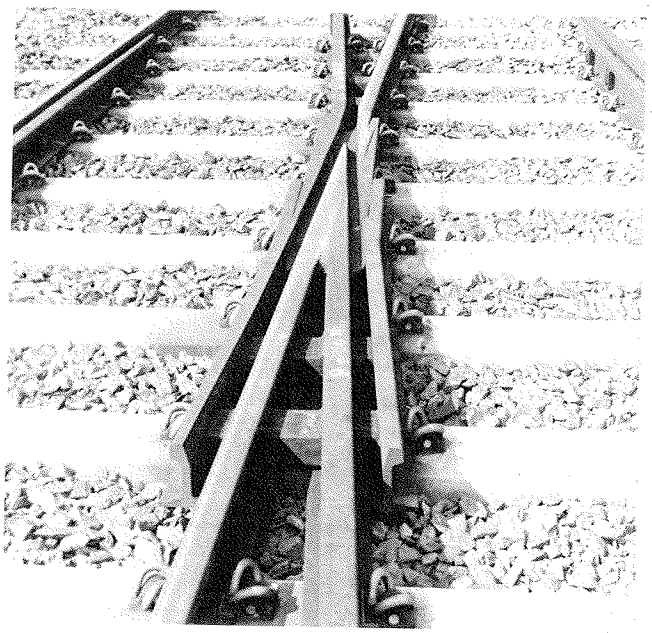

FIGURE 17 Bainitic cast center crossing with welded-on legs.

in, then concrete bearers could be competitive in cost with hardwood.

The position and angle for each housing were calculated by computer and the housings cast in during manufacturer of the bearers. Despite the large number of individual mold plates required, this method is now established and a range of standard turnouts and crossovers is available. Replacement bearers, if required, can be supplied quickly. Bearers up to 6 m long for plain rails and crossings with standard concrete sleeper-type clip housings, rail pads, and insulators have proved reliable (Figure 18).

Following the development work, carried out in collaboration with Dow-Mac Concrete Ltd. and Costain Concrete Ltd., some 30 turnouts and crossovers with a variety of switch and crossing combinations have been installed to date, with rail clip housings cast directly into the concrete. A further refinement has been the casting in of the plastic plugs for the slide baseplate screws (Figure 19).

Early problems with splitting of a few shallow bearers under switches were overcome by providing adequate drainage of the plastic plug to obviate freezing of entrapped water, and by redesigning of the screw and plug assembly to make sure that high tensile stresses were not generated in the concrete on insertion of the screws.

As with any railway track, it is considered essential to provide an adequate depth of clean, level, and well-compacted ballast for the satisfactory performance of concrete bearers. The layouts installed so far, in lines with speeds up to 90 mph, have behaved well. Geometry has been maintained well and reduced maintenance attention has been required compared with timbered layouts.

CONCLUSIONS

1. British Rail's track engineers have responded to demands for shorter journey times by designing and installing junctions for progressively higher speeds. A recent one on a major route diversion allows for a 125-mph (200-km/hr) running speed, and has proved satisfactory in service.

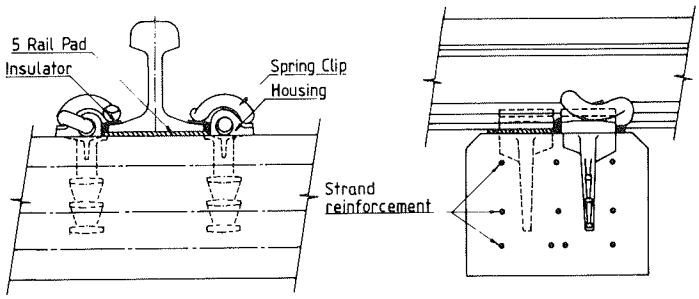

FIGURE 18 Deep concrete bearer with spring clips.

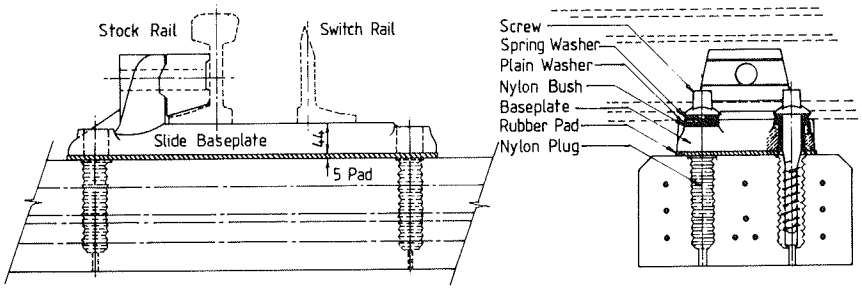

FIGURE 19 Shallow depth bearer with slide baseplates.

2. Computer models of wheel/rail interaction at switches have been validated by site running tests and used to examine design proposals. Significant reductions of lateral impact forces are considered possible with attendant economies in maintenance and component renewal costs. Crossing forces, too, have been measured by instrumented wheelsets, and computer models of wheel/rail interaction are being developed.
3. Careful choice of crossing geometry could make a significant reduction in forces causing batter. Computer-aided drawing facilities have enabled modified railhead shapes to be assessed and it has been shown that vertical ramp angles to be negotiated by wheels at crossings can be more severe than those at plain rail joints.
4. Work on improved materials has led to the adoption of a higher strength steel for part-welded crossings and evaluation of a weldable alloy steel for castings is well advanced. Substantial economies are anticipated from using these materials.
5. Increasingly, switches and crossings are being supported on concrete bearers and maintenance periods have been extended.

ACKNOWLEDGMENTS

The authors wish to thank the British Railways Board for permission to present and publish this paper and acknowledge the help and advice of colleagues in its preparation.

REFERENCES

1. British Railway Track: Design, Construction and Maintenance, 5th ed. (C.L. Heller, ed.). The Permanent Way Institution, London, England, 1979.
2. Journal of the Permanent Way Institution (A. Blower, ed.), Vol. 102, Part, 1, London, England, 1984.
3. C.O. Frederick. The Effect of Wheel and Rail Irregularities on the Track. Proc., Heavy Haul Railway Conference, Institution of Engineers (Australia) and Australasian Institute of Mining and Metallurgy, Perth, Western Australia, Sept. 1978.

Publication of this paper sponsored by Committee on Railroad Track Structure System Design.

Basic French Technology for Crossings, Switches, and Special Trackwork

GERARD E. CERVI

ABSTRACT

A modern track has to cope with modern rolling stock and increasing load and speed and has to be cost-effective. This is why the French national railroads have developed continuous welded rails on their main lines. As a result, new techniques are being developed to weld or glue switches and crossings into continuous welded rail track. Also, it is essential to increase the resistance of the material to make it more cost effective (longer lifetime, less maintenance). The results of this effort to improve cost effectiveness and cope with increasing loads and speeds are tangent, constant, or continuously varying radius geometry; flexible, thick-web, solid switch points (high or low web); solid cast manganese steel frogs (glued or welded); movable point frogs; and concrete and very hard wood ties.

Turnouts and special trackwork provide the various route arrangements needed by railroad traffic. The speed requested on the diverted track and the comfort required for passenger trains determine the geometry. Increasing speeds and axle loads as well as the improvement of cost effectiveness require a constant effort to improve the design and the engineering of switches and crossings (e.g., flexible thick-web switch rails, solid cast manganese steel frogs, welded switches and frogs, movable point frogs, and resilient fasteners) are the result of this search for improvement.

Diverging and converging routes require turnouts (switches and crossings). Crossing routes simply require crossings. Single- or double-slip switches allow for diverging, converging, and crossing in small spaces. The components of a turnout are (a) the switch (points, stock rails, and braces), which splits the route into two, (b) the crossing (frog and guard rails), and (c) the closure and turnout rails. The components of a diamond crossing are (a) two obtuse frogs or central frogs and (b) two acute frogs or end frogs.

In most cases, the main line in a turnout is on a tangent run. If necessary, it can be curved, opposite the direction of the curve of the diverted track (contra-curved) or curved to the same direction as the diverted track.

Diamond crossings can also be curved (one track or both tracks). The proper use of turnouts and crossings allows setting up single and double crossovers, pocket tracks, sidings, classification yards, and so forth.

GEOMETRY OF TURNOUTS

The radius in the diverted track will depend on the required speed. On the curved run, the centrifugal acceleration is expressed as

$$\gamma = K V^2/R$$

Techtrans, 1818 N Street, N.W., Suite 100, Washington, D.C. 20036.

The acceleration is proportional to the square of the speed and inversely proportional to the radius. To avoid this transversal acceleration, it is necessary to superelevate the high rail. This is commonly done in running tracks. The superelevation never absorbs the complete lateral acceleration. Depending on required comfort for passenger trains, there is a certain cant deficiency. In special trackwork and especially in turnouts, it is impossible to set the running surfaces of rails at different levels at a proper superelevation for each route.

To maintain the centrifugal acceleration within reasonable limits in such conditions, it is necessary to set up a proper ratio between speed and curvature.

The Union Internationale des Chemins de Fer Français/Office de Recherches et d'Essais (UIC/ORE) have determined that the maximum centrifugal acceleration acceptable, with good comfort and maintenance cost effectiveness, is 0.067 g (or 0.667 millisecond^2). This acceleration is obtained with a cant deficiency of 4 in. and takes into account the break-off of the curvature at the end of the point, which generates a sharp acceleration that is twice higher than in the regular curve. This cant deficiency value complies with the needs for maintenance. Examples of minimum radius on diverted track with corresponding cant deficiency follow.

Cant Deficiency (in.)	Speed 62.5 mph	Speed 100 mph
3 1/6	R = 5,000 ft (1.16°)	R = 15,800 ft (0.37°)
4	R = 4,000 ft (1.46°)	R = 10,000 ft (0.58°)

Generally, the geometry of the diverted track is a constant radius [e.g., a turnout n.20 with a constant radius (1) on the diverted track will allow a speed of 62.5 mph] (see Figure 1).

In crossovers, the diagram of centrifugal acceleration is different. The two opposite accelerations in a short lapse of time, due to the short distance, are prejudicial to comfort and limit the speed in the crossover to a lower value than on the diverted track of a single turnout (see Figure 2).

It is necessary to establish a portion of tangent

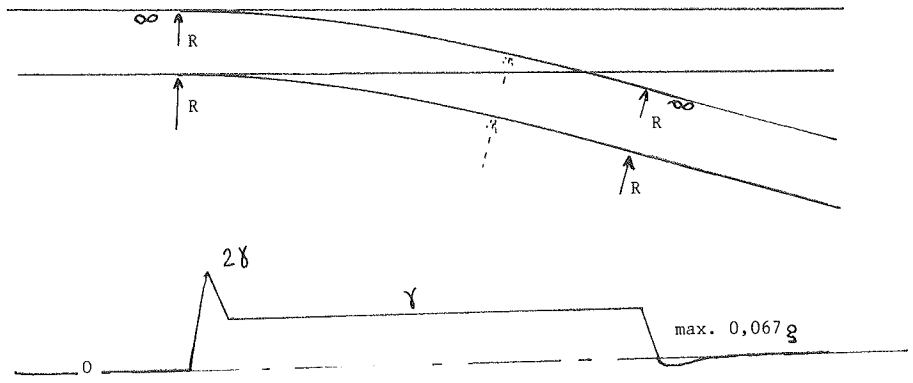

FIGURE 1 Diagram of centrifugal acceleration.

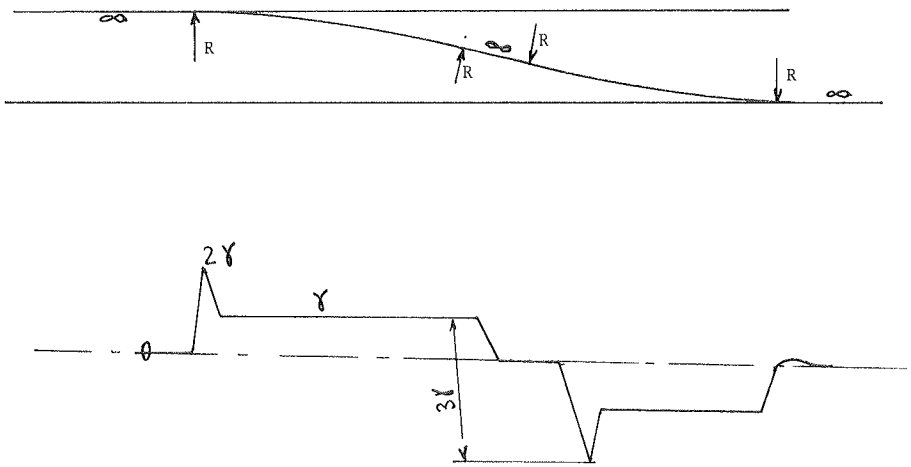

FIGURE 2 Diagram of centrifugal acceleration in a crossover.

track between the two opposite curves in order to allow the vehicles to stabilize (self frequency of vehicles is about 1 Hz). The required lapse of time is constant at 1 or 2 sec. The length of track required will thus depend on the speed. This may possibly have an effect on the distance between central lines on the two tracks.

In special conditions, such as high speed, parabola or curves with a constant variation of curvature can be used. The use of curves with constantly varying radius improves the performance of crossovers. For instance, on the Très Grande Vitesse (TGV) line, between Paris and Lyons, the Société Nationale des Chemins de Fer Français (SNCF) uses crossovers with parabolic curves with radii increasing steadily from their minimum value to infinite (see Figures 3 and 4).

Two turnouts have been developed by the SNCF for the Paris-Lyons high-speed line: (a) n.65 with a maximum speed of 138 mph on the diverted track, and (b) n.46, which is mostly used for crossovers with a maximum speed of 100 mph.

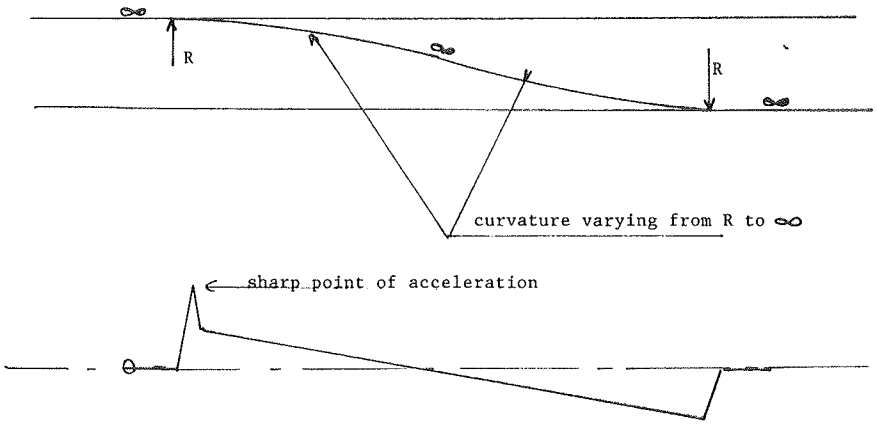

FIGURE 3 Diagram of centrifugal acceleration in a crossover with continuously varying radius.

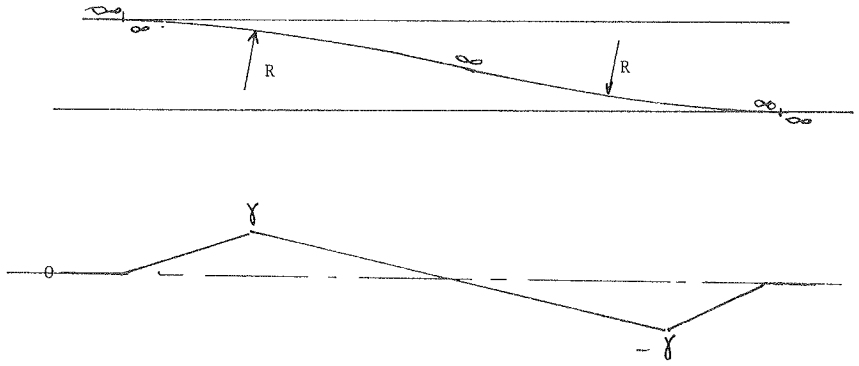

FIGURE 4 Centrifugal acceleration with double curvature variation.

POINT AND CROSSING TECHNOLOGY

Rails

The SNCF specifies UIC 60 rails (122 lb) with a 270 or 320 Brinell Hardness Number (BHN). The switch rails are machined in a special reinforced profile, called thick-web switch rail.

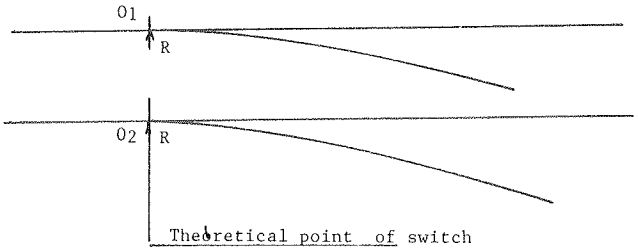

FIGURE 5 Theoretical point of switch.

Switches

In the previous section, the author mentioned the geometry where the diverted track is tangent to the main straight track at the point of the switch (see Figure 5). In fact, the physical point of the tongue is beyond the theoretical point of tangency, and the point of the curved tongue is straight when the thickness of the machined head is comprised between 3/32 and 7/32 in. (see Figure 6). Consequently, at the real point of the tongue, there is a small angle between the point and the stock rail (4.60 of a degree for an n.65). Nevertheless, this angle is small, and substantially inferior to the angles existing in straight switch points.

The gage on the diverted track is the same as on the main track, with the exception of small radii, or switches, or both, where low speed is acceptable on the diverted track. In such cases, two solutions can be used:

1. The theoretical point of the curved tongue is beyond the theoretical point of the straight tongue, the physical points of both tongues remaining square.

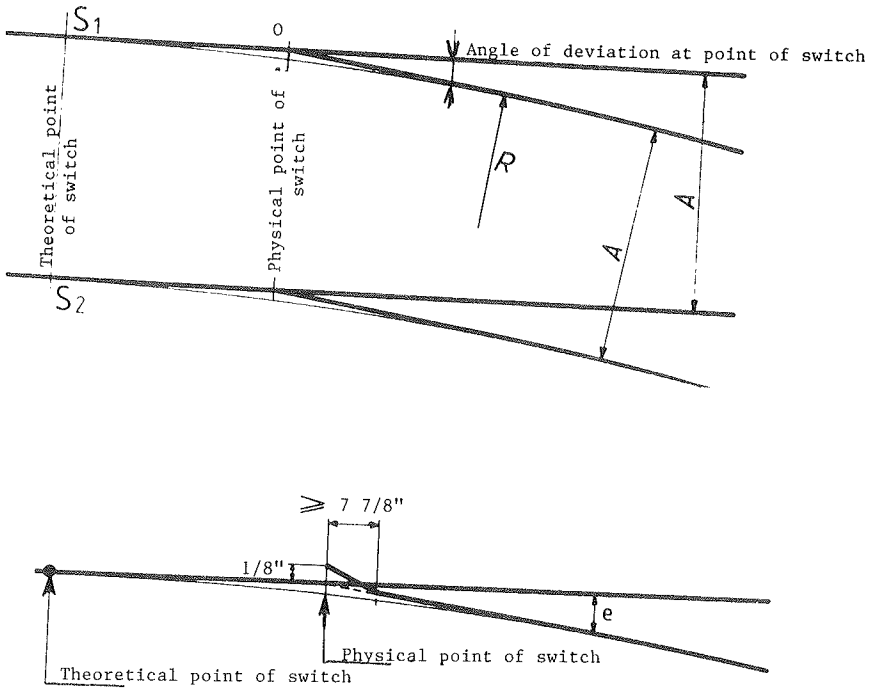

FIGURE 6 Angle of deviation at point of switch.

Consequently, the gage of the diverted track is wider, but there is a material swell at the gage line in the stock rail and at the point of the straight tongue (see Figure 7).

2. The theoretical point of the curved tongue remains beyond the theoretical point of the straight tongue, but, to avoid this drawback, it is wiser to cut the gage line of the straight stock rail with the gage line of the curved tongue. Consequently, the theoretical point of the curved tongue is beyond its physical point, which remains square to the physical point of the straight tongue.

This solution has the inconvenience to increase the value of the angle at the point of the curved switch. In any case, this value will be under 1 degree of angle (see Figure 8).

In the vertical plan, the points of switches are milled to avoid the wear by the wheel, in an area where the head of the tongue is thin. The undercutting and positioning of the point of the tongue under the running surface of the stock rail beyond the gage line guarantees that even sharp flanges will not force the point open.

The SNCF has generalized the use of flexible points for a long time. The movement of the tongue is allowed by the flexibility of the switch rail. There is no articulation or movement at the heel of the tongue, which is usually welded to the closure rail. It is also locked to the stock rail through a tightly bolted block and to the ties (see Figure 9). The minimum length of flexible switch point is 30 ft and the maximum driving effort is under 550 lb. The flexible switch points are milled in reinforced profiles with thick web, and heavier foot and head.

There are two types of switch rail: (a) high web

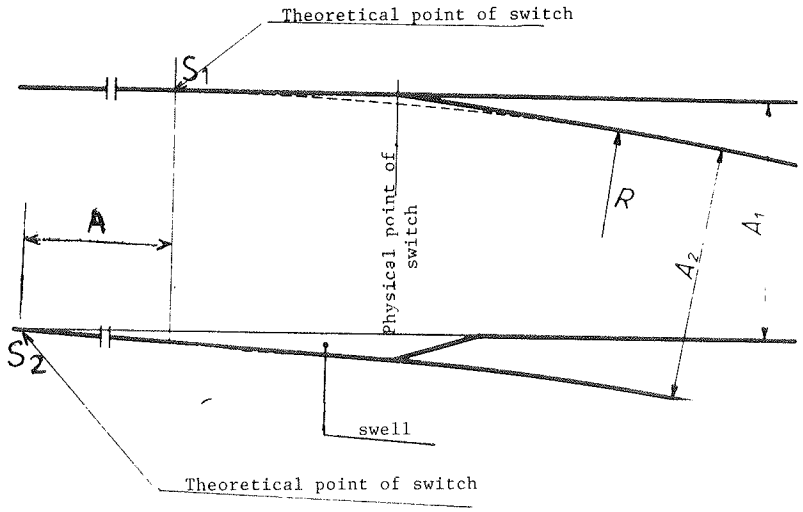

FIGURE 7 Gage widening on diverted track (Solution 1).

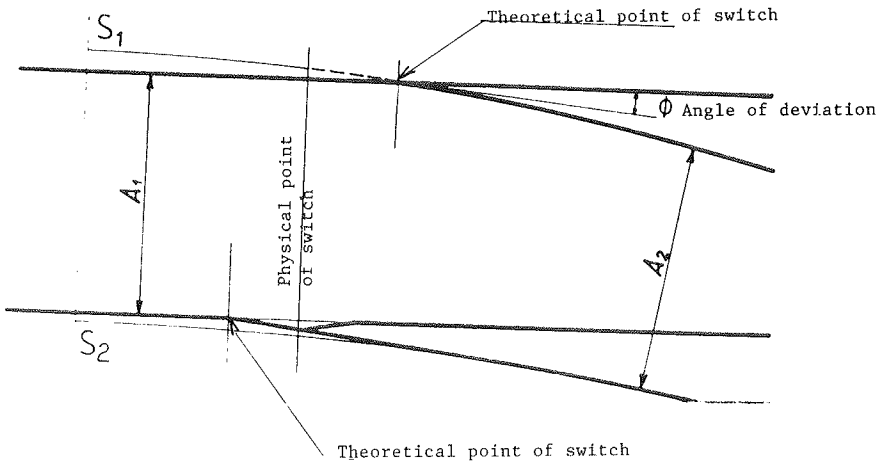

FIGURE 8 Gage widening on diverted track (Solution 2).

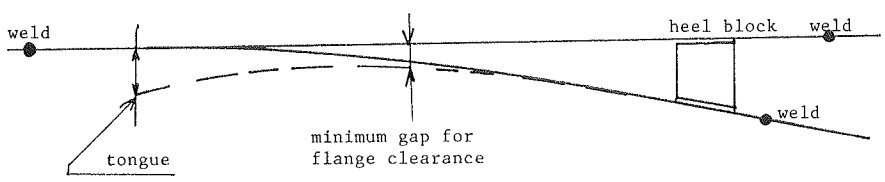

FIGURE 9 Diagram of a flexible thick web tongue.

(same height as the stock rail), and (b) low web (lower than the stock rail). In the high-web flexible switch point, both the switch and stock rails have the same height. The feet of both have to be machined to allow a proper contact. They are laid on flat sliding chairs, and the heel of the point is milled to the exact profile of the closure rail to allow easy field welding with standard equipment. Switch rails have also to be machined at the heel to increase the flexibility of the tongue (see Figure 10).

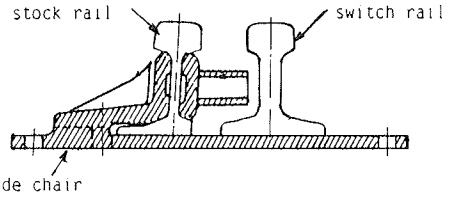

FIGURE 10 High-web switch rail.

The low-web flexible switch point is mostly used for long points. Because the switch rail is smaller than the stock rail, there is no need to machine the feet of both switch and stock rail. The foot of the switch rail comes over the foot of the stock rail, sliding on a two-level slideplate. The heel of the point is forged and welded to a piece of running rail to allow field welding to the closure rail (compromise weld) (see Figure 11). Flexible thick web points (low or high) allow for the elimination of the joint at the heel of the point and of the reinforcing bars with holes, bolts, and rivets.

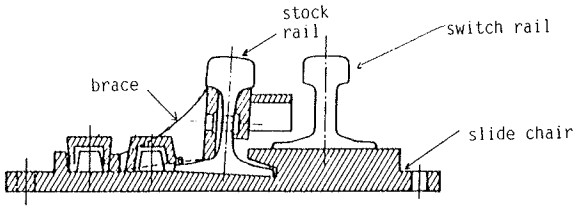

FIGURE 11 Low-web switch rail.

Crossings

Fixed-Point Frogs

The SNCF uses solid manganese steel frogs exclusively. The casting temperature is 1450°C. The longest units are 40 ft long. The thickness varies between 3/4 and 1 in. Heat-treated Hatfield steel with a manganese rate of 12 percent is used. The hardening is done on track by the vehicles and reaches an average value of 450 BHN. (Note that the French manufacturers are also able to preharden either by explosion or hammering.)

The running surfaces, the surfaces in contact with the ties, and the joint barring area are systematically milled, and holes are drilled.

Solid manganese steel frogs represent the large majority of frogs used on SNCF lines. They have proved to be highly reliable and long-lasting with low maintenance costs.

Movable-Point Frogs

The basic problem with crossings is the gap inherent to all frogs (see Figure 12); the lesser the angle, the longer the gap. The answer to this basic problem is the use of the movable-point frog, especially with heavy haul and high speed--that is, whenever it is necessary to suppress the gap and the shocks it generates.

The point of such frogs is generally milled in thick-web switch rail. It is machined, assembled, and adjusted to a solid cast manganese steel cradle. In cases like n.65 frog for the TGV, this cradle is assembled and bolted together in three pieces. The point moves in the cradle in coordination with the switch points. Interlocking between the switch and the movable point of the frog is necessary. The heel of the movable point is tightly locked to the cradle and the movement of the point is allowed by the flexibility of the rails (like flexible switch points).

Guard Rails

With convenient frogs, it is necessary to use guard rails to guide the axle through the proper track,

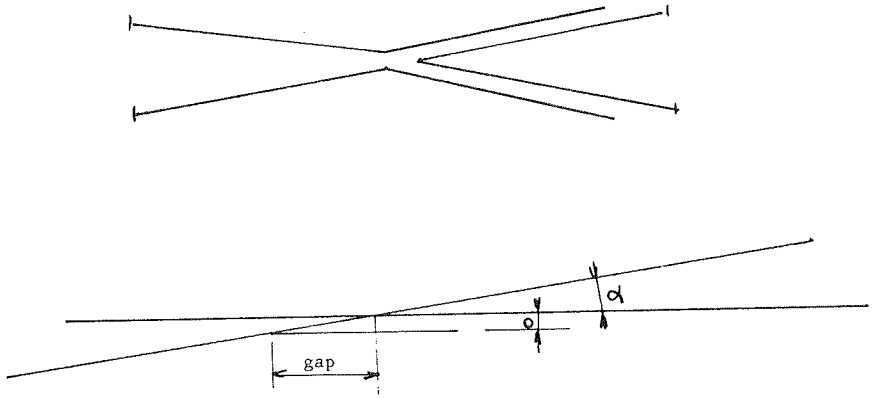

0 = flange clearance
α = crossing angle

$$\text{gap} = \frac{0}{\sin}$$

if $\alpha \searrow$ gap $\nearrow$

FIGURE 12 Gap value.

and to protect the frog point. There is no need for guard rails with movable-point frogs (see Figure 13). The SNCF has developed an interesting profile for guard rails, easily adjustable and replaceable, and with no link with the turnout rail. It has proved to be far more efficient than standard rails fixed to the turnout rails with blocks and bolts.

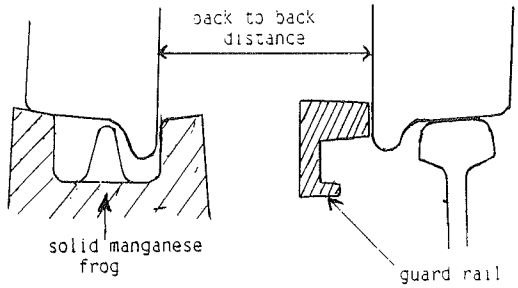

FIGURE 13 Guard rail.

Glued Frogs

Generally, frogs are glued into the continuous welded rail track (insulating glued joints), which allows for the necessary insulation related to track circuits. This also provides a continuous rolling surface with no gap and no risk of looseness. For the last 17 years, the SNCF has systematically welded turnouts into continuous welded rails. On main lines, expansion joints were suppressed with the exception of long bridges (movable ends).

It is necessary to anchor the turnout and junction rails into the ballast through the ties with resilient fasteners. Those fasteners have to avoid the canting and the creeping of the rail.

Ties

The SNCF prefers to use ekki wood ties under special trackwork. This African wood has a density of 1.2 and is far superior to oak as far as weight, hardness, and lifetime are concerned. In performance, it is more comparable to concrete ties than to soft or even hard wood.

Motors and Heating

Most switches are motorized and equipped with a locking or controlling system located on the stock rails. Both points move together since the motor is directly linked to the center of a rod located between the two points. When the length of the tongue is more than 30 ft, the motor is linked to two or more rods to ensure that the proper clearance between the open tongue and the stock rail is obtained. Also, additional control systems may be used to check that it is at this proper position. (Note that all these control and locking devices are linked to the signalling system. If anything goes wrong, the lights turn red to stop the train.)

The SNCF uses both gas and electric heating, depending on the situation of the track. Gas is cheaper but needs more maintenance, and is mostly used in stations and classification yards. Electric heating is more expensive but hardly needs any maintenance, and is used in remote places on main lines.

Diamond and Right-Angle Crossings, Double- and Single-Slip Switches

Central frogs (obtuse), end frogs (acute), and right-angle frogs for diamond and right-angle crossings are solid manganese steel, just like standard frogs for turnouts. Double- and single-slip switches are also designed and manufactured according to the same principles as the turnouts (i.e., solid cast manganese steel frogs and diamonds, thick-web flexible switch points, etc.). In some very special cases, solid manganese steel jump frogs are used.

CONSTRUCTION

Originally, most of the machining of the rails and cast manganese steel was done on conventional planing machines. Modern computerized planing machines are still used, but computerized milling machines are taking over. They are faster, more flexible, and more accurate; and allow long tables for the longest machining (120 ft for the switch point of the n.65 turnout of the TGV) with a tolerance of less than 0.01 in. The precutting and drilling of the rails is also done by computerized equipment. Timbers are preadzed and predrilled on computerized machines. They are thus ready for preassembly in the workshop before shipping to the site whenever this is necessary.

WELDING OF SPECIAL TRACKWORK INTO CONTINUOUS WELDED RAILS

Joints may be the main weakness in a track: the rolling stock and the wheels suffer, rail ends are beaten down, joint bars get loose, ties are stamped, and the ballast requires more frequent tamping. All this means shorter lifetime and heavier maintenance for both rolling stock and track: costwise, joints are a real nuisance. This is why, for more than 17 years, the SNCF has generalized continuous welded rails on its main tracks.

The key to welded track is the total rigidity of the rail/ties structure, and its fixed anchoring into the ballast (i.e., the fastening of the rail to the tie must remain square and restrain all creeping). The ladder structure of the rails and ties must be tightly anchored to the platform by a proper ballasting including high and heavy shoulders.

Forces in the closure rails are transferred to the turnout rails with increasing strengths at the switch heel. These increased strengths are restrained by longitudinal movements of the track skeleton in the ballast bed (see Figure 14).

With resilient fasteners, proper ties, and heavy ballasting, the experience of the SNCF railroads is such that the lateral forces are restrained, and the maximum longitudinal movement of the switch heel of ± 1/5 in. is perfectly acceptable.

NEW DEVELOPMENTS

Welded solid-cast manganese steel frogs have been on track for testing on SNCF main lines for several years. Several standard turnouts laid on prestressed concrete ties are also on track for testing under high-speed traffic (100 mph on the main track, 37.5 mph on the diverted track). The unique crosstie section has been studied so that the positive bending moment under the rail seat and the negative moment between rail seats support the dynamic efforts, whatever the position of the rails is. The unique cross section supports the highest bending efforts.

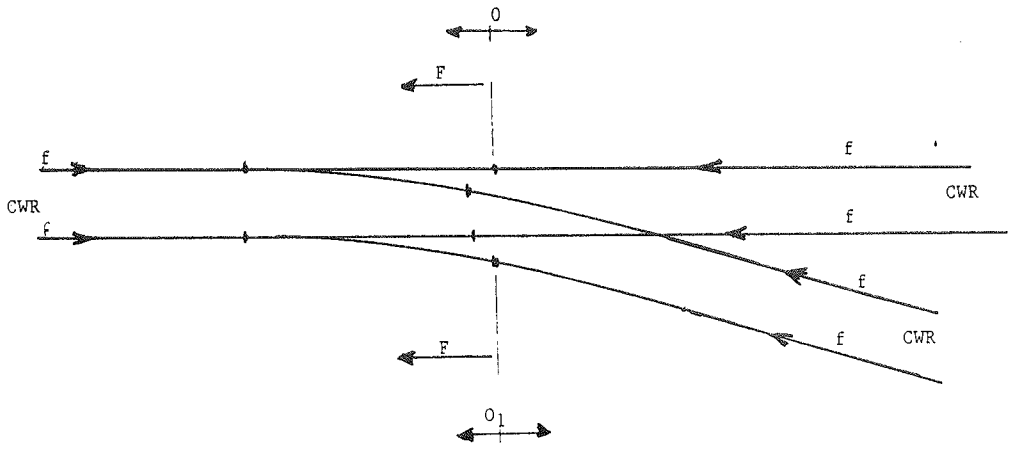

FIGURE 14 Welded turnout.

These turnouts are equipped with indirect fixation: a plate with a polyethylene high density pad underneath is first bolted into a plastic dowel anchored into the tie. The rail is bolted to the plate with another rubber pad in between, and with a resilient elastic fastener. The weight of the concrete ties is about twice the weight of creosote-treated oak ties. The concrete ties require a thickness of ballast of 10 in. minimum underneath. So far, turnouts equipped with concrete ties prove to have better stability and to require less leveling. The plastomere anchoring system and the rubber pads insulate the track.

CONCLUSION

The basic French technology for crossings, switches, and special trackwork has been described briefly. This technology results from constant studies to keep pace with this sensitive part of the track, while speed and axle loads have increased. Important factors such as safety and reliability have also been kept in mind. Both technology evolution and reduction in maintenance costs are necessary. Constant efforts have also been made to implement special trackwork maintenance as cost-effectively as possible, by means of mechanization and welding.

This special attention from the railroad engineers allows a wide range of applications such as

- Heavy loads of 30 gross tons or more (steel industry),
- A combination of high-speed (120 mph) passenger and freight trains, which is illustrated by the major part of the French network fixed plant,
- Commuter trains, rapid transit systems,
- A very high-speed dedicated line between Paris and Lyons (175 mph).

The French technology is the result of progressive engineering and permanent efforts to improve competition in coping with the demands of the transportation market.

Publication of this paper sponsored by Committee on Railroad Track Structure System Design.

Installation Factors That Affect Performance of Railroad Geotextiles

GERALD P. RAYMOND

ABSTRACT

The design of tracks on subgrades, which are identified as likely to be unstable if ballasted without the use of a separation layer, needs to have special attention paid to details that will prevent track pumping. These include, within the cross section, both good drainage practice and a suitably graded granular subballast or a granular-geotextile combination to function as a separation layer. Good drainage practice includes attention to side-ditch drainage, groundwater lowering, and internal track drainage. Particular attention is paid to internal track drainage because this topic has been found to receive insufficient consideration in numerous case histories investigated by the writer. Track that has been constructed with the deficiency of a suitable separation layer, or whose drainage is poor, or that is impacted at discontinuities of the rail such that segregation of fines from within the separation layer occurs, will need rehabilitation that should incorporate drainage improvement and possibly a heavy geotextile. These improvement requirements are explained for a number of typical locations where such problems are likely to occur. The requirements are illustrated with the description of a turnout pack geotextile used in Canadian National's Atlantic Region. Geotextiles must be correctly installed in order to maintain good track condition. Indeed, incorrect installation (particularly the lack of good drainage practice) may result in detrimental behavior.

Conventional ballasted railway track is essentially a loose assemblage of rail, crossties, ballast, granular subballast, and subgrade. These materials spread the load from the vehicle's axles and wheels to the earthen foundation beneath the track structure. In order that ballasted railway track ensure good riding qualities, there are two main requirements for adequate subgrade stability. First, a sufficient granular cover between the base of the crossties and the subgrade to reduce the loading intensity to a safe level for subgrade stability is required. Second, a granular filter blanket to be used in preventing fine-grained particles from the subgrade from penetrating upward into the ballast should be installed.

Both subgrade strength and the minimizing of particle migration are facilitated by good drainage practices. Such practices include (a) adequate side-ditch drainage to deal with surface water, (b) the lowering of the groundwater to increase the subgrade strength, and (c) the internal drainage or cross-fall sloping of subgrade and subballast surfaces to prevent water from seeping into the subgrade load-bearing area. Internal track drainage is by far the most difficult to ensure in rehabilitation work; however, in new construction, both the subgrade and subballast layers should be constructed with a 5 percent slope as illustrated in the typical cross section shown in Figure 1 for a two-track line.

In any corrective work involving the use of subballast or geotextiles, proper and adequate drainage must be incorporated into the planned maintenance. Although granular material for track support may be required to reduce the subgrade stresses to an acceptable level, geotextiles within the track structure should be selected only on the basis of their handling strength requirements and their ability to separate, filter, and facilitate drainage. Of particular importance is the geotextile's ability to facilitate drainage by transmitting water within its plane (1). Reinforcing can only occur if deformations are permitted to tension the geotextile, thus generating its tensile strength. Deformation failures are unacceptable as good design. Discussion of such deformation failures along with the depth of granular cover is beyond the scope of the work reported herein.

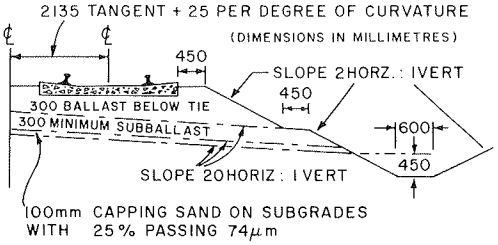

FIGURE 1 Typical track cross section for new double track construction.

UNSTABLE SUBGRADES CAUSED BY DEFICIENCY OF SEPARATION REQUIREMENTS

Irrespective of the amount of compaction a subgrade or a subballast receives during construction, some degree of permanent deformation occurs due to repetitive traffic loading. This loading is greatest below the rail causing the formation of a depression, which, if deep enough, would collect water during a

Department of Civil Engineering, Queen's University, Kingston, Ontario, Canada K7L 3N6.

rainstorm. On good subgrades, this depression may only be millimeters deep, but this could be sufficient to cause water ponding and considerable softening of any fine-grained subgrade soils. In order to prevent silt-sized fines from penetrating upwards from such subgrades, a separation layer will be required. Such a layer may be a subballast that incorporates nonplastic sand-sized materials grading down to the 74-micron (No. 200) sieve or a nonplastic sand-sized granular capping material. To be effective, whatever material is used must act as a filter to prevent subgrade fines from being vibrated or pumped upwards, or both. Similarly, subballast or capping sand should be either graded to prevent its finer particle sizes from vibrating upwards into the ballast, or a geotextile should be placed on the subballast or capping sand to prevent such movement (2,3). It is the author's opinion that the geotextile, if used, should be of a nonwoven type (1).

Geotextiles have been receiving considerable prominence as a possible alternative material for performing the separation function (4,5). Unfortunately, because of their equivalent opening size in relation to silt and clay-sized particles, if used alone, they only act as a partial filter to such silt- or clay-sized fines. Most geotextiles, if used alone, only retard ballast fouling. They are, however, beneficial where granular material is scarce or expensive. Geotextiles are also used on soft subgrades during new construction as reinforcement or as a working platform. However, as already noted, discussion of such reinforcement use is beyond the scope of the work presented herein.

In highway construction, modified clay layers are sometimes used as a subbase to perform the function of a separator layer. Unfortunately, dynamic loading experienced within a railway track support fill is much greater than that generally experienced by any highway support system. Impact loading from flat wheels can impose dynamic loads several times those resulting from static loading (6). Modified clay subgrades, which form a brittle, hard subgrade surface, are therefore generally subject to cracking, which, during wet conditions, results in erosion of the underlying subgrade. Consequently, they must be covered by a nonplastic granular filter material.

Should a granular subballast lacking finer sizes be used on a silt or clay subgrade, even if both are well compacted, summer dry weather may be expected to cause drying of the surfaces in contact with the subballast. Wetting after such dry weather may then be expected to cause, on the surface of the subgrade, collapse of the soil structure, which accelerates the erosion of fines upwards into the subballast. Over time, such erosion would be expected not only to foul the substandard subballast but also to foul the ballast. Once fouled, both materials may be expected to heave during freezing weather.

The importance of using a suitably graded subballast material on new construction projects, such that the material would remain unfouled by eroding fines from any underlying material and also be suitably graded (so as not to itself be vibrated upwards thereby fouling the ballast), cannot be overstressed. This material must be nonplastic so as to deform (or collapse) easily by flowing and not permit vertical fractures. On rehabilitation work, it is generally too expensive to undercut sufficiently to incorporate a subballast layer. Thus, geotextiles can be of great benefit (when correctly installed) and are often found to be the only economical solution.

GENERAL METHODS OF REHABILITATION OF FOULED BALLASTED TRACK

Rehabilitation of fouled ballast generally takes one of three forms. In the first form, undercutting of the track is performed using (a) a chainlike belt feeding down under one side of the track and up the other side, or (b) a chainsaw-type blade that extends under the track from one side only. In the belt technique, dirty ballast may be cleaned by sieving and the cleaned ballast returned for future use. Alternatively, like the chainsaw-type technique, ballast may be completely wasted. Where geotextiles are used, it is general practice to waste the ballast because it is difficult to install geotextiles between the undercutter chain and the discharge chute of the cleaned ballast.

In the second form, the track is removed by a crane, or by being pulled out of position, or by some mechanized removal equipment. Typical of the mechanized removal systems are the various switch and panel exchangers (7,8).

The third form of surface preparation for geotextiles involves the ploughing or sledding of fouled ballast. In the former technique, the plough's blades remove the crib ballast (i.e., the ballast above the base of the tie) and a small distance (about 50 mm) of ballast below the existing crosstie base level (9). Alternatively, the crib ballast may be flattened by sledding (10). When either ploughing or sledding is used, the track elevation (after rehabilitation) is raised as much as 300 mm, particularly if a geotextile is installed.

PURPOSE OF GEOTEXTILES

The accumulated fines in the dirty ballast may have come from many sources including subgrade migration, impermeable fines in the original subballast source, aggregate breakdown of either subballast or ballast, transported fines in flood water, freight car droppings, windblown sources, locomotive sand, and so forth. Geotextiles will not prevent fines from foreign sources such as freight car droppings, windblown sources, and so forth from contaminating any cleaned ballast but are of value where the foreign source has already contaminated the track support and action has been taken to prevent or minimize further foreign source contamination.

In the presence of excess water, most contaminating fines below a track, subject to repetitive wheel loads, will be pumped and migrate upwards through the track structure. The more free water there is, the faster (in general) the upward migration of fines. Thus, drainage improvement (whether the improvement of side-ditch drainage, or the lowering of the groundwater, or internal track drainage) is always the first and most essential item in any subgrade stabilization work. This is true whether or not geotextiles are used.

Special attention should be given to the undercutting of long lengths of track where, as shown in Figure 2, a "canal" effect is produced by undercutters. If, after or before undercutting, the shoulder ballast is not removed and cleaned, drainage cannot occur from the load-bearing area to the side ditches. Where possible, the shoulder undercutting should be deeper than the track undercut, as shown in Figure 3. On flat and marshy land, French drains (shown in Figure 4) may be required. Similarly, as shown in Figure 5, short lengths of undercut track such as grade crossings that are not subsequently (or during undercutting) provided with drainage will result in a "bathtub" effect. Grade crossings also suffer from the disadvantage of lacking drainage along the width of the highway. They should be provided with French drains through the crossing, as shown in Figures 6 and 7, that discharge into side ditches beyond the crossing's limits. Geotextiles should never be used as a substitute for good drainage. Indeed, if the geotextiles are in-

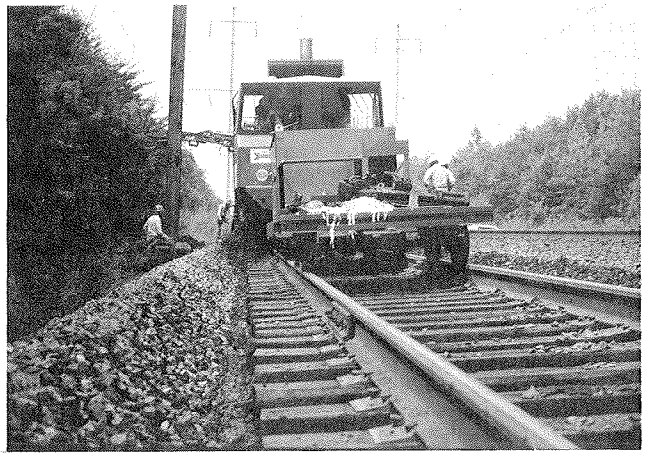

FIGURE 2 Canal effect created by undercutting operation before removal of shoulder ballast.

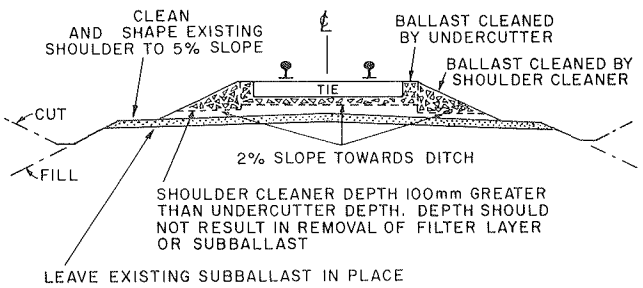

FIGURE 3 Recommended undercutting and shoulder ballast rehabilitation.

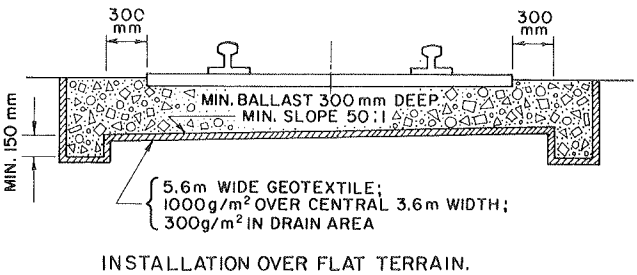

FIGURE 4 Recommended undercutting with French drains over flat terrain.

stalled without an ability to drain and discharge by gravity to side ditches or French drains, they will, as shown in Figure 8, facilitate the retention of water within the load-bearing area of the track. Water that is trapped within the load-bearing area of the track can be expected to provoke or stimulate the pumping phenomenon along with the possibility during cold weather of frost heave.

Geotextiles for tangent track have found their greatest use in terrain that is poorly drained, such as flat and marshy country. They are also being used at locations where it is difficult to maintain good drainage or at locations that have high localized impact loadings and where the geotextile, by facilitating drainage, reduces the amount of maintenance required. This is particularly true of places such as grade crossings, diamonds, turnouts, and track structures.

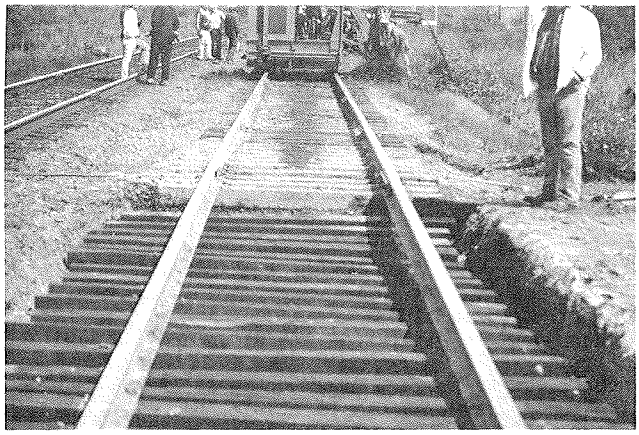

FIGURE 5 Bathtub effect produced at grade crossing rehabilitation before construction of outlet drains to ditches.

BASIC FUNCTIONAL REQUIREMENTS OF GEOTEXTILES

In general, when dealing with track rehabilitation problems, the track has been in existence for some time and excessive subgrade settlements have ceased. The use of a geotextile's strength for subgrade reinforcement will not, under these circumstances, be a major consideration. Rather, they should be highly abrasion-resistant and durable to withstand the harsh environment of ballast particle movement on ballast or subgrade aggregate. On undercut, ploughed, or sledded track in which the rail remains in place during rehabilitation, the prepared surface to receive a geotextile, as shown in Figure 9, will contain ballast particles either lying on the surface or protruding from the surface. Although raking would remove some of these protrusions, the prepared

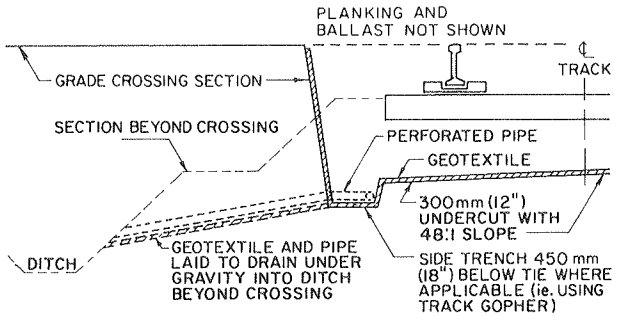

FIGURE 6 Typical grade crossing rehabilitation with geotextile.

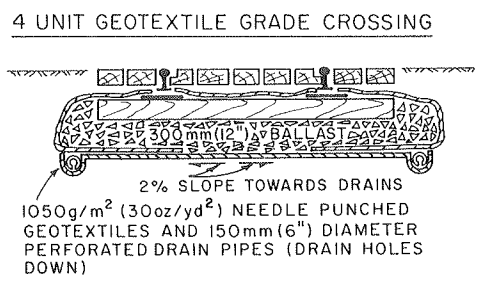

FIGURE 7 Recommended grade crossing rehabilitation with encapsulating geotextile to minimize fouling by salting and sanding.

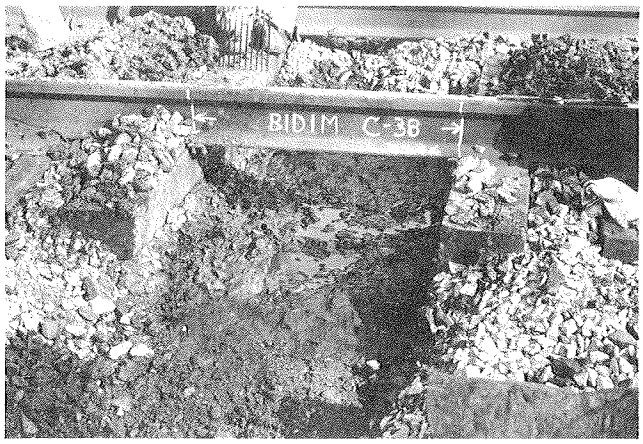

FIGURE 8 Effect of installing a geotextile without adequate drainage.

surface will remain rough and any geotextile placed on it will not only have to be abrasion-resistant, but should also have the ability to elongate around such protrusions without puncture or tear. If punctured or worn through, the geotextile will clearly lose some of its ability to filter and separate.

The ability to transmit water within the plane of the geotextile has been observed on a number of installations during the passage of a train. When an axle or group of axles passes a location, the track support compresses. If saturated or near-saturated, water will either escape or try to escape along the path of least resistance. Geotextiles with in-plane permeability offer such a path even when placed in sand or broadly graded gravel layers. Water pumping from the edge of a geotextile with the passage of each group of axles has been observed on a number of installations. Such water must be permitted to drain into the side ditch and not back into the load-bearing area of the track.

From the material already presented, it is apparent that the basic functional requirements of geotextiles in railroad bed rehabilitation technology are the capacity

1. To drain water away from the track roadbed (on a long-term basis, both laterally and by gravity) along the plane of the geotextile without build-up of excessive hydrostatic pressures;

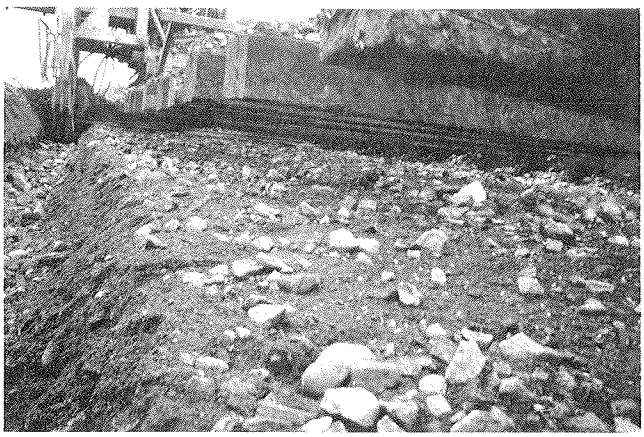

FIGURE 9 Typical condition of undercut surface prepared to receive geotextile.

2. To withstand the abrasive forces of moving aggregate caused by the tamping and compacting process during cyclic maintenance, tamping during initial compaction, and by the passage of trains on a frequent basis;
3. To filter or hold back soil particles while allowing the passage of water;
4. To separate two types of soils of different particle sizes and gradings that would readily mix under the influence of repeated loading and of water migration; and
5. To have the ability to elongate around protruding large angular gravel-sized particles while resisting rupture or puncture.

SHOULDER REMOVAL FOR DRAINAGE

When fouled ballast is removed from a track structure, it is important to achieve good drainage in the track shoulders. As shown in Figure 3, the ballast shoulders should be removed and cleaned or replaced to a level below the freshly prepared track surface. Care should also be taken to see that the excavated surface is sloped toward the side ditches. Where shoulder replacement is not practical, a French drain or equivalent should be used. Dirty ballast will retard lateral drainage to the side ditches or French drains unless care is taken to adequately remove the spoiled pile of dirty ballast at the shoulder, particularly when the spoil has been discharged on the shoulder. Another undesirable feature that has been frequently observed is the backfilling of undercutter trenches (typically produced by turnout or switch undercutters) with dirty ballast on the pretext of cost savings on ballast replacement. Unless water can drain away from the track-bearing area, it will pond within the track structure, softening the trackbed and facilitating its return to the original fouled condition. Such trenches should be used to advantage and converted into French drains. In multitrack areas, it may be necessary, as shown in Figure 4, to excavate additional French drains on both sides of the track. Underdrains should also be used to discharge the central French drains to the side ditches if side ditches exist. Excavated soil should not be deposited on the track because this allows water to wash the fouling fines back into the French drains or into the track-bearing area.

If, in cutting the trench, the subballast is removed so that the bottom of the trench is situated in the subgrade soil, a geotextile should be placed on the trench bottom and sides or a correctly graded subballast placed on the bottom of the trench as a separator. The geotextile should be engineered to be compatible with the surrounding soil so as to prevent or minimize fouling or in-filling. The trench should then be backfilled with clean ballast aggregate to aid side drainage. Fouled spoil that has been previously removed from the trackbed should not be used within the drainage trench. It is recommended that the depth of clean ballast within the trench be a minimum of 100 mm (4 in.) below the prepared undercut surface to allow for quick drainage away from the area below the track ties. Again, the fouled ballast should be deposited below the prepared trench bottom or removed completely so as to ensure good side drainage.

INSTALLATION BELOW LOCAL GROUND ELEVATION

In locations such as are shown in Figure 4, where the geotextile will be installed below the local ground elevation, steps should be taken to guard against the inflow of water from the ground surface

on any sides of the track that may be elevated above the geotextile. A number of installations inspected have shown that the ballast above the geotextile and the geotextile itself may be fouled with fines from beyond the end of the ties. This fouling results from water draining laterally from above the undercut elevation into the track structure, transporting fines into the ballast. To prevent this, a French drain may be installed along the edge of the track, which is lined or encapsulated in a geotextile. The geotextile should be selected so as to filter the inflow of water from above and beyond the prepared surface. The prevention of such water inflow into the track-bearing area is an added reason for establishing a trench along the side of the track during the undercutting process. In flat land areas, it may be necessary to construct soak-away pits away from the track structure to allow drainage of the water from the French drains.

INSTALLATION AT BRIDGE ABUTMENTS

A typical bridge abutment rehabilitation is shown in Figure 10 and incorporates a geotextile and French drain combination to increase drainage rates, decrease pumping, and generally increase track stability at the transition location from soil subgrade to bridge abutment.

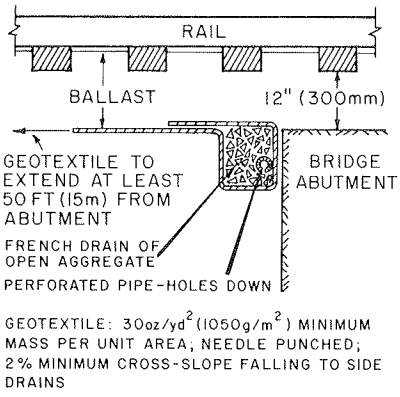

FIGURE 10 Typical method of rehabilitating bridge abutments using geotextiles.

INSTALLATION AT GRADE CROSSINGS

Grade crossings foul because of a lack of adequate drainage in the central region of the crossing and because of winter sanding of highways, as revealed by the removal of the crossing planks shown in Figure 11. High-impact loads may be expected at the crossing upon entering and leaving the more rigid track structure. The loads continue to overstress the track well beyond the grade crossing because of a harmonic motion established by the rolling stock. The higher stress placed on the subgrade will quite often generate localized pumping. For this reason, it is important to achieve a dry, stable subgrade at grade crossings, and it is also desirable to achieve similar conditions roughly 15 m (50 ft) to either side of it.

Drainage at a grade crossing is generally parallel to the rails until the road pavement and shoulders have been cleared. The drainage flow should then be turned perpendicular to the track to discharge into the ditch, or into a French drain leading to a soak-away pit. Perforated drain pipes are sometimes used and may be wrapped in a geotextile or purchased pre-wrapped. Either wrapped or unwrapped, the pipes will assist the flow of water from within the crossing to the ditches beyond the crossing. The pipes should be laid with the line of perforations pointing vertically downward. Such pipe can be placed on the geotextile in the trench prepared by the bucket wheel of the undercutter. The ends of the perforated drainpipes and the crossing geotextile should then be laid with a sufficient fall towards the side ditches as shown in Figures 6 and 7. Whether perforated pipes are used in the crossing nor not, it is advisable to remove the shoulders at the corner of the crossing and turn the geotextile ends down so that the geotextile facilitates drainage under gravity toward the side ditches as shown in Figure 6.

FIGURE 11 Typical condition of fouled grade crossing having inadequate drainage at centerline.

In cold weather climates, where it is common to salt and sand highways, including grade crossings, some railroad engineers require the grade-crossing geotextiles to encapsulate the ballast to prevent or minimize surface fouling from the salt and sanding process. Such an encapsulating geotextile is shown in Figure 7.

INSTALLATION OF TURNOUT PACK GEOTEXTILE

In the Atlantic Region of the Canadian National Railways (CN), a large number of turnout pack geotextiles have been installed since 1983. It was found that geotextiles are best installed using the same work gang. On August 27, 1985, the author was present at the site of a geotextile installation performed by CN's Altantic Region geotextile work crew. The geotextile was delivered to the site the previous day. Vandals had already removed the geotextile's weatherproof black polyethylene packaging. Fortunately, it did not rain overnight, otherwise, the geotextile would have absorbed water, which would have resulted in a dramatic increase in weight, making the geotextile difficult to handle. The delivered weight of these turnout packs when dry is between 300 and 500 kg. Because they have a porosity between 80 and 90 percent, saturation can increase their weight by a factor of 4, resulting in a saturated weight of between 1200 and 1500 kg, so that, where possible, delivery of the geotextile should be made on the day of installation. The turnout pack rolls are approximately 7 m long and were handled by six persons using three crowbars. The crowbars were

positioned, one near each end of the roll and one near the center. One person was situated at the end of a crowbar.

Work started at 10:10 a.m. local time as soon as a local passenger train had passed through the turnout to be rehabilitated. A ballast regulator first removed the ballast from the end of the ties to the ditch to a depth about 200 to 300 mm below the base of the tie on the turnout track side of the turnout. A passing siding ran parallel to the main-line track on the other side of the turnout so that ballast removal was not possible on that side. The ballast regulator completed its job in about 10 to 15 min, after which the gopher undercutter was moved to a position on the turnout about 9 m from the point of the turnout. The undercutting sequence is shown in Figure 12. The bucket excavator proceeded to excavate a trench about 4 m long and 700 mm deep so that the blade of the undercutter could be positioned to its full depth of about 300 mm below the base of the ties in order to start the undercutting operation.

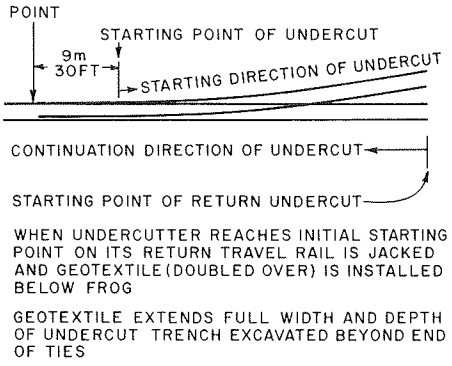

FIGURE 12 Turnout undercutting sequence observed on CN's Atlantic Region.

The track was then undercut to approximately below the closest tangent rail. This procedure continued until the undercutter had gone along the turnout track sufficiently so that its blade was extended fully under the turnout track and was well clear of the end of the ties of the tangent track. Measurements taken below both ends of a tie indicated that, although the undercutter blade was fixed horizontally during undercutting, it flexed sufficiently that the prepared surface had a 2 percent slope towards the bucket-made trench.

The undercutter was then repositioned on the tangent track with its bucket wheel swung through 180 degrees so as to undercut from the other side of the turnout. A 4-m trench was made by the bucket wheel to lower the undercutting blade below the tangent track portion of the turnout. Undercutting continued to well beyond the point of the turnout. When the undercutter had approximately 12 m more undercutting to reach the point of the turnout, the geotextile was unrolled so it could, if necessary, be shortened or positioned to fit the expected final undercut area of the turnout. Once this was done, the turnout point end of the geotextile was lifted and pulled to the wide-end portion of the turnout so that the geotextile lay doubled over for half its length. Rail jacks were then installed to raise the half length of turnout, which was to receive the doubled-over geotextile. The doubled-over geotextile was manually pulled under the wide end of the turnout as seen in Figure 13. Once in position with its edges

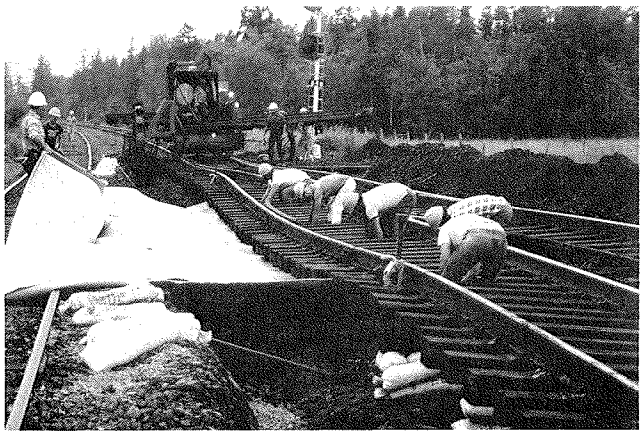

FIGURE 13 Placement of doubled-over geotextile below half area of turnout.

trailing into the ditch left by the bucket wheels, the upper layer of the geotextile was fanfolded toward the center of the turnout so that about three-eighths of the geotextile was ready to receive ballast.

Cotton bags, approximately 150 mm in diameter and 700 mm long, filled with fine-gravel-sized crushed aggregate, were then placed on the geotextile as spacers between the geotextile and the base of the crossties. Two bags were placed at each end of about every fourth to fifth tie so that when the rail jacks were removed, the bags supported the ties approximately 300 mm above the geotextile. Once the ballast bags were in place, the track jacks were released and the track gently lowered down onto the ballast bags. The jacks were then moved and repositioned. One pair was positioned at the end of the fanfolded geotextile on three ballast bags placed side by side, as shown in Figure 14. Figure 15 shows the turnout during the rail jack relocation procedures. The track was raised and the fanfolded portion of the geotextile was unfolded. It was not possible to extend the fanfolded portion fully in one unfolding so the procedure was repeated several times. Consideration could have been given to installing the turnout pack in two halves with a double heat-jointing seam. This would have simplified installation.

Once the turnout had been completely undercut, the geotextile completely extended, and ballast bags placed to support the track throughout its length, the turnout was ready to receive ballast. The ballast car first unloaded ballast into the French drain

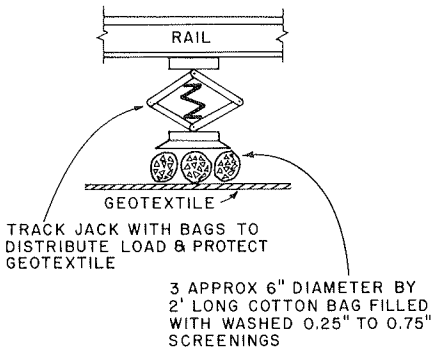

FIGURE 14 Method of protecting geotextiles from high imprint pressure of rail jack bases.

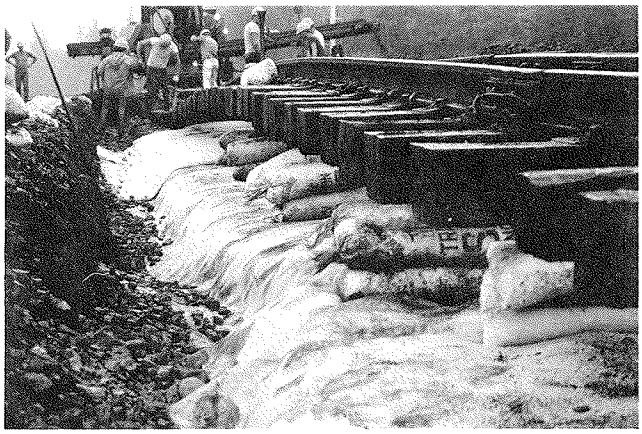

FIGURE 15 Geotextile in position below half of turnout with relocation of rail jacks taking place.

trench area beyond the end of the crossties, as shown in Figure 16. It then deposited ballast across the full undercut area. Ballast was placed until the cribs of the ties were overflowing. The turnout was left in this condition and traffic allowed through the turnout until the next day. On the next day, not only was the tamping and cleanup completed to permit traffic to proceed at the posted speed, but perpendicular trenching was performed at both ends of the bucket-made trench on both sides of the track so as to extend to the side ditching in a manner similar to that shown in Figure 17. In the case of the tangent turnout side-trench, the perpendicular trenching involved was under a passing siding. These four perpendicular trenches clearly benefit the exit of surface water during heavy rainstorms.

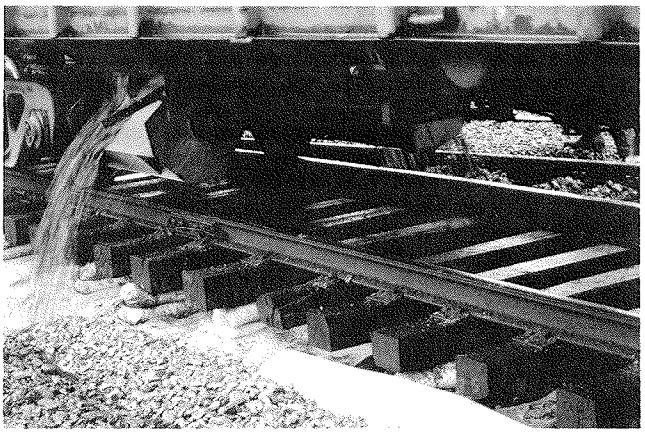

FIGURE 16 Filling French drain of turnout with ballast showing track supported by ballast bags.

DEPTH OF INSTALLATION

One of the contributing factors to a geotextile's performance in-track is the depth at which it is placed below the base of the ties. It is well known that the intensity of pressure generated from a standard wheel load is distributed through the track structure so that the pressure intensity decreases with depth. Depending on the abrasive or puncture resistance of the geotextile, or both, being installed, there should ideally be an optimum depth

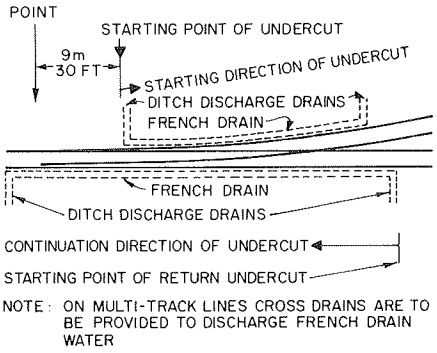

FIGURE 17 Illustration of positioning of perpendicular trench.

where the geotextile can be installed during a track upgrading process so that little or no damaging effects of ballast punctures and abrasion occur, thus prolonging the life of the geotextile. From a practical standpoint, abrasion depends on the deformations occurring at the geotextile level and, thus, subgrade modulus. The subgrade modulus is, to a large extent, controlled by track drainage, since soil behavior is very much dependent on soil suction and, thus, moisture content. Good drainage by the geotextile should result in decreased moisture and increased track modulus. Such an observed increased in track modulus when geotextiles are used is often incorrectly attributed to the geotextile's reinforcement effect. In fact, for reinforcement to occur, there must be an extension of the geotextile and, thus, a relatively large settlement of the subgrade. Such settlement is, in the opinion of the writer, undesirable. Rather, the geotextile should stiffen the subgrade by facilitating the drainage of moisture, thus reducing any chance of subgrade deformation and reducing any need for reinforcement. Increased track modulus also should mean reduced movements within the ballast and less abrasion to the geotextile from such movements.

To assess the effect of abrasion with installation depth, data were obtained from several sites installed with a needlepunched resin-treated geotextile--all having a mass per unit area between 450 and 510 g/m^2. After excavation, the estimated damage to each geotextile obtained from each location was obtained by measuring the percentage of completely worn-through areas in the worst 300- x 300-mm square section (generally below the intersection of the rail and tie). These results have been plotted against the measured geotextile's depth at the time of excavation in Figure 18. The values range from 0.3 percent at a depth of 350 mm to 4.1 percent at a depth of 175 mm. The results show that the amount of damage that the geotextile received increased as the depth of ballast between the crosstie base and the geotextile was reduced. The damage was also major once the depth of ballast was less than 200 mm. Below 250 mm, the amount and rate of change in damage was small.

Also measured on the same geotextiles was the amount of soil that penetrated each geotextile sample. This was estimated as the soil content (weight of internal soil divided by weight of fiber after cleaning expressed as a percentage). These results are shown plotted against excavation depth in Figure 19. From Figure 19, it may be seen that considerable geotextile fouling occured once the geotextile depth was less than 200 mm below the tie base.

The results shown in Figures 17 and 18 suggest that a depth of about 250 mm should be used as a minimum depth for the installation of geotextiles.

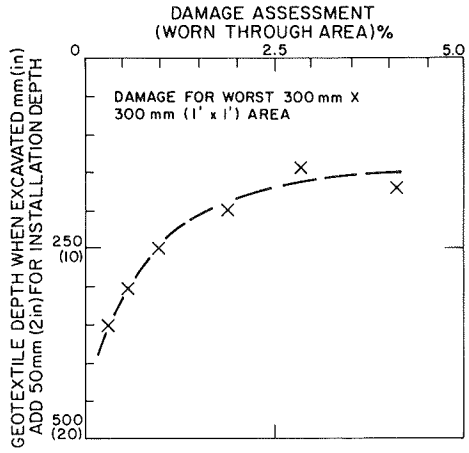

FIGURE 18 Depth of geotextile-abrasion assessment for recovered track geotextiles.

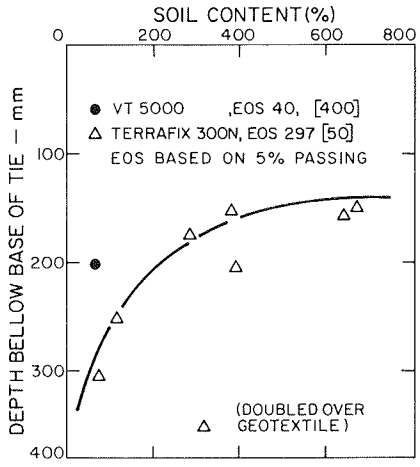

FIGURE 19 Depth of geotextile-soil content assessment for recovered track geotextiles.

Assuming that a 50-mm increase in ballast depths occurs during tamping, then a minimum 200-mm depth of ballast should be placed on a geotextile before the tamping of a rehabilitated ballasted track in which a geotextile has been installed. Where practical, a 300-mm ballast depth is recommended.

SUMMARY AND CONCLUSIONS

Design of tracks on subgrades identified as likely to be unstable if ballasted without the use of a separation layer (i.e., subgrades containing 25 percent or more passing 74 μm sieve) will need to incorporate within the cross section both good drainage practice (see Figure 1) and a suitably graded granular subballast or a granular-geotextile combination to function as a separation layer.

Track that has been constructed with the deficiency of a suitable separation layer, or whose drainage is poor, or that is impacted at discontinuities of the rail such that segregation of fines from within the separation layer occurs will need rehabilitation that should incorporate drainage improvement and, possibly, a heavy geotextile.

Particular attention needs to be directed to improving internal track drainage. This involves the sloping of interface layers or undercut surfaces toward drainage ditches or French drains. In particular, the creation of the canal or bathtub effects during rehabilitation should be avoided. Proper and adequate perpendicular drains to prevent water accumulating in the track structure or in French drains should be incorporated in rehabilitation work.

Recommended procedures for undercutting track without the use of geotextiles are shown in Figure 3. Rehabilitation with geotextiles is shown in Figures 4, 6, 7, and 10. The sequence for undercutting and installing geotextiles below turnouts is presented in the text and is shown in Figures 12 through 17, inclusive.

Highlighted is the incorporation of French drains in areas of the track difficult to drain. In particular, the discharge end of any installed geotextile must be located below the level of the undercut load-bearing area.

It is recommended (see Figures 18 and 19) that a minimum depth of 200 mm of ballast should be placed on a geotextile before the tamping of a rehabilitated ballasted track in which a geotextile has been installed. Where practical, a 300-mm ballast depth is recommended.

ACKNOWLEDGMENT

The work reported herein was performed under a Canadian Institute of Guided Ground Transport contract funded by CN Rail, CP Rail, and TDC of Transport Canada. Acknowledged is the kindness shown by R. Gillespie and B. Beaton of CN Rail who permitted excavations to be performed in CN's Atlantic Region.

REFERENCES

1. G.P. Raymond. Research on Geotextiles for Heavy Haul Railways. Canadian Geotechnical Journal, Vol. 21, 1984, pp. 259-276.
2. G.P. Raymond. Subgrade Requirements and the Application of Geotextiles. Proc., Conference on Track Technology for the Next Decade, Thomas Telford Ltd., London, England, 1984, pp. 159-166.
3. G.P. Raymond. Track Support Must be Right if Concrete Sleepers Are to Survive. Railway Gazette International, Vol. 140, 1984, pp. 528-530.
4. J.E. Newby. In Depth View of Geotextile Subgrade Stabilization. Railway Track and Structures, Vol. 76, No. 6, 1980, pp. 22-23.
5. J.E. Newby. Southern Pacific Transportation Co. Utilization of Geotextiles in Railroad Subgrade Stabilization. Proc., Second International Conference on Geotextiles, Vol. 2, Las Vegas, Nev., 1982, pp. 467-472.
6. Effect of Flat Wheels on Track and Equipment. Bull. 53. American Railway Engineering Association, Washington, D.C., 1952, pp. 423-448.
7. Panel Renewal System Spurs NEC Interlocking Work. Railway Track and Structures, Vol. 76, March 1980, pp. 27-30.
8. S and P Exchanger Simplifies Seaboard Track Work. Railway Track and Structures, Vol. 79, Sept. 1983, pp. 32-34.
9. Track Plows Modified to Boost Output. Railway Track and Structures, Vol. 77, Jan. 1981, pp. 42-44.
10. G.P. Raymond. New Options in Branch Line Rehabilitation. Progressive Railroading, Vol. 27, March 1984, pp. 71-74.

Publication of this paper sponsored by Committee on Engineering Fabrics and Committee on Railway Maintenance.

In-Track Performance of Geotextiles at Caldwell, Texas

S. M. CHRISMER and G. RICHARDSON

ABSTRACT

A performance test of geotextiles in track was performed jointly by the Monsanto Corporation and Southern Pacific Railroad. The test site at Caldwell, Texas, was chosen because of the poor subgrade conditions. The track was instrumented to determine the influence of the geotextiles on track behavior. The instrumentation measured the extent of the anticipated geotextile functions of reinforcement, subgrade moisture transport, filtration, and separation. There was no evidence of reinforcement or moisture transport, but filtration and separation appeared to be the main advantages.

In November 1977, an extensive field investigation was begun of geotextile performance and the associated influence on track behavior, which was a joint project of the Monsanto Corporation and Southern Pacific Railroad. The test site was located in Caldwell, Texas, in an area with significant track maintenance problems resulting from poor subgrade performance. The subgrade soil is comprised of a medium-to-soft consistency, highly expansive clay, which typifies some of the worst soil conditions under which geotextiles are placed.

The geotextiles were installed in a new siding constructed alongside the main line track. New track construction was selected for the test to eliminate problems related to ballast pockets and undercutting programs that would have been experienced if the fabric and instrumentation had been placed in existing track. The main line carries about 10 million gross tons (mgt) per year, which is considered moderate for a main line track.

The test was planned with the objective of determining the extent to which fabrics perform the anticipated functions of (a) reinforcement, (b) subgrade moisture transport, (c) filtration, and (d) separation. Extensive instrumentation was required to differentiate the role that each mechanism played in a given test section. Figure 1 shows the subgrade instrumentation that was installed in each section.

TEST SECTION CONDITIONS

The existing and design grades at each of the six individual test sections are shown in Figure 2. Test Sections 1 through 4 were constructed with nonwoven fabrics placed on the subgrade. The properties of the geotextiles are given in Table 1. Section 5 was a control section with no fabric, and Section 6 was a cement-stabilized zone. Section 6 was used to compare the performance of a conventional, but expensive, method of subgrade stabilization with the performance of the various fabric sections. The length of each of the fabric sections and the cement-stabilized section was 300 ft, whereas the control zone was only 150 ft in length. The control site was made shorter because it was believed that this track section might fail or experience a large amount of settlement.

S.M. Chrismer, Association of American Railroads, 3140 South Federal Street, Chicago, Ill. 60616. G. Richardson, Soils and Material Engineering, 1903 North Harrison Avenue, Cary, N.C. 27511.

An 8-in. layer of lightly cement-stabilized soil was compacted over the natural soil of the entire test area to provide a zone of intermediate strength between the ballast and subgrade. The natural soil had a range of liquid limits between 50 and 85 percent, and a plastic index of between 27 and 55 percent, and is therefore a CH-type soil (inorganic clay of high plasticity) under the Unified Classification System. The natural soil was about 95 percent saturated. The compacted soil layer is classified as a CL-type soil (clay of low plasticity). Field California Bearing Ratio (CBR) tests were performed on the compacted soil at three locations within each test section. The average CBR values at 0.1 in. penetration for the six sections were 24, 23, 21, 20, 32, and 15, respectively. The CBR values were much greater than would be expected for clayey loam, due to the surface cement stabilization and heavy compaction.

The effects of swelling soil were seen in the top-of-rail surveys and soil moisture measurements obtained periodically over a period of 1.5 yr. Upheaval of the track was observed after a hard rain, but the effect of this soil swelling on the dynamic instrument response should not have been appreciable. After the various fabrics were placed in Test Sections 1 through 4, 8 in. of ballast were placed over each section. No subballast was used. Section 6 had the ballast resting on 12 in. of cement-stabilized rock screenings.

TRACK LOADINGS

Switcher locomotives, running at speeds between 2 and 50 mph, provided the load input to the track structure for those tests that required a load. The cumulative wear on the track was provided by revenue trains that were allowed to run over the test sections. Unfortunately, records of the amount of actual traffic tonnage passing over the test sections were not kept. However, because approximately 50 percent of the main line traffic was diverted onto the siding test section, it may be assumed that the siding received about 5 mgt per year (i.e., one-half of the single track total of 10 mgt per year).

QUASI-STATIC TRACK SYSTEM RESPONSE

As mentioned earlier, there are four postulated mechanisms by which a geotextile is believed to influence track behavior in general:

- Reinforcement,
- Moisture transport,
- Filtration, and
- Separation.

The data from instrumentation that are used to measure such influences will be presented next. Near the end of the paper, the measurements are reviewed to determine if and how much any of the preceding mechanisms influenced behavior.

Soil Moisture Measurements

Soil moisture in the compacted clay loam and the natural clay subgrade was measured to monitor the water content (relative percentage ratio of pore water to soil solids). A smaller seasonal change in soil moisture contents in the fabric test sections as compared to the control section would indicate that a fabric may keep the subgrade drier.

Drainage in the test sections was dependent on the topography and local soil properties. Figure 2 shows the grade conditions for the overall test site. The steeper grade in Section 1 provided better drainage; however, this section also received runoff from Sections 2 and 3. Thus, various combinations of grade and watershed did not appear to favor any particular section.

Three methods were used to monitor the soil water content: (a) manual corings, (b) electrical resistance transducers, and (c) electrical capacitance transducers. The last two methods (those using instrumentation) gave values of moisture content that were close to those of the field corings. However, the instrumentation responses were flatter and did not show the increase resulting from the rainy months of March through June as did the samples recovered from the field. Because the water content measurements from the manual corings are believed to be the most reliable, only the data from the field corings will be given. Soil samples were obtained every 6 in. to a depth of 24 in. at the middle of each test section. Figure 3 shows the variation of subgrade water content in the test sections over approximately 1.5 yr. Figure 4 shows the test section differences between the seasonal maximum and minimum soil moistures that occurred during the 17 months.

Pore Water Pressures

Pore water pressures in the natural subgrade were monitored using piezometers. It was believed that subgrade moisture transport in the fabric test sections might be apparent from reduced pore water pressures compared to the control section. The piezometers were implanted within the subgrade in each section in a plane perpendicular to the rails. Shallow piezometers were placed 15 in. beneath the finished subgrade at locations below the south edge of the ties, the south rails, and the centerline of

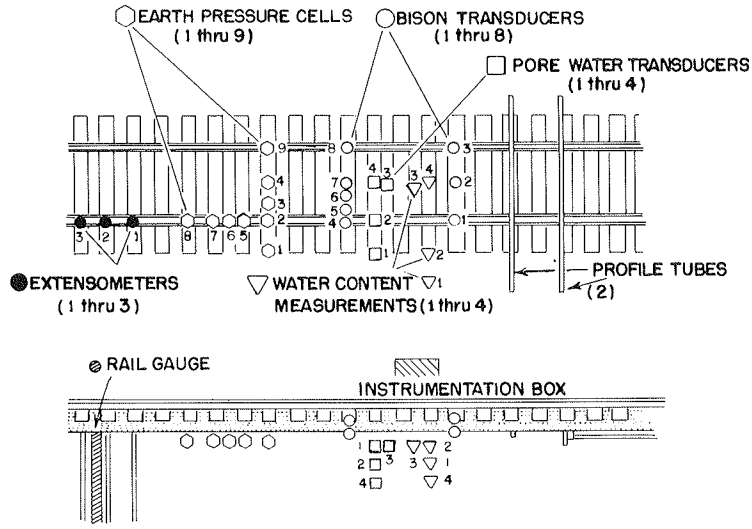

FIGURE 1 Schematic diagram showing typical subgrade test instrumentation.

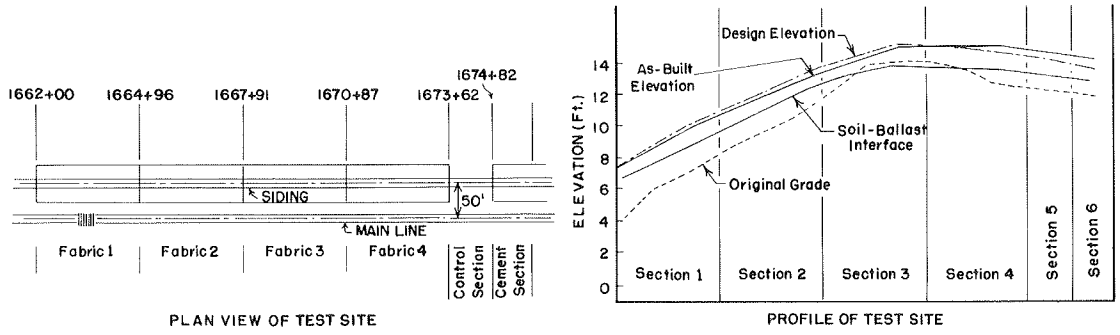

FIGURE 2 Caldwell test site configuration.

TABLE 1 Physical Properties of the Caldwell Test Site Geotextiles

Property	Fabric 1	2	3	4
Weight (oz/yd^2)	10.7	10.7	6.1	6.7
Thickness at 0.03 bar (mils)	173	99	22	78
Porosity (%)	91	90	60	92
Density (kg/m^3)	83	144	364	114
Puncture strength (lb)	113	143	74	88
Puncture toughness (lb)	40	34	24	25
Burst strength (psi)	344	458	270	311
Grab strength (lb)				
MD[a]	165	279	233	238
TD[b]	271	301	225	184
Apparent elongation (%)				
MD	129	66	61	63
TD	112	61	75	75
Toughness (lb)				
MD	106	92	71	75
TD	152	92	84	69
Trap. tear strength (lb)				
MD	62	114	76	95
TD	88	109	102	86
Abrasion (grab strength) (lb)	104	177	184	71
Lateral permeability (cm/sec)				
At 0.24 bar	0.27	0.32	0.06	0.38
At 2.00 bar	0.08	0.13	0.01	0.14
Normal permeability				
cm/sec	0.57	0.45	0.02	0.44
liter/sec/cm^2	0.022	0.022	0.004	0.034
Equivalent opening size	50	Unknown	200	Unknown
Denier	7	7	12	7
Polymer	Polypropylene	Polyester	Polyester	Polyester
Structure	Needled	Needled	Thermal-bonded	Needled

[a]Machine direction.
[b]Transverse direction.

the siding. An additional piezometer was placed to a depth of 4 ft beneath the finished subgrade at the centerline of each test section.

Maximum static positive pore water pressures would occur if the water table is assumed to be at the surface of the subgrade. Thus, the maximum positive pore water pressures measured at Caldwell should be 0.54 psi for the shallow piezometers and 1.73 psi for the deep piezometers, based on the depth below the water table. However, pore water pressures in excess of 0.54 psi (some approaching 3.6 psi) were measured by the shallow piezometers at Sections 1-3, and 6, which conflicts with the maximum pore water pressure model just mentioned.

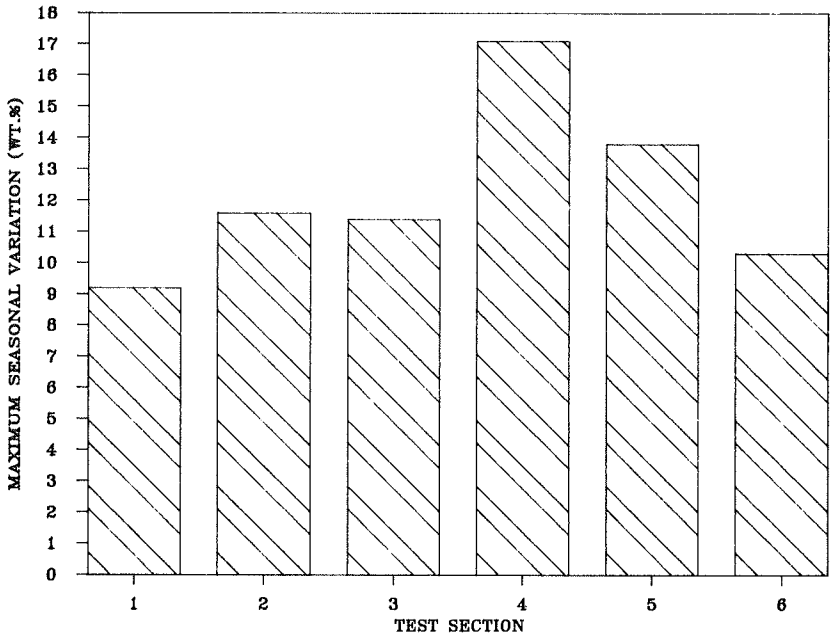

FIGURE 3 Maximum seasonal variations in soil moisture content from July 1978 to March 1980 for Sections 1-6.

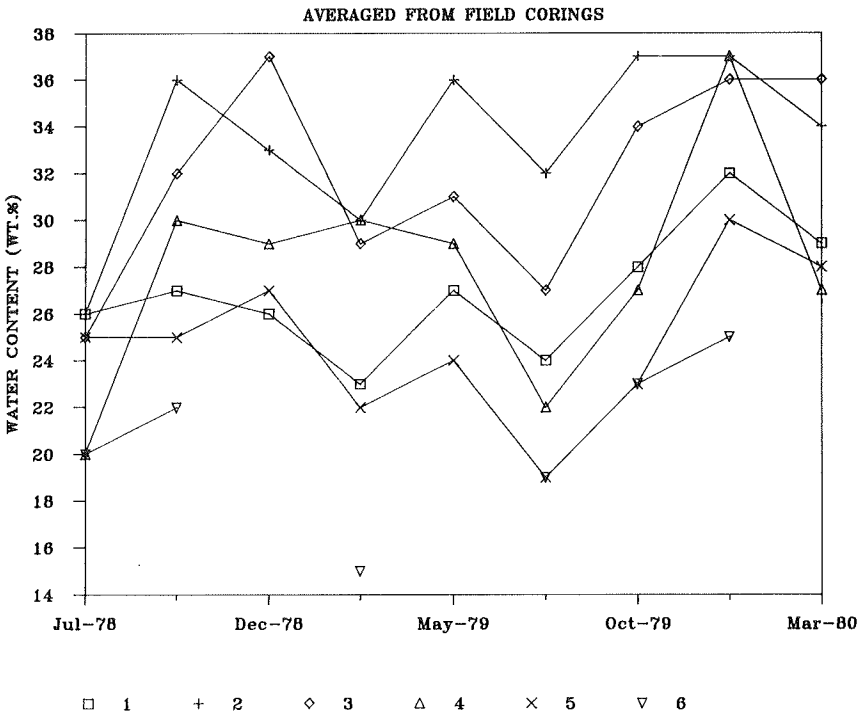

FIGURE 4 Variations in average soil water content with time in Sections 1-6.

Excess positive pore water pressures would lead to reduced subgrade strengths and increased settlements, caused by reduced effective stress. However, Sections 1, 2, and 6 did not experience significant settlements and certainly did not appear to be showing any signs of weak or failing subgrades.

Although there were erratic readings from a few of the piezometers, the others gave reasonable measurements. From these data, the reduced pore water pressures expected to be seen if soil moisture transport was occurring were not apparent. Therefore, no systematic test section differences were observed with this instrumentation.

Subgrade Geometry

Static vertical extensometer readings were recorded to monitor the vertical movement of the soil-ballast interface with respect to a point 10 ft below. The static extensometer readings are shown in Figure 5. All of the curves show a consistent trend in the rise and fall of the interface. Section 5, the control section, clearly experienced greater vertical settlements than the remaining sections. Note also that the vertical movement of Section 3 began to accelerate rapidly during December 1979. The failure of Section 3 occurred in January 1980, as shown in Figure 5.

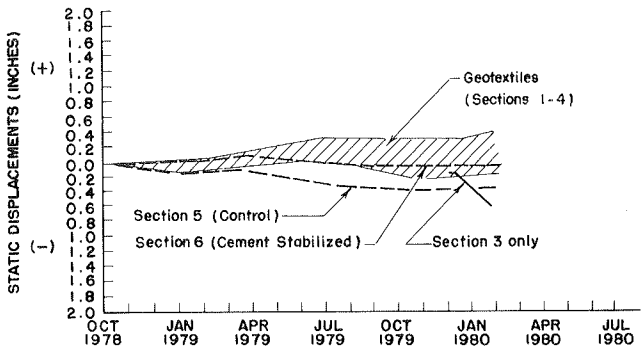

FIGURE 5 Extensometer data showing static soil displacement variations with time in Sections 1-6.

Track excavations were made in each of the fabric sections to observe the transverse subgrade profile under both a tie and a crib. Elevations were taken at the top of the fabric in each excavation before it was removed to reveal the subgrade. Large subgrade displacements were indicated for Section 3. The excavation in Section 3 was made in an area where the top-of-rail (TOR) profile had indicated large settlements. This provided further evidence of the soil-related failure of Section 3. The subgrade profiles from all of the geotextile sections and the control section showed a depression of the subgrade below the tie-rail seats. The depth of this depression ranged from less than 1 in. in Section 4 to more than 6 in. in Section 3.

The most significant finding in the excavations was made at Site 3 where a layer of weak clay slurry was located just under the fabric. The penetrometer unconfined compression strength of the clay slurry was less than 0.25 tons per ft^2. The slurry layer appeared to be extruding from beneath the fabric. The existence of this layer pointed to a near surface soil failure as contributing to the excessive settlement in Section 3. The low permeability of the fabric appeared to be the cause of the slurry formation. This problem site will be discussed in greater detail later.

DYNAMIC TRACK SYSTEM RESPONSE

Subgrade Response--Earth Pressures

The transducers for measuring vertical earth pressures were installed 3 to 4 in. below the top of the

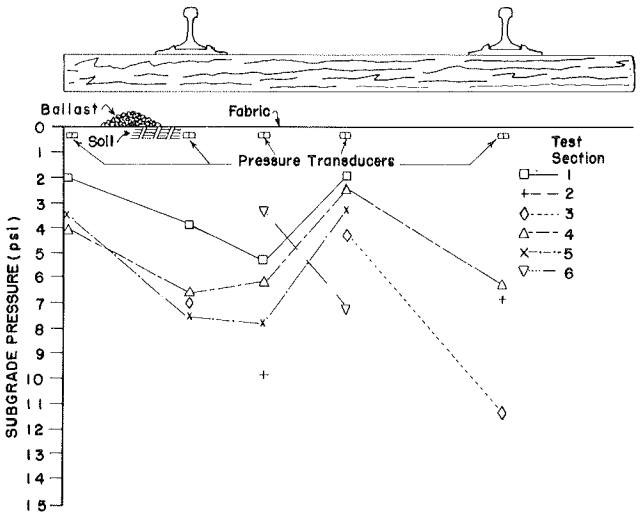

FIGURE 6 Subgrade pressures under one tie in each of Sections 1-6.

subgrade. Figures 6 and 7 show the transverse and longitudinal layout of the transducers in the soil. The earth pressure measurements shown in these figures were obtained by selecting the maximum pressure registered by each transducer during each locomotive pass. These maximum pressures were generated under the wheel loads of switcher locomotives traveling at velocities ranging from 2 to 50 mph. Because the maximum pressures varied somewhat with locomotive speed (a small variation in most cases and with no definite trend), the average for each of the various speeds was calculated and plotted in Figures 6 and 7.

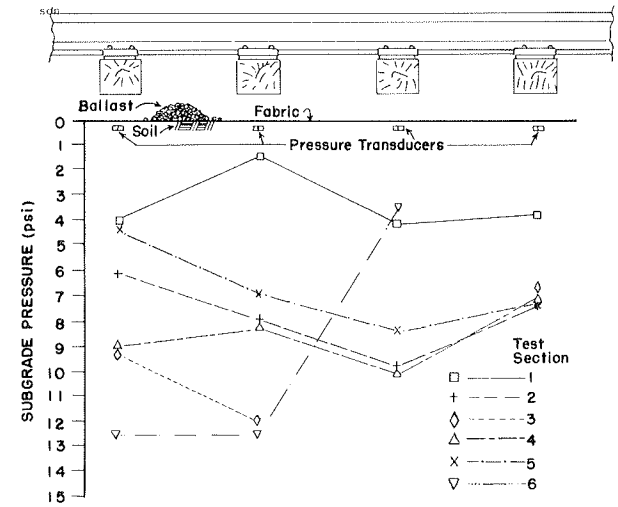

FIGURE 7 Subgrade pressures under four ties in each of Sections 1-6.

The transverse and longitudinal earth pressure measurements showed approximately the same pressure profiles for each site. No significant differences could be observed between the pressure profiles in the fabric sections and those in the control section.

Elastic Subgrade Deformations

Measurements of elastic subgrade deformations under load were obtained using three extensometers per section, which were installed under the rail-tie seats. The mean values obtained under loading are plotted in Figure 8 for the respective test dates. The elastic deformations measured in Sections 2-4, and 6 showed the same climatic variations, with Section 6 having consistently smaller amplitudes. General weather data obtained from Caldwell, Texas, showed that March through June were months that had significant amounts of rainfall, which would explain the increase in dynamic displacements in all but Section 5.

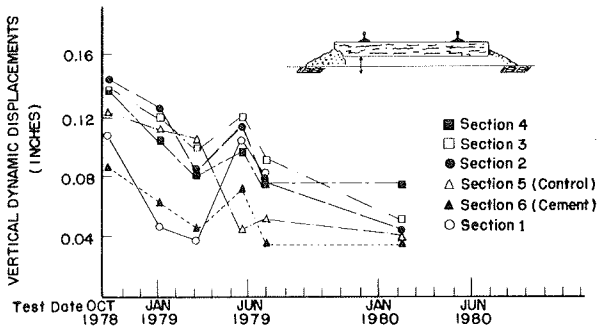

FIGURE 8 Variations in mean values of elastic deformation under load at the ballast/subgrade interface with time, for Sections 1-6.

The anomalous behavior of Section 5 during the wet season was shown by decreasing elastic deformation, while the other sections were experiencing increasing deformations. Section 1 also had anomalous behavior, as evidenced by the wide range in deformation with the seasons. The soil moisture content data did not indicate that the soil in Section 1 experienced greater variation of moisture content; the moisture content in Section 1 was the most uniform during this period.

Because there was no consistent trend in subgrade elastic deformations between test sections, no section differences are noted. The control section had lower-than-average elastic subgrade deflections.

Superstructural Response--Tie Plate Loads

The portion of the wheel load that was distributed to the single tie over which the wheel was located was measured at one tie in each section, using a load cell tie plate. The load cell tie plates were installed just before the time of measurement and then replaced with ordinary tie plates after the testing was completed.

The maximum tie plate loadings for all six sections were 19, 18, 14, 10, 11, and 20 kips, respectively. Sections 1, 2, and 6 appeared to have the largest loads. However, tie loads can be variable from one tie to the next, even in new construction. Tests elsewhere have shown that the percentage of a wheel load taken by the tie directly under that wheel may vary between 20 and 50 percent (1), depending on the tie support conditions and rail stiffness. In these tests, the range of the tie loads divided by the wheel loads (about 33 kips) for all six sections was between 30 and 60 percent. Because the test results were within the natural variations of the tie load spectrum, and because only one tie per section was instrumented, data from the instrumented tie plates could not be used to explain the observed differences in test section behavior.

Tie Strains

The tie strains were measured by gauges attached to the top of one tie in each test section. This enabled the dynamic bending strains in the longitudinal plane of a tie in each section to be monitored. The ties in Sections 5 and 6 were straining somewhat more in the tie middle than near the rail seats, whereas the fabric section ties were strained more uniformly. However, as mentioned previously, the tie support conditions, and, therefore, the bending, could vary considerably from tie to tie. Therefore, because only one tie per section was instrumented, differences in section response could not be confirmed from these data.

BALLAST CONTAMINATION

Filtration and separation are two of the attributes most commonly associated with the use of geotextiles in railroad applications. To assess the performance of the fabric sections with respect to these two characteristics, samples of ballast, soil, and fabric were taken from the field for laboratory analysis.

Differentiating the subgrade fines from fines of other sources, for example, from ballast abrasion, windblown, and so forth, was essential to evaluating the performance of the various geotextiles. Section 6, the cement-stabilized section, played a key role in this investigation, because it contained fines from all sources other than those associated with the subgrade. Assuming reasonably uniform ballast and surface conditions, the contaminating fines measured in Section 6 should represent a control for the other test sections.

Ballast samples were taken at uniform increments of depth below the top of the ties in Sections 1 through 6. Additional samples were obtained from the top of, and beneath, the fabric in Sections 1 through 4. Samples were also taken at the soil-ballast interface, and at the top of the cement at Sections 5 and 6, respectively. Samples were obtained from holes dug by hand in the ballast. A water spray mist was used to prevent the fines from being displaced due to the sampling disturbance. Approximately 700 to 800 g of ballast were taken at each depth.

The amount of contamination, as quantified by measuring the amount of fines that passed through a No. 200 sieve (0.074 mm), consisted of both silt and clay-sized particles, and were assumed to be representative of the ballast contamination.

Mean values were established for the percentage of contamination versus depth data from each test section, and are presented in Figure 9. In the ballast above the level of 12 in. from the top of the tie, only Sections 3 and 5 had contamination in excess of that measured in Section 6 (the "control" section in this case). (Note the contamination of the ballast just above the fabric. Section 5, with no fabric, had significantly more contamination at this level than the remaining sections, and only Sections 3 and 4 of the fabric sections had contamination greater than Section 6.)

In addition to the amount of contamination, laboratory hydrometer analyses were performed to measure the percentage of clay particles in the contaminant fines. Clay particles in the contaminant can originate only as windblown particles or in the subgrade. Crushing and abrasion of the ballast would produce coarser silt-sized particles. The subgrade beneath the track consisted of both clay and silt-sized particles; therefore, the presence of excessive amounts of clay fines would indicate a filtering of the silts by the fabrics, as the fines tried to pass through the fabric.

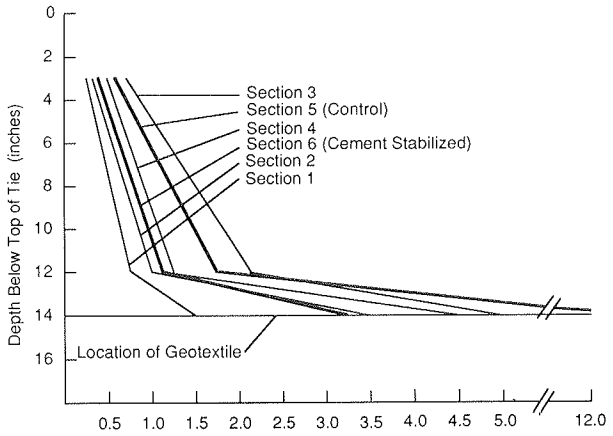

FIGURE 9 Percentage of fines passing a No. 200 sieve versus sampling depth in Sections 1-6.

The average percentages of clay particles in the contaminant fines for Sections 1 through 6 were, respectively, 50.3, 45.7, 43.6, 40.6, 32.6, and 25.3. Therefore, using Section 6 as the control, it appears that the fabric sections received much of their subgrade contamination in the form of clay particles. Because Control Section 5 (the most fouled section) exhibited a significantly lower percentage of clay within its ballast fines, this indicates that large quantities of subgrade silts in addition to the clay were moving into the Section 5 ballast because no fabric was present. This substantiates the filtering capabilities of the fabrics with respect to silt-sized particles.

The quantities of clay-sized particles present within the ballast in Fabric Sections 1, 2, and 4 were between 2 and 3 percent by weight of the total ballast sample. Fabric Section 3 and Control Section 5 had about 8 percent clay fines near the bottom of the ballast layer. [In Fabric Section 3, this may be explained by the extrusion of the soil-slurry that had built up just under the fabric.] Percentages less than 4 or 5 are normally considered negligible in that they will not influence the ballast performance. The amount of clay in Sections 3 and 5, however, may contribute to a degradation of the engineering properties of the ballast. An example of such degradation is the possible increased lateral spreading of the bottom layer of ballast under the lateral shear forces caused by traffic. Excessive track settlement can result. It appears that the use of fabrics can control the pumping of silt-sized particles into the ballast. Fabrics will allow a small amount of clay to pump into the ballast. However, this amount of clay will be significantly smaller than would have occurred if no fabric had been used.

PROPERTIES OF RECOVERED GEOTEXTILES

After 17 months of service, several ties were removed and the ballast was excavated so that samples of fabric could be taken from each test section. The fabric samples were taken to a laboratory, tested for their permeability, both in-plane and normal to the fabric, and compared with the permeability of a clean sample of fabric (shown as the control sample in Figure 10). Also, the strength in tension, as measured by the Grab Tensile Strength test, was determined.

Figure 10 shows the measured decrease in fabric permeabilities when tested in the soiled condition

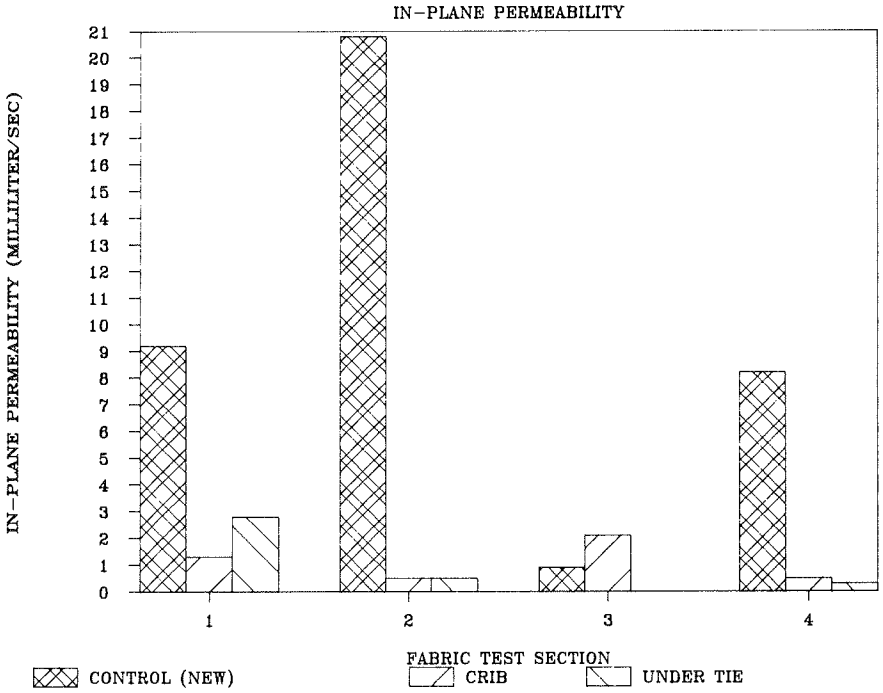

FIGURE 10 In-plane permeability of geotextiles recovered from the field and tested at a pressure of 3.4 psi, applied normal to the surface.

after removal from the field. As shown, the in-plane permeability of the fabric samples after 17 months in track have decreased by as much as a factor of 100. The fabric in Section 1 retained the greatest percentage of its initial in-plane permeability. The test performed on the fabric from Section 3 appeared to show a gain in permeability in the field; however, this test was reported by the technician to be in error. The fabric in Section 3 is known to have clogged more severely in the field than any of the other fabrics based on the observed performance in the field.

A combination of visual and microscopic inspections revealed that all of the fabrics had soil particles in the voids of the fibers and on the fabric surfaces. Fabric 1 had the least amount of soil in the fibers, while the other three fabrics had a greater (approximately equal to each other) degree of soil particles in them. These observations confirmed the laboratory permeability results.

The tests that were conducted to determine the permeability normal to the plane of the fabric again showed the fabric from Section 1 to have the smallest percentage decrease and the greatest permeability. However, even with permeability decreases on the order of 100, the soiled fabric permeability was still much greater than that of the soil itself.

It appears desirable to permit a certain amount of clay to pass into and through the fabric, while the silt is retained in the surrounding soil. If some clay fines are not allowed to pass into the fabric, they are retained just under the fabric and, after a time, may form a weak soil layer. The behavior of pore water pressure at the soil-fabric interface is crucial to system performance. The soil immediately adjacent to the fabric apparently has a tendency to increase in water content as a result of soil suction and local shearing by ballast particles (2). Hoare has found that the water content of this thin layer of clay soil layer may increase to the liquid limit and beyond. The fabric must remain sufficiently permeable to allow pore water, carrying the clay fines under pressure from transient loads, to escape into the fabric. In other words, the filtration properties of the geotextile should not be 100 percent efficient.

As evidence of this phenomenon, consider the fabric-related soil failure in Section 3. A derailment occurred that was directly related to the weak layer of clay particles that built up just under the clogged fabric. Although it is not clear to what extent the derailment was due to the differential rail settlement caused by the weak soil in Section 3, or the track sliding horizontally under load, or both, the failure was clearly exacerbated because of an impermeable geotextile. Ballast sliding laterally on top of the fabric due to a low coefficient of friction of Fabric 3, also contributed to the track settlement, although to a lesser degree than soil failure, which caused 6-in. rutting.

The grab strength test was used to determine the tensile resistance to tearing, when subjected to a slowly increasing load applied to either end of a standard sized strip. Fabric in a soiled and wet condition was tested in this manner; the results are shown in Figure 11 for samples recovered from under the tie and in the crib area. The fabric with the largest loss of strength, as compared to a new control sample, was Fabric 1, which exhibited a 56 percent decrease. Fabric 2 had the least amount of strength loss, with only a 35 percent decrease.

A visual inspection at the time of fabric sampling from the field revealed that Fabrics 3 and 4 had the most holes from tamper and traffic-induced ballast puncturing. Also, despite the relatively low amount of retained grab strength, Fabric 1 was observed in track to have the least number of puncture holes. The fabric holes appeared to be caused by puncturing rather than abrasion.

ANALYSIS OF RESULTS

Any final analysis of the effect of geotextiles on track behavior should compare how the track was

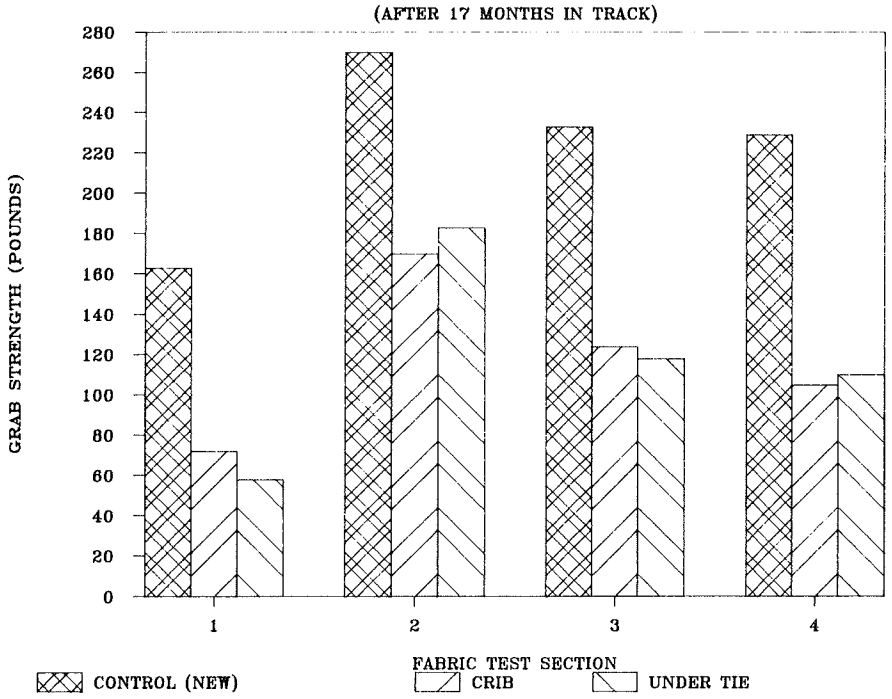

FIGURE 11 Grab strength of geotextiles recovered from the field and tested under wet and soiled conditions (after 17 months in track).

postulated to be improved and determine to what extent, if any, the testing indicated such an improvement. Data gathered over the 1.5 yr of testing will be analyzed in more detail in this section. The four postulated beneficial effects mentioned earlier will now be reviewed in light of what the various track measurements indicated.

Reinforcement

If track reinforcement was occurring, these effects would probably manifest themselves in a decreased amount of vertical deformation under load and decreased pressure transmitted to the subgrade. A review of the data from the subgrade pressure and extensometer transducers indicated that no such reinforcement effect was observed, when the instrument readings of Fabric Sections 1 through 4 were compared to those of the control (Section 5) and the cement-stabilized (Section 6) locations.

The control section did experience somewhat more ballast/soil interface settlement than the other sections (Figure 5). However, this most likely is due to ballast penetration into the subgrade in Section 5. Therefore, rather than a reinforcement function, the decreased settlement in the fabric sections is probably attributable to the separation function of geotextiles.

Subgrade Moisture Transport

Another anticipated benefit of geotextiles, that of moisture transport in the subgrade, could be assessed by the soil moisture measurements and the pore water pressure readings. Although the soil moisture measurements were not consistent between the different measurement methods, there was still enough evidence to conclude that there was no apparent subgrade moisture transport in the fabric sections as compared to the control section. The maximum seasonal variation of subgrade moisture content in Section 5 was not significantly greater than that of the average of all of the fabric sections (see Figure 4).

The pore water pressure readings, although somewhat difficult to interpret, also did not support the moisture transport mechanism. The reduced pore pressures that would be expected to be observed in the fabric sections, relative to the control section, if the fabrics did transport moisture, were not apparent.

Filtration/Separation

The real success of these geotextiles in separating the layers, and limiting intermixing of the ballast and subgrade, could be seen by comparing the amount of fines above the fabric with the amount at the ballast/soil interface in the control section (Figure 9). The silty and clayey fines in the ballast of each fabric test section could be used to assess the filtration and separation functions of these geotextiles. There was a clear difference within the fabric sections with respect to the amount of subgrade fines contamination in the ballast. Of the fabric sections, Section 1 had the lowest amount of fines in the ballast, whereas Section 3 had the highest.

However, as mentioned previously, filtration should not be 100 percent efficient. Passing some of the clayey fines that have access to the fabric should continue in order to prevent a buildup of these particles and a resulting weak soil layer. The acceptable amount of clay is difficult to determine, but it should not be more than about 3 or 4 percent of the ballast by weight.

Durability

The types of geotextiles in this test allow a comparison of needle-bonded with thermal-bonded fabrics, and polyester with polypropylene fabrics. The ther-

mal-bonded type of fabric structure appears unsuitable for use in railroad track because of its low permeability and low ballast-fabric frictional resistance. The fabric with the polypropylene structure (Fabric 1) seemed to perform best with respect to resistance to both clogging and puncture damage. Although not mentioned before, Fabric 1 had the highest retained filament strength of all the fabrics recovered from the field. The retained strength of filaments from the tops (sides that faced the ballast) of Fabrics 1 to 4 were, respectively, 90, 57, 34, and 56 percent. There was, however, somewhat more abrasion on the surface of Fabric 1. Also, Fabric 1 had the greatest loss in grab strength.

CONCLUSIONS

Geotextiles apparently provide varying degrees of filtration and separation to the track structure. These two functions could be enough to justify the inclusion of fabric in the track. If reinforcement or subgrade moisture transport, or both, also resulted, then this would be an added bonus. However, the data collected from this extensively instrumented test showed no evidence of moisture transport or reinforcement attributable to the fabric.

The graphs of subgrade moisture from the soils (obtained by hand sampling for over 1.5 yr) indicate seasonal changes in the soil in each section, but the observed moisture variations were virtually the same among the fabric sections and the control section. It is in the variation of subgrade moisture that one would expect to observe evidence of fabric-induced subgrade drainage. Reinforcement as a result of fabric membrane support was also not indicated from either the earth pressure measurements or the soil extensometers.

Perhaps one of the most interesting findings was the geotextile-related track failure, which resulted in a derailment in Section 3. The soil failure was in the form of a clay slurry that had built up under a fabric with a low initial permeability. The structure of the polymer (thermal bonded) may have had something to do with the failure as well. Because the clay particles in the compacted clay loam were displaced upwards under the loading conditions, these fines accumulated at the fabric-soil interface. Furthermore, the water in the clay fines did not escape through the fabric because of apparent fabric clogging. This clogging is believed to have been caused by the initially low permeability of the fabric. The low ballast-fabric friction resistance may also have contributed to the excessive settlement in Section 3, because of low lateral ballast restraint.

It appears that the installation of a geotextile that clogs can be more harmful than not installing one at all, as shown by the fact that Fabric Section 3 failed, while control Section 5 was remarkably stable. Even though this particular type of thermal-bonded fabric is no longer used in track, it does illustrate what could happen if a fabric became clogged. With the more permeable fabrics that railroads are using currently, clogging may not occur for many years. However, these fabric properties that resist clogging should be further investigated.

In summary, the Caldwell geotextile tests indicated that these fabrics did not play a direct structural role or modify the soil conditions in an active manner. The benefit of these materials appeared to be in their application as barriers to intermixing of the ballast and subgrade.

REFERENCES

1. J.F. Scott. Granular Depth Requirement for Railroad Track. In Transportation Research Record 1006, TRB, National Research Council, Washington, D.C., 1985, pp. 17-23.
2. D.J. Hoare. A Laboratory Study into Pumping Clay Through Geotextiles Under Dynamic Loading. Presented at the Second International Conference on Geotextiles, Las Vegas, Nev., 1982.

Publication of this paper sponsored by the Committee on Engineering Fabrics and the Committee on Railway Maintenance.